Design and implementation of a synthetic pre-miR switch for controlling miRNA biogenesis in mammals

Vom Fachbereich Biologie der Technischen Universität Darmstadt

zur

Erlangung des akademischen Grades

eines Doctor rerum naturalium

genehmigte Dissertation von

Janina Atanasov, M. Sc.

aus Nürnberg

1. Referentin: Prof. Dr. Beatrix Süß

2. Referent: Prof. Dr. Alexander Löwer

Tag der Einreichung: 06.03.2017

Tag der mündlichen Prüfung: 28.03.2017

Darmstadt 2017

D 17

Danksagung

Frau Prof. Dr. Beatrix Süß gilt mein ausdrücklicher Dank für die Vergabe des interessanten Themas und für die Möglichkeit der Durchführung meiner Doktorarbeit in Ihrem Labor. Zudem bin ich dankbar für die hervorragende Betreuung, die hilfreichen Diskussionen und die Möglichkeit zur Teilnahme an interessanten Tagungen und Konferenzen.

Frau Dr. Julia Weigand danke ich für die inspirierenden wissenschaftlichen Gespräche und Diskussionen, die meine Arbeit maßgeblich unterstützt haben.

Ich danke Herrn Prof. Dr. Alexander Löwer für die freundliche Übernahme des Zweitgutachtens.

Natürlich möchte ich mich auch bei meinen Kollegen für eine gute Zusammenarbeit und eine nette Zeit im Labor bedanken. Mein Dank gilt besonders den Kollegen im Labor, die über die Zeit ebenso meine Freunde geworden sind und mit denen ich im Lab sowie in meiner Freizeit sehr viel lachen konnte.

Meiner ganzen Familie bin ich unglaublich dankbar für die großartige Unterstützung, die ich auf meinem ganzen bisherigen Lebensweg genießen durfte und die mich zu dem Menschen gemacht hat, der ich heute bin.

Chrissi danke ich dafür, dass er immer an meiner Seite war.

Julia Atanasov und Christopher Schneider danke ich außerdem für das Korrekturlesen meiner Arbeit.

Parts of this thesis will be published in:

Atanasov J, Weigand JE and Suess B: **Design and implementation of a synthetic pre-miR switch for controlling miRNA biogenesis in mammals.** (2017), manuscript submitted

Table of Contents

1 Zusammenfassung/ Summary ..... - 1 -

2 Introduction ..... - 5 -

2.1 The potential of synthetic biology ..... - 5 -

2.2 Regulation of gene expression in eukaryotes ..... - 6 -

2.2.1 DNA-based control mechanisms ..... - 6 -

2.2.1.1 Engineering and application of TFs in synthetic biology ..... - 7 -

2.2.2 RNA-based control mechanisms ..... - 9 -

2.2.2.1 Small non-coding RNAs and their involvement in gene regulation ..... - 9 -

2.2.2.2 Synthetic riboswitches as post-transcriptional control elements ..... - 17 -

2.3 Scope of the study ..... - 24 -

3 Results ..... - 25 -

3.1 Design and functionality of a reversible pre-miR switch ..... - 25 -

3.2 Transfer of the pre-miR switch design to further miRNA precursors ..... - 29 -

3.3 Proof of the functionality of the pre-miR switches in a reporter gene assay ..... - 33 -

3.4 Determination of the pre-miR switch miR-199a_2 onset kinetics ..... - 40 -

3.5 Regulatory function of the pre-miR switches targeting endogenous genes ..... - 41 -

3.5.1 Transient transfection of pre-miR switch miR-199a_2 ..... - 41 -

3.5.2 Genomic integration of pre-miR switch miR-199a_2 ..... - 43 -

3.5.3 Genomic integration of pre-miR switch miR-199a_2 and TetR ..... - 47 -

4 Discussion ..... - 55 -

4.1 Evaluation of design and functionality of the pre-miR switches ..... - 55 -

4.2 Regulation of reporter gene expression dependent on TetR and dox ..... - 57 -

4.3 Regulation of endogenous miRNA-199a-5p targets with miR-199a_2 ..... - 60 -

4.4 Comparison between transient and genomic expression ..... - 62 -

4.5 Evaluation of the experimental setup to investigate endogenous regulation ..... - 63 -

4.6 Synthetic regulatory tools for controlling RNAi in mammals ..... - 64 -

4.7 Conclusion and perspectives ..... - 65 -

5 Material and Methods ..... - 67 -

5.1 Chemicals, instrumentation and consumables ..... - 67 -

5.2 Prokaryotic and eukaryotic cell strains ..... - 71 -

5.3 Buffers and solutions ..... - 72 -

5.4 Oligonucleotides ..... - 73 -

5.5 Plasmids ..... - 77 -

5.5.1 Basic plasmids ..... - 80 -

5.5.2 Construction of plasmids ..... - 83 -

5.6 Methods ..... - 89 -
5.6.1 Treatment of prokaryotic cells ..... - 89 -
5.6.2 Treatment of eukaryotic cells ..... - 89 -
5.6.3 Treatment of proteins ..... - 92 -
5.6.4 Treatment of nucleic acids ..... - 93 -
6 Appendix ..... - 101 -
6.1 Abbreviations ..... - 101 -
6.2 Units ..... - 102 -
6.3 Prefixes ..... - 102 -
6.4 Nucleobases ..... - 102 -
7 References ..... - 103 -
8 Talks and Poster Presentations ..... - 114 -
9 Publications ..... - 115 -
10 Curriculum Vitae ..... - 116 -
11 Ehrenwörtliche Erklärung ..... - 117 -

1 Zusammenfassung

Mit der Entschlüsselung des humanen Genoms stellte sich heraus, dass nur ein geringer Anteil der genetischen Information von ca. 2% für Proteine kodiert. Das verbleibende Genom wird aber größtenteils auch transkribiert und es entstehen ribosomale und transfer RNAs sowie verschiedene längere und kleine RNAs, von denen ein Großteil maßgeblich an der Regulation zellulärer Prozesse beteiligt ist. Obwohl die genaue Funktion vieler nicht-kodierender RNAs noch unklar ist, spielen besonders die kleinen, nicht-kodierenden RNAs eine große Rolle in der Regulation der Genexpression. Zur Gruppe der kleinen, nicht-kodierenden RNAs gehören die microRNAs (miRNAs). Die 20-25 Nukleotide langen Ribonukleinsäuren erfüllen wichtige Aufgaben bei der Steuerung grundlegender biologischer Prozesse wie der Entwicklung und Zelldifferenzierung. Es wird vermutet, dass ca. 60% der Protein-kodierenden Gene von miRNAs reguliert werden. Dementsprechend sind sie auch mit der Entstehung von verschiedenen Krankheiten wie Stoffwechselstörungen und Krebs assoziiert. Mittlerweile wurden ungefähr 2.500 verschiedene humane miRNAs gefunden, doch über ihren genauen Regulationsmechanismus liegen noch wenige Informationen vor. Die genomisch kodierten, kleinen RNAs werden als Vorläufer transkribiert und anschließend schrittweise durch die Enzyme Drosha und Dicer zur reifen miRNA prozessiert. Die reife miRNA bildet dann einen Komplex mit verschiedenen Proteinen und bindet an eine Ziel-mRNA. Dadurch kommt es im Rahmen der RNA-Interferenz entweder zur Degradation der mRNA oder zur Inhibition der Translation.

Die synthetische Biologie besitzt ein hohes Potential, die direkten Zusammenhänge zwischen Erkrankungen und spezifischen miRNAs aufzuklären. Durch die wachsende Bedeutung dieses Forschungsfeldes wird die Entwicklung geeigneter Werkzeuge und Methoden immer wichtiger. Durch die gezielte Herstellung von RNA-basierten Werkzeugen zur Steuerung bestimmter zellulärer Prozesse kann beispielsweise die Interaktion einer miRNA mit einem potentiellen endogenen Ziel untersucht werden. Im Rahmen dieser Arbeit wurde ein RNA-Schalter basierend auf der natürlichen miRNA-Vorläuferstruktur der miRNA-126 designt, der die Prozessierung zur maturen miRNA durch Dicer steuern sollte. Zu diesem Zweck wurde der miRNA-Vorläufer modifiziert, indem die natürliche Endschleife entfernt und durch eine regulatorische Domäne, das TetR-bindende Aptamer, ersetzt wurde. Die Positionierung des TetR-bindenden Aptamers erfolgte an besagter Stelle, da hierdurch die Nähe zur Schnittstelle des Enzyms Dicer gewährleistet werden konnte. Somit konnte der Zugang der Schnittstellen durch Zugabe des Liganden TetR direkt kontrolliert werden. Zur Verknüpfung der zwei verschiedenen RNA-Bausteine zu einem funktionellen Schaltelement wurden verschiedene sogenannte Kommunikationsmodule getestet. Diese wurden am Übergang vom natürlichen Vorläufer zum TetR-bindenden Aptamer eingebracht und sollten zum einen die erfolgreiche Prozessierung und zum anderen die effektive Regulation des Vorläufer-basierten Systems ermöglichen. Mit Hilfe dieser strukturellen Modifikation gelang es einen Schalter zu generieren, der die Prozessierung des miRNA-Vorläufers effektiv und in Abhängigkeit des Liganden TetR regulierte. Dadurch konnte eine 44-fache Inhibition der Prozessierung zur reifen miRNA erzielt werden. Die Verwendung des TetR-basierten Systems ermöglichte es zudem ein reversibles Schaltelement zu entwickeln, das nach der Zugabe von Doxyzyklin und der darauffolgenden Ablösung des Liganden vom Aptamer die Wiederherstellung der natürlichen Prozessierung zur maturen miRNA erlaubte. Es wurde zudem festgestellt, dass die

verschiedenen Kommunikationsmodule, abhängig von deren Länge und Volumen, und der Ersatz der natürlichen terminalen Schleife die Prozessierung in unterschiedlichem Maß beeinflussten. Letztendlich stellte sich heraus, dass die Verknüpfung über ein G-C Basenpaar die beste Möglichkeit bot, um die Prozessierung aufrecht zu erhalten und ein effektives Schaltverhalten herbeizuführen.

Basierend auf dieser Erkenntnis konnte das Design erfolgreich auf weitere miRNA Vorläufer (miRNA-34a und -199a) übertragen werden, die sich hinsichtlich ihrer Struktur von der miR-126 unterschieden. Auch hier konnte eine effektive Schaltaktivität von bis zu 400-fach nachgewiesen werden. Die Inhibition der Prozessierung des miRNA Vorläufers konnte durch die Zugabe von Doxyzyklin auch hier vollständig aufgehoben werden. Die entwickelten RNA-Schalter wurden daraufhin mit Hilfe eines Reportergen-Assays auf ihre Aktivität bezüglich der Regulation von miRNA Zielgenen überprüft. Hierzu wurden natürliche miRNA-Zielsequenzen hinter ein Reportergen eingebracht und die Bindung der miRNAs in Abhängigkeit von der Aktivität der Schaltelemente getestet. Es konnte gezeigt werden, dass der Großteil der Schaltelemente zur Regulation der Reportergenexpression geeignet war. Um Informationen über die Kinetik des Schalters miR-199a_2 zu gewinnen, wurden zeitaufgelöste Messungen zur Bestimmung der Ansprechverhaltens des Schalters auf die Zugabe von Doxyzyklin durchgeführt. Es konnte gezeigt werden, dass bis zu 30% der Prozessierungsaktivität bereits 1 h nach Doxycyklinzugabe wiederhergestellt und innerhalb von 24 h vollständig wiedergewonnen werden konnte. Im Anschluss wurde das regulatorische Potential der Schalter bezüglich endogener miRNA Ziele betrachtet. Dazu wurde die für den Schalter miR-199a_2 kodierende Sequenz entweder transient in die Zelle eingebracht oder in das Genom der Zelle integriert. Durch die genomische Integration wurde eine geringere Expression der Schalter-basierten miRNA beobachtet, was mit einer Verringerung des Schaltfaktors einherging. Eine Regulation der endogenen Ziel-mRNAs *SMAD4*, *DDR1* und *CAV1* in Abhängigkeit von Liganden- und Doxyzyklinpräsenz konnte allerdings weder im Fall der transienten Expression des Schaltelements noch nach der genomischen Integration des Konstrukts unter den vorliegenden experimentellen Bedingungen gezeigt werden.

Zusammenfassend kann man sagen, dass das entwickelte Schalterdesign die effektive und robuste RNA-basierte Regulation der miRNA Biogenese ermöglichte. Die in dieser Studie generierten Schaltelemente besitzen ein hohes Potential, in zukünftigen Anwendungen die physiologische Relevanz verschiedener miRNAs aufzuklären.

Summary

In recent years, the discovery of small non-coding RNAs has unveiled the essential role of RNAs for the regulation of gene expression. The largest group within the small non-coding RNAs is constituted by the class of micro RNAs (miRNAs). These 20 to 25 nucleotide long molecules fulfill important tasks concerning the control of fundamental biological processes like cell differentiation and development. This class of small non-coding RNAs impacts on post-transcriptional gene regulation in eukaryotes in a process called RNA interference. Acting on translation and mRNA stability, miRNAs influence the functionality of at least 60% of the human protein-coding genes. In this context the development of many diseases has been associated with miRNA dysregulation. Accounting for the importance of miRNAs, current research is focused on the elucidation of their exact function. 2,500 human miRNAs have been identified so far, but their detailed regulatory mechanism still remains elusive. MiRNAs are encoded in the genome and transcribed as primary precursors that are processed in a two-step mechanism to the mature miRNA by the enzymes Drosha and Dicer. Together with several protein factors, the mature miRNA builds the RNA-induced silencing complex and functions as a guide to target the respective mRNA. The consequence of a miRNA-target interaction is either mRNA degradation or translational repression.

Synthetic biology offers various opportunities to shed light on the detailed relation between miRNA abundance and disease development. To deepen the knowledge about miRNAs and their respective function, the repertoire of existing methods and tools has to be adapted to the research objective. For an experimental setup it would be advantageous to make use of switchable systems which allow for the control over the abundance of the respective miRNA, thereby investigating its physiological relevance. In this study a natural miRNA precursor was modified by replacing the natural terminal loop with a regulatory sensor domain, the TetR-binding aptamer to enable the ligand-dependent control of the processing of precursor miRNA-126 (pre-miR-126) to mature miRNA-126-3p. The TetR aptamer was positioned in close proximity to the Dicer cleavage sites, conferring steric control over pre-miR processing by Dicer dependent on absence and presence of the ligand TetR. For the fusion of the two inherently different parts to a functional unit different communication modules were tested. These modules were introduced at the transition region between miRNA precursor and TetR aptamer to enable an adequate pre-miR cleavage as well as an effective regulation of processing. Here, switching factors of 44-fold could be yielded for pre-miR switch miR-126_5 in the presence of TetR that resulted in nearly complete inhibition of processing. The employment of the TetR-based system allowed the development of a completely reversible switching element, since the supplementation with doxycycline resulted in a dissociation of the ligand from the aptamer and the total recovery of pre-miRNA processing. Furthermore, the application of different communication modules turned out to essentially affect the processing to mature miRNA dependent on length and size of the resulting Dicer substrate. A single C-G base pair proved to provide an adequate connection between precursor and aptamer that preserved pre-miR processing und facilitated effective regulation at the same time.
In analogy to this design concept further functional pre-miR switches were developed based on the precursors of miR-34a and -199a. These switches showed comparable features and regulatory factors of up to 400-fold as determined in qPCR assays. The addition of doxycycline resulted in the complete

recovery of pre-miRNA processing. The functional riboswitches were further tested for their regulatory activity in reporter gene assays. The natural target sites were introduced downstream of a reporter gene and miRNA binding to its target was investigated dependent on the regulatory performance of the respective switches. It could be shown that most of the switching elements were well suited to regulate reporter gene expression dependent on the presence of TetR and doxycycline. To gain information on the kinetics of the switch miR-199a_2 time-course experiments were performed to test the responsiveness of the switch to the presence of doxycycline. Within the hour of doxycycline addition already 30% of the processing activity were restored. 24 h after doxycycline addition the full recovery of switching activity could be observed in this experiment. At last, the regulatory potential of the switch to control endogenously expressed miRNA targets was investigated. Therefore, cells were either transiently transfected with the plasmid bearing the miR-199a_2 or a genomic integration of this switch was performed. As a consequence of genomic integration the expression of the switch as well as the regulatory factor were reduced compared to the effects obtained after transient transfection. All in all, the robust regulation of none of the miR-199a-5p targets *SMAD4*, *DDR1* and *CAV1* could be shown under the present experimental conditions.

However, the developed design enabled the robust and effective RNA-based regulation of miRNA biogenesis. The generated pre-miR switches thus exhibit a high potential to contribute to the elucidation of the physiological relevance of different miRNAs in future applications.

2 Introduction

2.1 The potential of synthetic biology

Among various options a very simple, but appropriate definition of the term synthetic biology is “1. the design and construction of biological parts, devices and systems, and; 2. the redesign of existing, natural biological systems for useful purposes” [1].

Based on the knowledge of molecular biology, synthetic biology unites different disciplines of science reaching from nanotechnology to immunology and connects concepts from engineering and biology. It separates itself from other disciplines like systems biology or biotechnology by the aspect of engineering that is to develop new properties and functions. Characterized by a “plug and play” mentality, the combination of various parts and devices by employing different engineering principles allows the rational design of novel, artificial functional frameworks and biological systems.

Driven by the purpose of implementing new biological functions to organisms or modifying existing systems, the applicability of these artificial constructs is rather extensive. Reprogramming stem cells, the development of biosensors or the production of chemical entities in modified bacteria merely represent a small part of the current repertoire. A well-known example that emphasizes the high potential of the synthetic biology field is the production of terpenoid compounds in *Escherichia coli* and *Saccharomyces cerevisiae* as precursor for the development of the antimalaria drug Artemisinin [2–4]. This approach demonstrates that engineering of a metabolic pathway for employing cells as small factories for compound production is feasible in an applicable way.

Providing a huge space for genetically modifying an organism, synthetic biology also has to face several challenges that set boundaries to the theoretically endless possibilities of manipulating systems by the help of artificial structures. In order to increase the researcher’s toolbox it is mandatory to create a variety of well-characterized functional building blocks that can be assembled to complex genetic circuits and expression systems. In an ideal case, these parts should be modularized as well as standardized for the robustly use in different organisms. Furthermore, a predictable and targeted modification of an organism requires detailed knowledge about the biology of the respective organism itself and the possible influence this modification has on cellular processes. Given that especially higher eukaryotic systems are rather complex and the mostly naturally derived devices often exhibit a strong dependence on the genetic context, the construction of robustly and predictably working devices is a complicated adventure. To counteract the issues stemming from interactions of artificial components with the deployed natural system, a valuable approach is the design of orthogonal biosystems. The ability to combine various independent, orthogonal parts and their implementation without affecting other natural processes is a basic requirement in synthetic biology and renders specific modifications of the organism possible.

This doctoral thesis focuses on a special application area in the field of synthetic biology that intends to manipulate gene expression by using RNA-based regulators. Here, approaches are quite manifold with regard to the various factors involved in regulating gene expression. Over the years synthetic biologists have designed various synthetic tools that can be combined to achieve conditional gene

expression. It is a fact that there are more devices available for the usage in prokaryotes and lower eukaryotes than for the modification of higher eukaryotes [5]. That in turn might be associated with the higher complexity of eukaryotic gene regulation.
Synthetic biology is a continuously expanding field with a multitude of promising developments for industry and for basic research. But there is still some effort required to fully exploit the power of synthetic biology and to build up complex systems by the constructive combination of various synthetic units to predictably engineer an organism.

2.2 Regulation of gene expression in eukaryotes

During evolution, gene regulation of all organisms perfectly adapted to the environmental requirements through the development of a system that is defined by a complex interplay of various factors. Compared to prokaryotes, eukaryotes typically possess a much larger repertoire of genes that is organized into chromosomes. Although the whole genome of an organism is present in every cell, differentiation into single macrostructures like tissues and organs occurs during development. This leads to the conclusion that gene expression has to be an individual process in each cell type. To enable a precise temporal and spatial regulation of gene expression, eukaryotes are dependent on a highly sophisticated operation framework that decides about gene activation and the amount of RNA and protein product. The regulatory mechanisms can be classified into transcriptional and post-transcriptional events. Transcription is regulated by adjusting the transcript amount of a gene, whereas regulation at the post-transcriptional level directly influences the translation of an mRNA into a protein.

2.2.1 DNA-based control mechanisms

A basic prerequisite for transcriptional control is the accessibility of the DNA for the RNA polymerase and specific regulatory factors. These factors mainly have an effect on transcription initiation. To find a compromise between a large genome and merely limited space in the nucleus and to coordinate cellular processes like transcription and replication, eukaryotic genes are arranged in an elaborate and highly dynamic higher order structure (Fig. 2.1). In the nucleus, the double stranded genomic DNA is stably coupled to histone proteins, thereby forming a complex, the nucleosome that constitutes the basic structural unit in chromatin. These nucleosomes are further organized into chromatin fibers (reviewed in [6]). Metaphase chromosomes exhibit the most compact form of chromatin that occurs during nuclear division. The term heterochromatin describes the state of chromatin that appears to be relatively condensed and mainly contains genomic DNA that is not transcribed and is therefore referred to as inactive part of the genome. In order to grant the transcription machinery access to a gene, partial unpacking of the condensed heterochromatin structure is necessary to form the euchromatin. With its lightly packed structure, the euchromatin allows the binding of protein factors and RNA polymerase to the DNA to initiate transcription [7].

The dynamic features of the nucleosomes are dependent on the intensity of interactions between DNA and histone and also strongly influenced by the processes of chromatin remodeling [8]. By covalently modifying the protein structure of histones through acetylation, methylation or phosphorylation of

specific amino acid residues, the stability of the nucleosome is changed. Another mechanism to influence DNA-histone contact formation is used by an ATP-dependent set of chromatin-remodeling enzymes that utilizes ATP-hydrolysis for targeted movement or eviction histones and restructuring nucleosomes (reviewed in [9]).

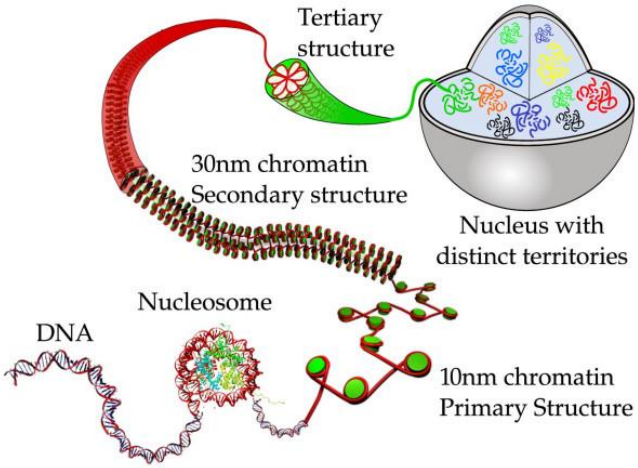

Figure 2.1 The organization of the eukaryotic genome.
To condense the eukaryotic genome, the DNA double strand is wrapped around a core octamer of histones to form the core particles of the nucleosomes. These nucleosome particles are separated by a 50-70 base pair (bp) DNA linker and further compacted to a chromatin fiber. The secondary and tertiary structures of chromatin are stabilized by architectural proteins leading to higher organization of the chromatin structure. The tertiary structure chromatin is then spatially organized within defined territories in the nucleus. (adopted from [10])

The presence of transcription factors (TFs), a group of sequence-specific DNA binding proteins mandatory for recruitment, adequate binding and the activity of the RNA-Polymerase II in eukaryotes, constitutes another level of regulation [11]. The recognition and binding sites of TFs are either located directly in the promoter region or up- or downstream in a gene dependent on the family of TFs and their specific function. The mechanisms of these transcription regulation elements are manifold and often based on the recruiting of further factors to form the transcription (pre-)initiation complex, the promotion or repression of transcription by binding to distant-dependent (Promoter, Promoter-proximal elements, enhancer, silencer) and –independent (enhancer, silencer) *cis* regulatory elements in the DNA sequence and even influencing histone modification [12–14]. Thus, the different transcription factor families significantly contribute to selective gene expression in the cell.

2.2.1.1 Engineering and application of TFs in synthetic biology

For the design of large synthetic networks, a well-characterized library of different parts and precise design principles for their assembly are required. Such parts can be promoters, terminators, reporters and also TFs. Eukaryotic cells use their complex network of TFs to precisely control gene expression. At present, the number of well-characterized and orthogonal natural TFs is limited and therefore restricts the application of TFs for the construction of complex synthetic networks in eukaryotes [15].
Basically, a TF can be compartmentalized into three functional substructures for binding to DNA through specific protein-DNA interactions, one for recruiting or blocking RNA polymerase and interacting with further TFs. The modular nature of a TF enables the synthetic engineer to create designer TFs *de novo* by combining tailored DNA-binding and effector domains that execute either

activating or repressive function. Regarding the modifiability and adaptability of expression strength and specificity, the application of synthetic promoters and TFs provides a great advantage over their natural counterparts.

The two main classes of engineered, site-specific DNA-binding domains are the Cys2-His2 zinc finger domains and the transcription activator-like effector (TALE) DNA-binding domains. Due to the modifiability of their binding regions, these domains can be engineered to specifically "read" virtually any promoter sequence of choice.

A zinc finger-based TF usually employs a zinc finger protein domain to recognize a specific DNA sequence as well as an effector domain to recruit further factors for transcription initiation. A zinc finger domain consists of an array of finger domains and each finger domain recognizes an overlapping four bp sequence. That modular composition renders engineering of single finger domains for the recognition of specific three to four bp motifs possible (reviewed in [16]). The fusion of single finger domains to one artificial zinc finger domain allows the design of tailored zinc finger-TFs for the binding to custom promoter sequences. In 2012, Collins and coworkers demonstrated that a complete synthetic TF could be established based on the modulation hypothesis [17]. They combined an artificial zinc finger for DNA binding with a VP16 activator domain that regulates RNA polymerase recruitment and activity. A further protein-protein interaction domain was fused to the complex to allow the cooperative binding with adjacent TFs.

TALE-based TFs constitute another powerful tool to selectively regulate gene expression in mammalian cells [18]. TALE DNA-binding domains consist of multiple 34 amino acid repeats. Two polymorphic amino acids in position 12 and 13 of each repeat mediate the recognition of one specific DNA base [19]. The knowledge about the unique domain organization and the DNA-recognition mode of such a DNA-binding domain can be exploited to engineer custom TFs for custom DNA recognition. TFs with activating or repressive characteristics can be designed by coupling the TF with an RNA polymerase interacting element. Zhang *et al.* have developed an activator TALE-TF by combining a truncated TALE scaffold with a VP46 activation domain and have shown the successful induction of gene expression in mammals [20]. Custom TALE DNA-binding domains have also often been used for positive or negative transcription regulation in plants [21,22]. Mercer *et al*. developed a ligand-dependent TALE-TF by inserting one or more ligand receptors between the DNA-binding and the regulatory domain, thereby creating a switchable synthetic TF [22].

The dCas9-based TFs constitute a rather new class of artificial TFs that employ the catalytically inactivated CRISPR-Cas9 associated nuclease (dCas9) for the purpose of Clustered Regularly Interspaced Short Palindromic Repeats (CRISPR) RNA-guided DNA sequence recognition. The dCas9 protein has been fused to a VP64 activator domain and this hybrid protein has been co-expressed with a guide RNA (gRNA) for the formation of a DNA recognition complex. That complex has been shown to facilitate gene activation of specific endogenous human genes [23]. In contrast, Gilbert *et al*. have used a dCas9-repressor fusion protein for efficiently silencing transcription in eukaryotes [24]. The design of dCas9-TFs offers some advantages over the ZF- and TALE-based TFs. Since target DNA recognition is based on a sequence-specific gRNA, dCas9-based TFs are easier to design. However, due to the necessity of engineering the respective ZF or TALE motifs as well as the related promoters, the development of ZF- and TALE-based TFs is rather laborious. Furthermore, by

using one dCas9-TF interacting with various specific gRNAs one may be capable of building a circuit with many orthogonal parts regulating multiple target genes at once.

2.2.2 RNA-based control mechanisms

For regulating a complex eukaryotic system further specific natural mechanisms are necessary to define the amount of mature mRNA designated for translation. In contrast to prokaryotes, eukaryotes possess a precursor (pre-) mRNA processing system that represents a unique level of gene expression control. Whereas the addition of a 5'-cap structure and the process of splicing out the intronic regions of the pre-mRNA already occurs during transcription, the modification of the transcript with a 3' poly(A)-tail takes place post-transcriptionally in higher eukaryotes [25]. RNA editing is also a common process to vary RNA nucleotide identity [26]. This enzyme-based mechanism results in the chemical modification of RNA molecules and thereby extends the diversity of gene products. Altogether, these structural alterations strongly influence transcript stability, distribution in the cell`s compartments and the process of translation [27].

2.2.2.1 Small non-coding RNAs and their involvement in gene regulation

For a long time it has been assumed that mainly protein factors are relevant for gene regulation. In the meantime it became obvious that functional RNAs play a key role in determining differential gene expression and thus constitute another group of relevant *trans* regulators. Although the existence of non-coding (nc) RNAs has been known for many years, their meaning for the organism still has to be elucidated in large part [28]. Many of these ncRNAs are transcribed at very low level and no specific function has been attributed to them yet. Still, there is also increasing evidence that some of them are strongly involved in a multitude of cellular processes [29]. Due to their activity in gene expression regulation especially the small ncRNAs are of great interest. The 20-30 nucleotide long main representatives of this class have been categorized according to origin, function and associated effector proteins in Piwi-interacting (pi) RNAs, small interfering (si) RNAs and micro (mi) RNAs. These molecules are exclusively present in eukaryotes and constitute the key players of RNA interference (RNAi) [30]. RNAi is a biological mechanism that was first discovered in 1993 in *Caenorhabditis elegans*, when Ambros and coworkers found the miRNA lin-4 to be an active endogenous regulator of developmental genes [31]. The term "RNAi" was later defined by Mello and Conte [32]. Over the years, this mechanism has turned out to be present in a huge variety of eukaryotic organisms, namely plants, fungi and animals, where it leads to the targeted silencing of specific genes during development or serves as defense mechanism from invasive nucleic acids [33]. The small ncRNAs exhibit a common mode of action that is the specific binding of a ribonucleoprotein complex to its target gene (reviewed in [34]).

Within the group of small ncRNAs, piRNAs constitute the largest class (reviewed in [35]). The piRNAs exhibit a size between 26 to 31 nucleotides (nt) and form complexes with piwi-proteins that are involved in the post-transcriptional gene silencing of transposons to guard germline cells against transposable elements (reviewed in [36]).

Both, siRNAs and miRNAs, have a similar size of 20 to 25 nt (reviewed in[37]). Furthermore, siRNAs and miRNAs share that part of the processing machinery located in the cytoplasm during biogenesis. To perform their task as sequence-specific gene silencers, the siRNA as well as the miRNA have to be assembled in the RNA-induced silencing complex (RISC) [38]. The RISC is composed of an RNA and protein compounds. The incorporated small RNA serves as a guide for the RISC by base-pairing to the target gene. One of the protein components is a member of the AGO protein family and acts as a recruiting factor for effector molecules. After binding to their target region, siRNAs and miRNAs either cause degradation or translational repression, dependent on the extent of complementarity between RNA and target sequence (reviewed in[37]). Whereas the precursor of a piRNA is assumed to be present as a single-strand (ss), siRNAs and miRNA both originate from double-stranded (ds) precursors [30]. A huge difference is revealed in the character of their precursors. The siRNA precursors distinguish themselves from miRNA precursors through perfectly-matched duplex structures. In contrast, miRNA precursors exhibit mismatches in their helical stem structure as well as a more extended terminal loop. Furthermore, siRNAs may be endogenous, arise from virus infection or are derived from other exogenous sources. However, miRNAs are encoded as an individual species in the genome (reviewed in [30,34]).

2.2.2.1.1 A class of small ncRNAs: miRNAs

To date, there are 2500 miRNAs catalogued for humans (miRbase, release 21, http://mirbase.org/), but most of their targets and related functions still have to be elucidated. It is generally believed that miRNAs are involved in the regulation of about 60% of the protein-coding genes in humans [39]. The transcription of a miRNA precursor is usually performed by RNA polymerase II. The miRNA precursors are typically encoded by independent miRNA genes or located in introns and, to a much smaller extent, in exons of (non)-coding genes (reviewed in [40]). Some miRNAs are clustered in a polycistronic transcription unit and therefore co-transcribed [41]. In this case, individual regulation of the single miRNAs from one cluster occurs at the post-transcriptional level. In mammals, the miRNA target sequence is usually located in the 3' untranslated region (UTR) of the target mRNA and often present in multiple copies to intensify the regulatory effect (reviewed in [30]).

A typical, very promiscuous binding mode has been observed for miRNAs in mammals that enables one single miRNA to interact with multiple different target sequences. Perfect match binding within the miRNA-mRNA duplex structure occurs in the 5' region of the miRNA through the heptamerical "seed" region of the miRNA (Fig. 2.2) [42]. This "seed" region is the primary determinant of the binding specificity. The 3' region of the miRNA is characterized by a partial, more flexible base pairing to the target sequence and functions as a modulator of suppression [43,44].

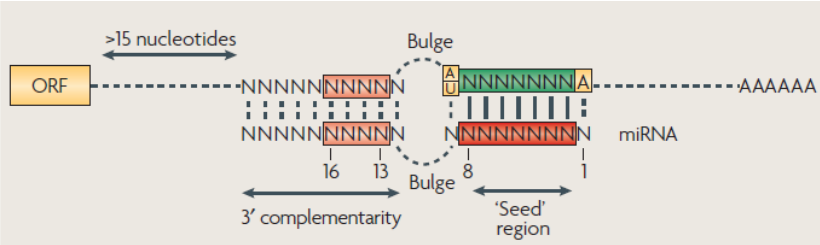

Figure 2.2 Typical miRNA-mRNA target interaction.
The "seed" region of the miRNA consists of nucleotides 2 to 8 and is essential for miRNA-mRNA binding. The conserved heptameric sequence exhibits perfect complementarity to the mRNA target sequence. An A residue at position 1 or an A or U residue at position 9 additionally support efficient binding, although base pairing with the miRNA is not mandatory. Usually a bulge or a mismatch region is present in the centre of the miRNA-mRNA duplex. The 3' region of the miRNA often shows imperfect binding to the mRNA. However, partial complementarity is a prerequisite for adequate duplex stability. **ORF** open reading frame (adopted from [40])

Once bound to its target, RISC either induces mRNA degradation or translational repression. Direct target mRNA degradation via Argonaute 2 cleavage is quite rare in mammals (reviewed in [45]). Most of the mRNAs seem to be degraded by the recruitment of further protein factors that in turn contribute to mRNA deadenylation and decapping [46,47]. Although being a highly controversial topic, there is evidence that translational repression as the primary event followed by mRNA degradation accounts for the main regulatory effect for miRNAs (reviewed in [48]). In order to facilitate an efficient translational repression, several target mRNAs exhibit multiple miRNA binding sites for either the same or a combination of different miRNAs (reviewed in [49]).

2.2.2.1.1.1 The miRNA processing machinery and regulation of miRNA biogenesis

Being aware of the distinct involvement of miRNAs in gene regulation, an association of miRNA dysregulation with various diseases becomes evident. This highlights the importance of a tight regulation and accuracy of miRNA biogenesis to ensure an adequate functionality of gene regulation. The process of miRNA biogenesis is depicted in Fig. 2.3.

The miRNA biogenesis starts with the transcription of the primary (pri-) miRNA from the respective miRNA gene in the nucleus. Due to the fact that usually RNA polymerase II is responsible for this step, pri-miRNAs are equipped with a cap structure at their 5' end and a poly(A) tail at the 3' end. The processing of the pri-miRNA requires the presence of the microprocessor complex consisting of the RNase III Drosha and the DiGeorge syndrome critical region 8 (DGCR8) [50]. The microprocessor facilitates the processing of the pri-miRNA to the precursor (pre-) miRNA. For substrate recognition as well as the correct positioning of the pri-miRNA for Drosha cleavage, a basal stem ss junction is a prerequisite as the pri-miRNA is cleaved at a position about 11 bp distant from aforesaid junction. Furthermore, the features of the apical junction significantly contribute to the precise cleavage of the pri-miRNA [51]. An accurate determination of the cleavage site by the involved RNase III is critical to prevent possible alterations in processing that could change abundance or miRNA target specificity. Besides the RNase III domains, Drosha harbors a double-stranded RNA binding domain which, however, is not sufficient for interacting with the substrate (Fig. 2.4). The presence of the RNA-binding protein DGCR8 is necessary to complement the complex with two additional double-stranded RNA binding domains (dsRBDs) (Fig. 2.4) [52]. Further factors that influence Drosha cleavage efficiency are

the loop size and the stem structure of the terminal loop region of the respective precursor as well as the sequence of the flanking areas around the Drosha cleavage sites [50,53]. The location of bulges within the pri-miRNA also significantly affects Drosha processing efficiency [54]. Before Dicer cleavage can occur in cytoplasm, the pre-miRNA has to be transported out of the nucleus with the help of exportin 5, a Ras-related nuclear protein (Ran)-GTP dependent transporter [55].

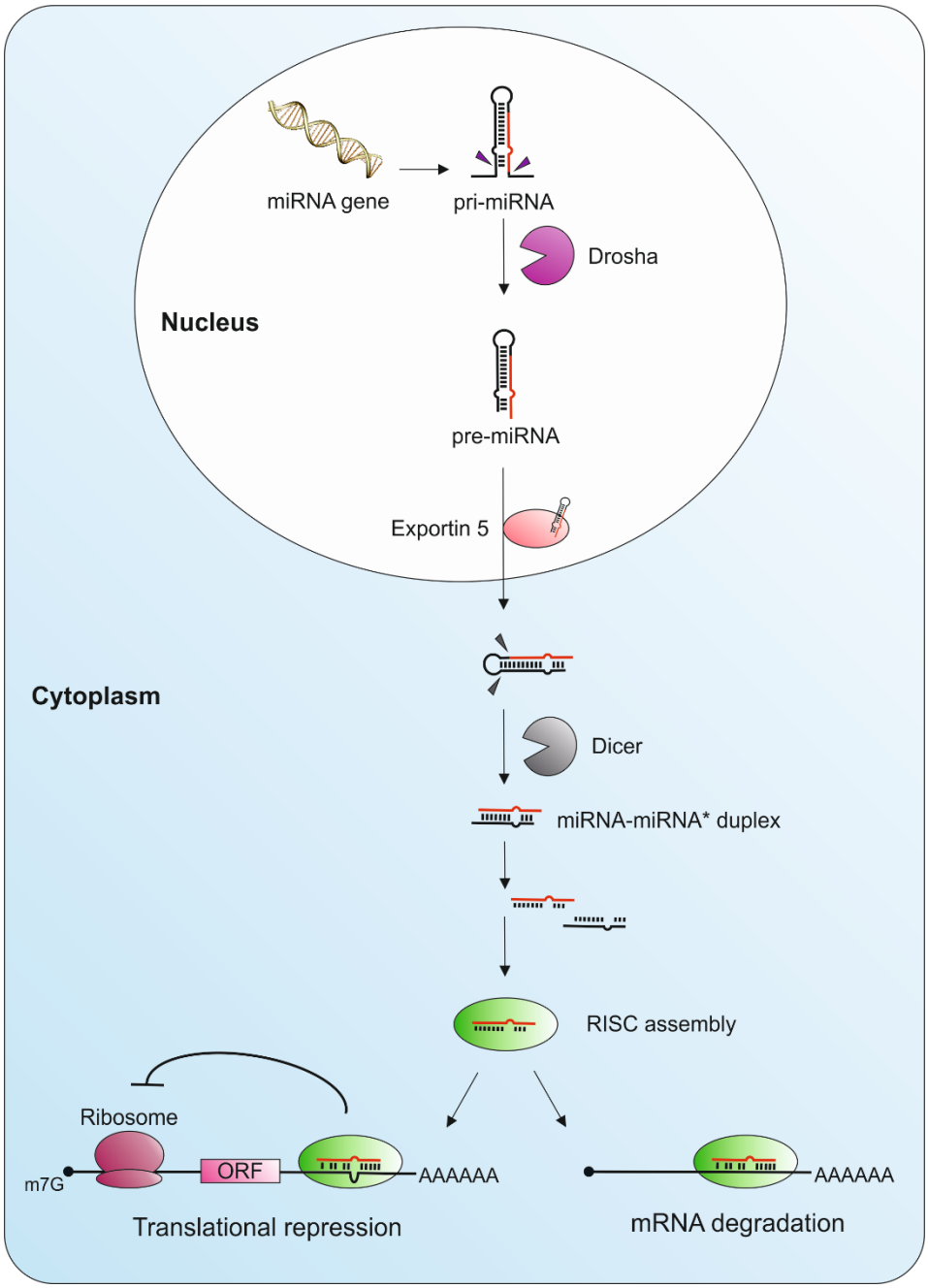

Figure 2.3 The process of miRNA biogenesis.
The first step in miRNA biogenesis is the transcription of the miRNA gene by RNA polymerase II. After transcription the primary miRNA (pri-miRNA) is processed by Drosha to a hairpin-like pre-miRNA with a 2nt 3' overhang. The pre-miRNA is exported from the nucleus to the cytoplasm via exportin 5 and cleaved by Dicer at defined positions (arrows) next to the terminal loop. The emerging miRNA-miRNA* duplex strand is then unwound and the guide strand (red) is integrated into the RISC which either triggers translational repression or mRNA degradation. **ORF** open reading frame, **m^{7}G** cap structure

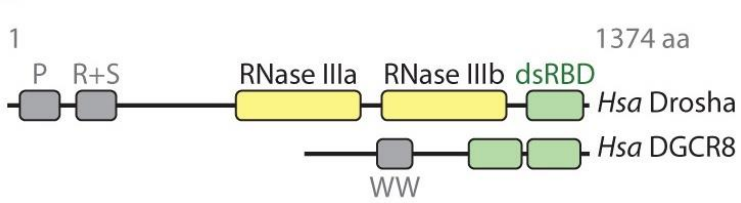

Figure 2.4 Schematic illustration of the structural organization of Drosha and DGCR8.
The domain structures of Drosha and DGCR8 are delineated. Drosha consists of two RNase III domains and a C-terminal dsRBD domain. DGCR8 shows two dsRBDs at its C terminus that significantly contribute to substrate binding and recognition. Furthermore, DGCR8s tryptophan-rich (WW) region is hypothesized to interact with the prolin-rich region (P) of the N terminus of Drosha. (adopted from [34])

Dicer is another RNase III enzyme that slices the pre-miRNA near the terminal loop to produce a miRNA:miRNA* duplex consisting of the guide miRNA and the passenger miRNA*. To pose an eligible Dicer substrate, the pre-miRNA is typically hairpin shaped and usually exhibits a 2 nt 3' terminal overhang as well as a 5' terminal phosphate group that are relevant for recognition by the PAZ (Piwi/Argonaute/Zwille) domain of Dicer [56,57] (Fig. 2.5). Figure 2.6 illustrates the typical composition of the human Dicer. In mammals as well as in flies, the PAZ domain features two binding pockets, one for the 3' hydroxyl end (3' counting rule) and the other for the 5' phosphate end (5' counting rule), and thereby defines the distance to the cleavage sites [58,59]. Thus, the region between PAZ domain and RNase III domain can be seen as a molecular ruler. In *Drosophila*, the helicase domain of Dicer-1 recognizes the single stranded terminal loop structure and facilitates pre-miRNA recognition [60]. So far, the exact function of the helicase domain of human Dicer has not been elucidated. Other structural features, such as the nature of the terminal loop (loop size, stem length) and the pre-miRNA sequence, are also of importance for recognition and accurate processing by Dicer [61,62]. Furthermore, Dicer contributes to RISC loading of the miRNA strand [63]. Therefore, the enzyme possesses two additional binding sites, one for associating with dsRBPs as the TAR-RNA binding protein (TRBP), the other for binding to an Argonaute (Ago) protein [64]. TRBP is supposed to be involved in modulating pre-miR processing efficiency, in the adjustment of the mature miRNA`s length as well as in transferring the dsRNA from Dicer to Ago for strand selection [65–67]. The Ago protein has the task to recognize the guide strand and to either cleave the target dependent on binding mode and Ago protein or to recruit other protein factors required for gene silencing (reviewed in [68]).

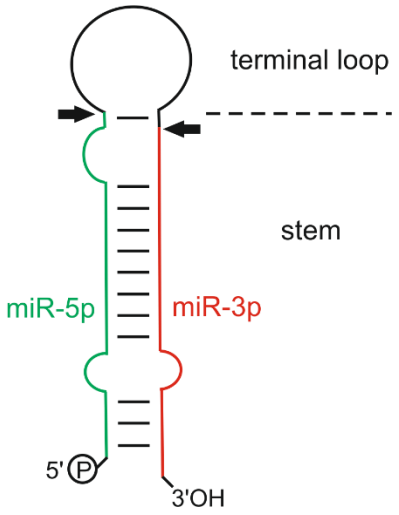

Figure 2.5 Schematic secondary structure of a pre-miRNA.
The typically hairpin-like structure of a pre-miRNA is depicted. The upper part of the pre-miRNA consists of the terminal loop, whereas the lower part is formed by a stem of incomplete complementarity. The 5' arm of the pre-miRNA harbors the miR-5p (green), the 3' arm the miR-3p (red). After being processed by Drosha the pre-miRNA features a 5' phosphate group (circled P) and a 2 nt 3' overhang. The arrows indicate the Dicer cleavage sites.

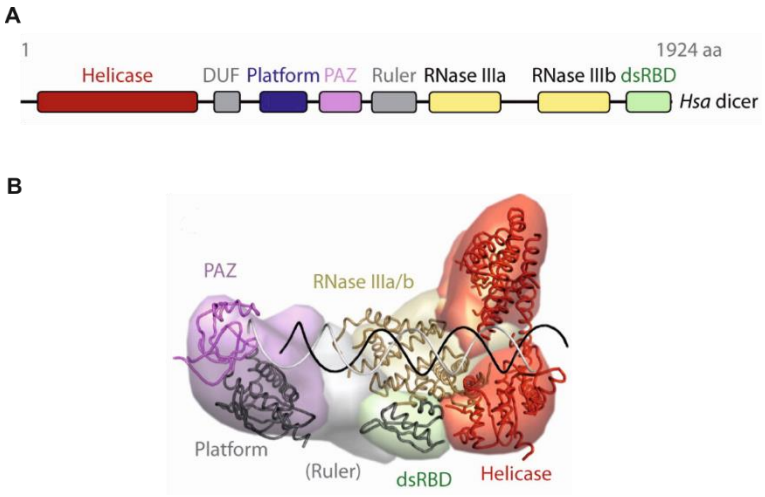

Figure 2.6 (A) Domain structures of human Dicer. Depicted are the C-terminal dsRBD, the two RNase III domains and the PAZ domain responsible for the recognition of the pre-miRNA ends. In between the PAZ and RNase III domain, the anticipated ruler is located. Furthermore, a domain of unknown function (DUF) and a platform domain are depicted. The N-terminal helicase domain with over 600 amino acids constitutes the largest domain of Dicer. **(B) Global architecture of human Dicer.** The helicase domain (red) is shaped like a clamp and oriented in a suited position to navigate the incoming dsRNA substrate (black and grey coil) to the RNase active centre and the PAZ domain. The PAZ domain is reoriented to the catalytically active centre. The ruler is located between the PAZ domain and the RNases III. (adopted from [69] and modified)

After Dicer cleavage the originated duplex structure miRNA:miRNA* is unwound by a helicase and, dependent on the thermodynamic stability of the respective 5' end of the duplex, the guide strand (miRNA) is loaded onto the RISC to perform RNAi whereas the passenger strand (miRNA*) is degraded [70,71]. For tightly regulating miRNA biogenesis, a control system similar to that of protein-coding genes has evolved. This system is of the utmost importance for a precise spatiotemporal miRNA expression and comprises various modes of action. As such, several miRNAs are able to regulate their own transcription in an autoregulatory feedback-loop mechanism by binding to their

transcription factors [72]. There are also numerous paths to control the processing to mature miRNA operating through the regulation of protein factors that participate in biogenesis itself or bind to the respective miRNA precursor thereby preventing processing [73]. A well-characterized example for a protein-precursor miRNA interaction in the terminal loop region is the LIN-28-let-7 system that regulates access of both Drosha and Dicer to the two precursors pri-/ pre-let-7 [74]. RNA editing as well as methylation of the miRNA precursor also turned out to negatively influence pri-/ pre-miRNA processing by Drosha and Dicer due to poor substrate recognition [75].

2.2.2.1.1.2 A selection of clinically relevant miRNAs: miR-34a, -92a, -101, -126 and -199a

Due to their participation in the regulation of a multitude of target genes, miRNAs are involved in controlling lots of different processes in the organism. Altered miRNA expression is often found to be associated with disease development and there is strong evidence for a connection between miRNAs and oncogenesis, metastasis and resistance in cancer (reviewed in [76]). Dependent on their role in cancer, miRNAs can be further classified as oncogenes or tumor-suppressor genes. Since miRNAs often have a causal connection with disease development and due to their tissue specificity, they also present themselves as ideal candidates for biomarker-related early diagnosis and treatment [77,78]. Due to the identification of thousands of miRNAs across different species, a systematic nomenclature has been established. The numbering of newly identified miRNAs is sequential and the connection between structurally related miRNAs is indicated with lower case letters. Dependent on their origin, miRNAs derived from the 5' or 3' end are denoted with a "-5p" or "-3p" suffix. Considering their abundance after processing, the miRNAs derived from one precursor are referred to as miR-x for the main miRNA and miR-x* for the less abundant one.

Five miRNAs have been chosen for investigation in this work because of their relevance in the emergence of frequently occurring diseases. One of these miRNAs is miRNA-34a that belongs to the highly conserved miRNA-34 family and has been shown to be a master regulator of tumor suppression [79]. It has been observed that the overexpression of miR-34a repressed several oncogenes and led to an increase of cell apoptosis as well as an inhibition of metastasis. Generally, miRNA-34a is ubiquitous in all tissues, but the highest level of expression is detectable in ovary, testes and prostate (reviewed in [80]). An ectopic expression induces either cell cycle arrest or apoptosis and its dysregulation is strongly associated with cancer progression in numerous cell types [81,82]. The transcription factor p53 has been proven to regulate the expression of the miRNA-34 family. It has been asserted that most targets of miRNA-34a are related to the p53 pathway. *SIRT1* turned out to be a target of miRNA-34a and thus p53 dependent apoptosis is controlled through acetylation and activaton of p53 in a positive feedback loop [83,84]. Another relevant target of miR-34a-5p is the proto-oncogene receptor tyrosine kinase mRNA *MET*. The MET protein is associated with tumor cell migration and invasion and its expression was shown to be downregulated by miRNA-34a. In hepatocellular carcinoma (HCC), an inverse correlation between miR-34a and MET expression has been observed suggesting a function of miR-34a in the MET signaling pathway [85]. On top of that a direct relationship between the E2F pathway and miR-34a has been found. The overexpression of miR-34a led to an immense downregulation of the E2F pathway and to an up-regulation of the p53

pathway activity. Through a direct interaction with *E2F3*, miRNA-34a seems to function as a potent suppressor of cell proliferation [86].

MiRNA-92a belongs to the miRNA-17~92 family and arises from the miR-17/92 cluster. This cluster is composed of three highly conserved, polycistronic genes that encode for 15 miRNAs that are essential for development and homeostasis [87]. MiRNA-92a is expressed in the majority of cells and in human blood plasma [88]. It has been demonstrated that miRNA contributes to tumorigenesis via regulating tumor proliferation, apoptosis as well as tumor invasion and metastasis [89]. Integrin α-5 expression was shown to be directly regulated through miR-92a. The expression of miR-92a resulted in a downregulation of Integrin α-5 expression in ovarian cancer cells resulting in the inhibition of cell adhesion, invasion and proliferation [90]. Furthermore, miR-92a regulates the expression of the tropomyosin receptor kinase. The miRNA was shown to downregulate protein expression and thereby to promote proliferation and migration of human neuroblastoma cells [91]. Furthermore, miRNA-92a regulates angiogenesis and viability of endothelial cells under oxidative stress [92].

MiRNA-101 acts as a tumor suppressor in various cancer types. It belongs to a family of miRNAs that is involved in a series of cellular activities such as proliferation, cell invasion and angiogenesis. MiRNA-101 was often shown to be downregulated in prostate cancer, hepatocellular carcinomas and bladder cancers [93–95]. This miRNA suppresses the proliferation of breast cancer cells by directing cell apoptosis and cell cycle arrest through the regulation of the expression of Von-Hippel-Lindau tumor suppressor, a negative regulator of the hypoxia-induced factor 1α [96]. In cervical cancer cells, miRNA-101 has been linked to the regulation of viability and invasion through affecting cyclooxigenase-2 expression [97].

Another miRNA with a distinct link to disease development is miRNA-126. MiRNA-126 is highly abundant in endothelial cells and hematopoietic stem cells [98]. The miRNA-126 host gene is *EGFL7* which leads to transcription of both the miRNA and the *EGFL7* transcript at the same time. In turn, this transcription is regulated by a negative feedback loop due to the presence of a miRNA-126 binding site in the host gene transcript itself [99]. EGFL7 is a key factor in cell migration pathways and also associated with the process of angiogenesis [100]. Being implicated in processes like inflammation and angiogenesis, this miRNA plays a role in the development of a multitude of cancer types (reviewed in [101,102]). With regard to this, vascular cell adhesion molecule 1 (VCAM1) expression is controlled through miRNA-126 [103]. By inhibiting the VCAM1 expression in endothelial cells, adhesion and infiltration of leukocytes into the vasculature wall is hampered and inflammation is interrupted. *SPRED1* encoding for the sprout-related, EVH1 domain-containing protein-1 (SPRED1) constitutes a further target of miRNA-126 that has been shown to regulate vascular integrity and angiogenesis [104].

An interesting miRNA with numerous links to different diseases is miR-199a. MiRNA-199a shows a strong correlation with the development of chronic obstructive pulmonary disease (COPD) due to its regulation of HIF-1α [105]. Also the participation in various cancer types via either up- or down regulation dependent on the specific tissue is known (reviewed in [106]). There are results that indicate that miR-199a-5p functions via inhibition of cell proliferation and induction of cell death [107–109]. Furthermore, the expression of the mothers against decapentaplegic homolog 4 (SMAD4) protein has also been shown to be directly regulated through miRNA-199a. The overexpression of miRNA-199a resulted in the downregulation of SMAD4 protein expression thereby demonstrating a regulatory effect on the TGF-β

signaling pathway [110]. The discoidin domain receptor 1 (DDR1) affects human hepatocellular carcinoma invasion and its expression was demonstrated to depend on the presence of miR-199a-5p [111]. A strong correlation between caveolin-1 (CAV1) and miR-199a-5p expression has also been found [112]. MiR-199a-3p is also involved in disease development, as well. MiRNA-199a-3p was shown to regulate cell proliferation and survival by affecting caveolin-2 (CAV2) expression [113]. Besides *CAV2*, *MET* and the transcript encoding for the cell-surface glycoprotein CD44 constitute validated targets of miRNA-199a-3p [114,115].

The above mentioned functions of the miRNAs are merely a small excerpt of the huge repertoire of functions. However, most of their roles in the regulation of cellular processes are not known today and still have to be elucidated. To extend the existing knowledge on these molecules and their respective function, the repertoire of existing methods and tools has to be adapted to the features of the research objectives. Therefore, the synthetic biology poses a promising field of research that extensively employs artificially built systems for the purpose of investigating and controlling cellular processes.

2.2.2.2 Synthetic riboswitches as post-transcriptional control elements

Scientists from the field of synthetic biology have been inspired by the fact that nature extensively utilizes RNA to regulate gene expression through various mechanisms. Basically, RNA molecules consist of four bases and interact with their surroundings via a combination of intra- and intermolecular interactions. For the formation of a highly selective binding pocket of a RNA-based switch merely four types of monomers are available. Nonetheless, the resulting interactions between ligand and binding domain are suited to warrant highly precise and efficient gene regulation. For this reason, ribonucleic acids with their structural and functional diversity are predestinated to serve as basic building blocks for the development of engineered regulatory systems.

A specific regulatory RNA-based mechanism to execute control over gene expression was first discovered by Breaker and coworkers when they found a flavin mononucleotide (FMN) binding riboswitch in the 5'UTR of a prokaryotic mRNA [116]. Upon direct binding of the metabolite FMN, the premature termination of transcription is triggered to regulate genes participating in biosynthesis and transport of FMN. Riboswitches are defined as autonomous, *cis*-acting RNA elements consisting of a ligand sensing aptamer domain and an expression platform that undergoes a conformational change as a consequence to ligand binding [117]. The switching event between two mutually exclusive structures enables the expression platform to directly intervene with gene expression. Riboswitches have been found to be encoded in the genome of fungi, plants, archea and bacteria [118].
Due to their modular characteristic, synthetic riboswitches can be designed *de novo* in analog to their natural counterparts by combining RNA-based sensing modules and versatile regulatory domains. For that purpose, RNA aptamers are highly suitable components for the application as sensing modules.

2.2.2.2.1 RNA aptamers and their application in conditional gene expression

The term RNA aptamer refers to an oligonucleotide-based structure that is capable of binding a ligand with high affinity and specificity. Besides aptamers consisting of RNA, also DNA and peptide aptamers

can be developed to specifically bind to molecules with their 3D structure. In a process named systematic evolution of ligands by exponential enrichment (SELEX), aptamers against a variety of components like organic compounds, proteins, oligonucleotides as well as whole cells can be created [119,120] (reviewed in [121]). With regard to size, production, immunogenicity, thermodynamic stability and due to their structural versatility, RNA aptamers show significant advantages over their functional protein-based counterparts, the antibodies (reviewed in [122]). Besides their applicability as a sensing unit for building synthetic riboswitches, aptamers can also be applied for therapeutic and diagnostic purposes or as biosensors (reviewed in [122]) [123]. To be classified as a riboswitch, an RNA structure has to possess essential features such as high affinity binding to a ligand, undergoing a conformational change in response to ligand binding and fast ligand association kinetic. Aptamers sometimes feature riboswitching activity and can therefore be used for interference with gene expression without employing further regulatory elements. In 1998, Werstuck and Green showed for the first time that the insertion of aptamers into a 5'UTR of an mRNA actually leads to translational repression upon ligand binding [124]. Indeed, merely a small percentage of the presently selected aptamers show this behavior because the SELEX approach is focused on finding high affinity binders to the respective target. The combination of *in vitro* and *in vivo* selection methods in one approach is by far more constructive to obtain aptamers with adequate switching capability (reviewed in [125]). The neomycin aptamer as well as the tetracycline aptamer are two examples of aptamers that can be employed to confer control over translation in yeast [126,127]. Upon binding the respective ligand, a structural rearrangement resulting in the stabilization of the aptamer structure occurs in the 5'UTR which, in turn, inhibits binding or scanning of a ribosomal subunit to the mRNA (Fig. 2.7 A). Besides manipulating translation initiation, other mechanisms have also been exploited to control gene expression. Dependent on ligand presence, the positioning of an aptamer in proximity to recognition sequences relevant to the splicing machinery leads to the impairment of pre-mRNA splicing (Fig. 2.7 B) [128]. RNAi can also be controlled by replacing the terminal loop of a small hairpin (sh) RNA with an aptamer (Fig. 2.7 C)[129]. Demonstrating the variability of applications for riboswitches, Wang and White used the theophylline aptamer to regulate virus replication (Fig. 2.7 D) [130].

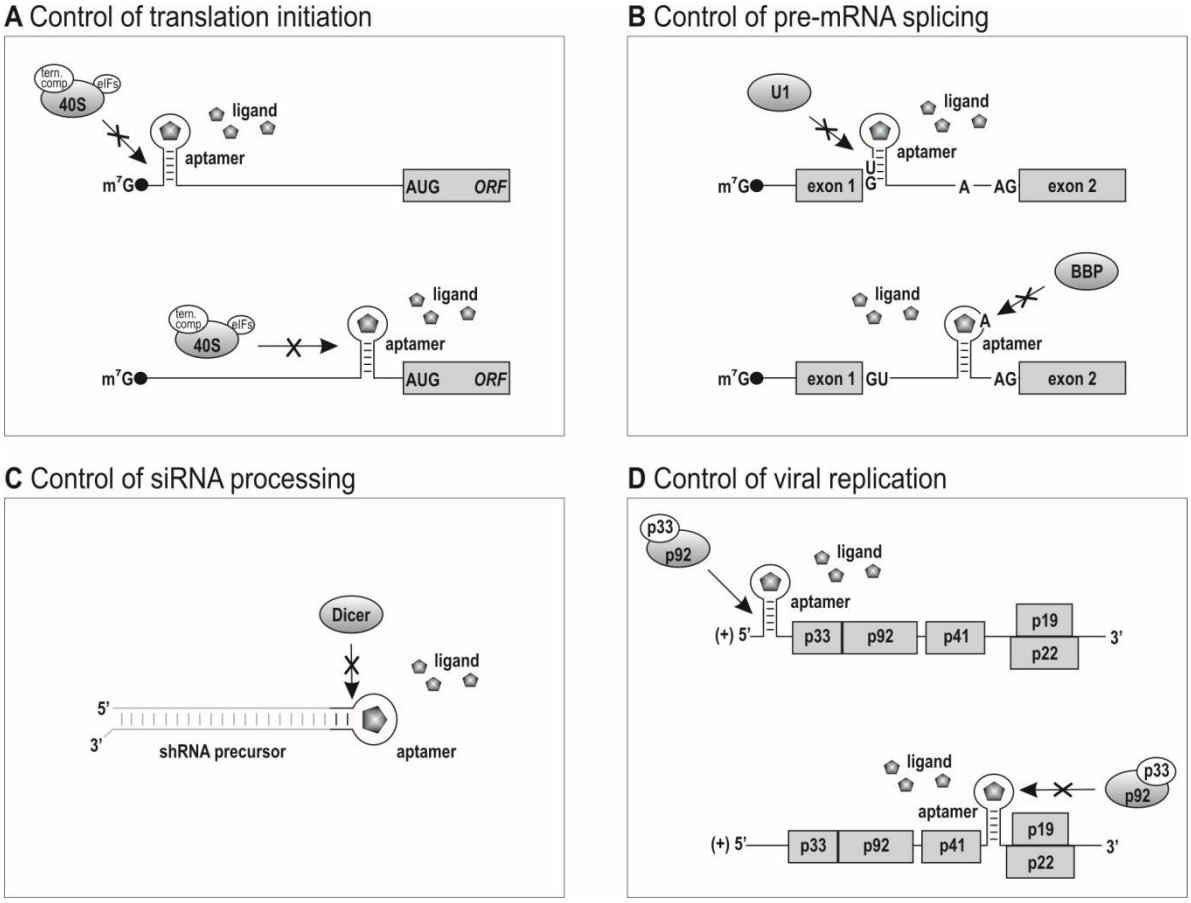

Figure 2.7 Mechanisms of gene expression control with synthetic riboswitches.
(A) Control of translation initiation. The aptamer is positioned either in proximity to the m^7G cap or to the start codon AUG. In the presence of the ligand a stable secondary structure is formed that either interrupts binding of the small ribosomal unit to the mRNA (upper part) or alternatively the scanning process (lower part). **(B) Control of pre-mRNA splicing**. The sequestration of a recognition site of the splicing machinery through the introduction of an aptamer interrupts pre-mRNA splicing. **(C) Control of siRNA processing.** The structural modification of an shRNA by replacing the terminal loop with an aptamer sequence can affect Dicer processing by blocking the cleavage sites through the conformational change of the aptamer. **(D) Control of viral replication.** The replacement of an endogenous signal structure in the 5'UTR of an mRNA with an aptamer leads to a malfunction of structure recognition of the virus replication machinery which disturbs viral replication.
(adopted from [131])

In bacteria, synthetic riboswitches can also be utilized to gain control over translational initiation. By positioning an aptamer in a way, that sequesters the Shine-Dalgarno (SD) sequence, it is possible to regulate the accessibility of the 30S ribosome subunit to its binding sequence (Fig. 2.8 A) [132]. Another approach employs a slippage element for removing the theophylline aptamer that functions as a steric hindrance for ribosome binding to the SD sequence upon ligand binding (Fig. 2.8 B) [133].

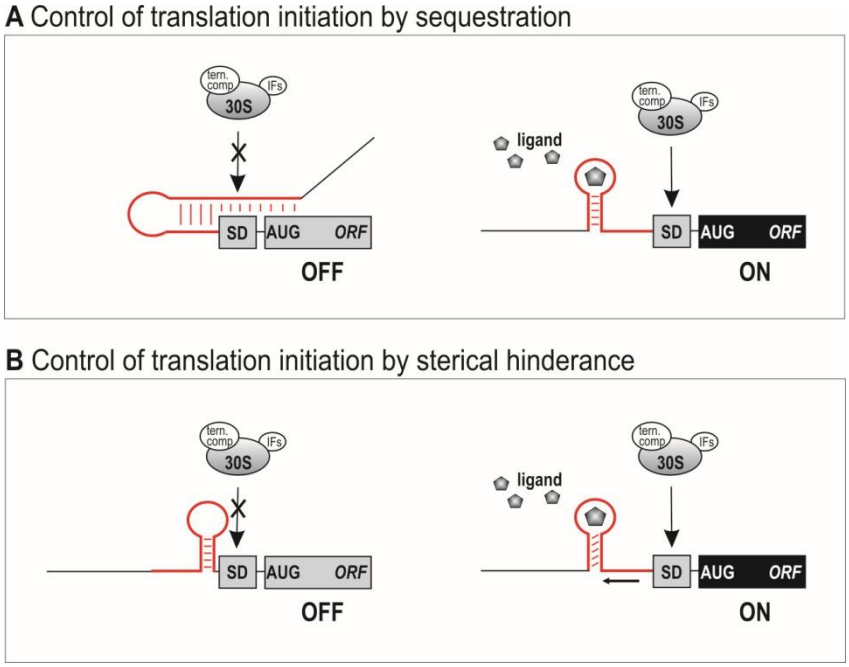

Figure 2.8 Mechanisms of gene expression control in bacteria.
(A) Control of translational initiation by sequestration. The incorporation of both the SD sequence and the start codon into a secondary structure interferes with the binding of the small ribosomal subunit to the mRNA. This sequestration can be eliminated through ligand binding to the aptamer that leads to a conformational change and thus the release of the recognition elements. **(B) Control of translation initiation by steric hindrance.** Positioning a stable aptamer structure next to the SD sequence can result in an impairment of binding of the ribosomal subunit. Through ligand binding the steric hindrance can be removed from the recognition sequence thereby granting access to the SD sequence. (adopted from [131])

The coupling of an aptamer to various expression platforms is possible to create versatile genetic manipulation devices. With a connection module that communicates ligand binding to an expression platform, an allosterically controllable ribozyme can be created by fusing an aptamer to a self-cleaving ribozyme, thus providing another RNA-based tool for gene expression regulation (reviewed in [134]). Besides small-molecule binding systems, approaches employing protein-binding motifs and aptamers for the creation of protein-driven switches were established. Their high potential for the conditional regulation of cellular pathways was demonstrated by the Saito group that developed a protein-responsive shRNA [135].

2.2.2.2.1 The tetracycline (tc) repressor (TetR) and the TetR-binding aptamer

In a combined approach of an *in vitro* screening for TetR-binding sequences and an *in vivo* screening for TetR-related induction of gene expression, the TetR aptamer was originally identified as an aptamer that is able to induce transcription in *E. coli* [136]. The aptamer binding ligand is the TetR which is a 46.6 kDa homodimeric transcription factor of bacterial origin and belongs to the Tet/Cam family of regulators [137]. Naturally, TetR exerts control over the expression of the *Tn10* encoded tc resistance in gram-negative bacteria and equips the organism with the ability to actively export the antibiotic tc from the cell (reviewed in [138]). In the absence of tc, TetR occupies the operator *tetO* and prevents the transcription of *tetA* that encodes for the tc antiporter. The presence of tc results in binding of a $[tc \cdot Mg]^+$ complex to the TetR binding pocket located in the core region and induces a conformational

change in the homodimer. This conformational change is accompanied by the reorientation of the DNA reading heads that are directly connected to the protein binding core [139]. The rearrangement leads to dissociation of TetR from the operator sequence and enables the expression of the resistance conferring transport protein [140].

Tc-dependent regulation is an often used mechanism to control gene expression in a variety of organisms since the TetR system provides a high binding affinity and specificity as well as good pharmacokinetic properties [141,142]. The small molecules tc and doxycycline (dox), which is an analog of tetracycline (Fig. 2.9), are often applied in combination with the TetR system. With $10^9\ M^{-1}$ and $10^{10}\ M^{-1}$ respectively, they exhibit very high affinities to TetR [140]. The binding of two molecules of $[tc{\cdot}Mg]^+$ to each TetR monomer (Fig. 2.10) reduces the affinity of TetR to the operator by nine orders of magnitude [140]. This characteristic and the good permeability of the compounds facilitate the use of very low amounts of tc and dox in experiments, thereby preventing an effect on other cellular processes. Another advantage of the original system is its modularity and the concomitant potential to fuse TetR to eukaryotic regulation domains [143].

Nowadays, the TetR system is often used for regulation of gene expression in eukaryotes. The first published application of this system in eukaryotes using the features of the unmodified TetR showed the regulation of transcription by employing TetR as a steric roadblock for RNA polymerase binding [144]. Furthermore, the Tet-Off and the Tet-On system have been established through the modification of TetR and its binding mode. For the Tet-Off system, the tc-controlled transactivator (tTA) hybrid protein was built by fusing a VP16 activator domain to TetR. Applied in combination with the Tet operator placed upstream of a promoter, the stimulation of an ensuing gene can be accomplished. Upon the addition of tc or dox to the system, tTA dissociates from the operator and gene expression is abolished. In contrast, the Tet-On system employs a VP16 activator domain coupled with the reverse TetR (rtTA) that has been created through a point mutation within the protein. In that case, the modified TetR binds to the operator sequence in presence of tc and induces gene expression [145,146].

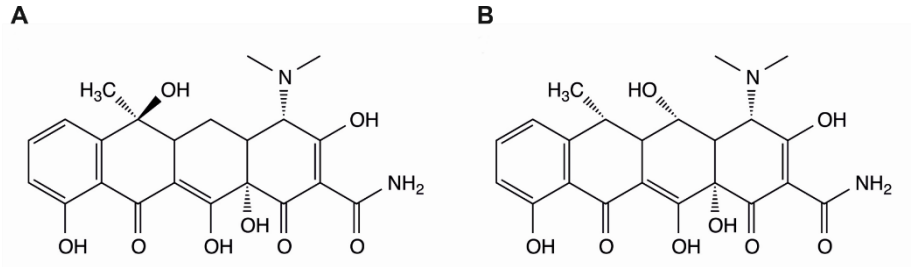

Figure 2.9 Molecular structures of **(A) tc** and (**B) dox.**

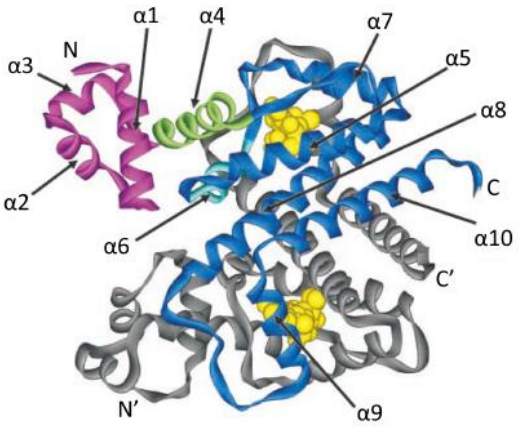

Figure 2.10 Crystal structure of the TetR-[tc·Mg]$^{+}_{2}$ complex.
The TetR homodimer is illustrated as a ribbon with one monomer in grey and the other monomer substructured by utilizing the following color code: the DNA binding helix is highlighted in magenta. The connecting helix α4 that is located between the DNA binding helix and the protein core is displayed in green. The protein core is shown in blue and tc depicted as space-filling model in yellow. (adopted from [140])

The discovery of the TetR aptamer creates new opportunities to apply the TetR system. Comparable to the original TetR system, binding of tc to TetR results in the dissociation of TetR from the aptamer. It has been demonstrated that the achievable *in vivo* activity of the RNA-based system is comparable to that of the original inducer tc [136]. The aptamer folds into a stem loop structure harboring a highly conserved internal loop structure that was shown to constitute the ligand binding site (Fig. 2.11 A). The thermodynamic stability of the stem and the terminal loop structure are of the utmost importance because they were shown to directly affect the induction efficiency and therefore the functionality of the aptamer [136]. Suess and coworkers shed light on the mechanistic basis of the TetR aptamer-based induction and revealed that the aptamer interacts with amino acids from both monomers of the TetR homodimer by binding to the DNA reading heads (Fig. 2.11 B) [147]. This observation is strongly linked to another finding, namely the capability of the aptamer to actively compete with the operator for TetR binding. Besides the observed competition, the active displacement of the operator by the TetR aptamer was determined in further experiments[147]. A prerequisite for this feature is that *tetO* and the aptamer possess similar binding affinities for TetR, as demonstrated by Steber *et al.* [147]. The detailed characterization and the special features of the TetR aptamer system render it a well suited component for its employment in the synthetic biology.

The universal applicability as well as the genetic modularity of the TetR aptamer in different organisms have already been confirmed in various experimental approaches. Demonstrating the functional independence of the system from the organism, Niles and coworkers illustrated the portability of the *E.coli* derived TetR aptamer system to the protozoon *Plasmodium falciparum* and also to the lower eukaryote *S. cerevisiae* [148,149]. With their ligand-dependent intramer, Fussenegger and coworkers added an additional layer of regulation to the TetR aptamer based system and designed a small-molecule responsive switch functional in mammals [150].

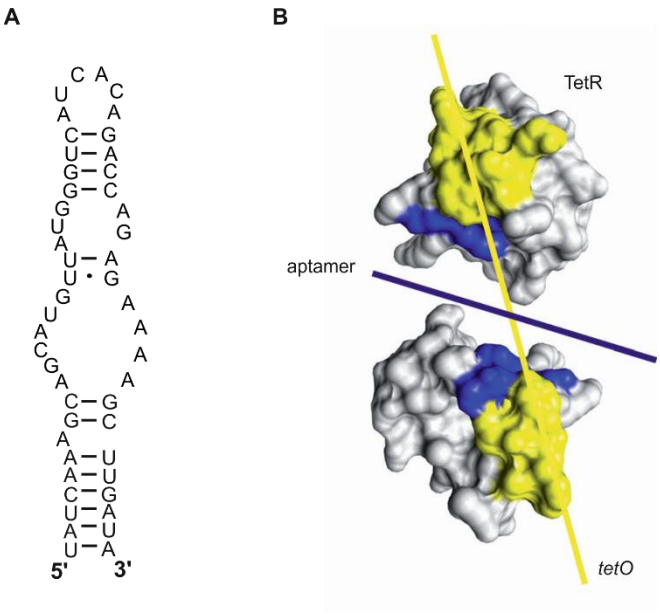

Figure 2.11 (A) Secondary structure of the TetR aptamer. The aptamer is predicted to fold into a stem loop structure. The internal loop is responsible for ligand binding, whereas the surrounding structural elements stabilize the binding structure. **(B) Illustration of the TetR-aptamer interaction.** The DNA binding site, recognition helix α3 of TetR (yellow) and the aptamer recognition epitope (blue) are illustrated. (partly adopted from [147] and modified)

2.3 Scope of the study

Due to the variety of synthetic building blocks and devices as well as a continuously growing knowledge about biological systems, the opportunities to genetically manipulate an organism are seemingly infinite. In the last years, several studies have focused on the significance of small ncRNAs for eukaryotic gene regulation and revealed their important role for various biologically relevant processes (reviewed in [151]). To deepen the knowledge about these molecules and their respective function, the repertoire of existing methods and tools has to be adapted to the features of the research objectives.

One very promising and simultaneously complex target for synthetic engineering represents RNAi with miRNAs as the key components of the mechanism. The direct involvement of miRNAs in the regulation of gene expression offers the possibility to control the expression of specific target genes by affecting miRNA abundance. MiRNA abundance, in turn, is dependent on a magnitude of factors. A relevant process determining miRNA levels is the regulation of miRNA biogenesis, which therefore poses an attractive interference point for manipulation.

Thus, the scope of this study was the design and implementation of an RNA-based device to create a switchable unit, consisting of a synthetic aptamer component functioning as a ligand sensing module coupled to a natural miRNA precursor structure, to enable ligand-controlled miRNA abundance. In order to control pre-miRNA processing in a ligand-dependent fashion, the TetR aptamer should be connected to the miRNA precursor, intending to directly control the access of Dicer to its cleavage sites by the presence of the ligand. Concerning the special interest in miRNA function and its involvement in pathogenesis, a specific and transferable design for regulating the biogenesis of various miRNAs was sought to be established to provide a useful tool for the investigation of cellular malfunctions caused by different miRNAs. To prove the functionality, applicability and robustness of the designed pre-miR switches, their ligand-dependent regulatory activity should be demonstrated at the protein level.

3 Results

3.1 Design and functionality of a reversible pre-miR switch

Accounting for the strong correlation between miRNA dysregulation and human disease, the development of a specific device to regulate miRNA levels in a ligand-dependent way provides a useful tool for investigating the impact of specific miRNAs on cellular malfunction. One approach to systematically control miRNA levels is constituted by the direct interference with the processing machinery. Although miRNA precursors display high structural variability like different extents of stem complementarity and varying loop size, most of these precursors are recognized by the same miRNA processing machinery. Thus, the processing machinery seems to feature a certain structural tolerance with regard to substrate recognition that can be exploited for the modification of a precursor molecule. Due to the current knowledge about substrate recognition features and specific cleavage positions of Dicer, a pre-miRNA molecule can be modified to allow the controlled and directed processing to a specific miRNA. Such an adjustable precursor tool could be realized by the integration of a regulatory synthetic component into the natural precursor structure.

In this study, the TetR aptamer was chosen as a regulatory sensor domain for the development of a pre-miR switch to conditionally control miRNA maturation [136]. The application of this TetR-based system provides several advantages over other small molecule- and protein-based systems. TetR is bound as a homodimer of 46.6 kDa to the aptamer and thus functions as a sterically demanding protein ligand that is theoretically eligible to block the binding of Dicer or other cofactors to the processing sites [137,147]. Since one characteristic of the TetR-based system is reversibility, TetR and its aptamer constitute an ideal basis for the design of a reversible pre-miR switch. Additionally, the supplementation with a low concentration of dox is sufficient to efficiently relieve TetR from the aptamer. Furthermore, as TetR originates from bacteria, it is not endogenously expressed in mammals and therefore well suited to be applied as a regulatory protein. Two critical aspects had to be considered for the design with respect to the sensor domain. (i) TetR aptamer functionality turned out to be strongly dependent on the stability of its closing stem, whereas the exact nucleotide identity was negligible [136]. (ii) For the purpose of directly regulating miRNA processing through ligand presence, the aptamer had to be introduced in direct proximity to the cleavage sites of Dicer.

Besides, an appropriate communication module had to be established to connect the two inherently different parts, the aptamer and the miRNA precursor, to a functional unit. This module was sought to be designed in order to retain pre-miRNA processing and contemporaneously to enable efficient control over pre-miRNA cleavage. Therefore, the optimal distance between the ligand binding site and the cleavage sites had to be determined to satisfy both requirements. Figure 3.1 schematically illustrates the proposed mechanism of the TetR-controlled regulation of pre-miRNA processing. In the absence of TetR the Dicer processing sites are supposed to be readily accessible for the processing machinery and the precursor is converted into mature miRNA. In contrast, the expression of TetR followed by binding to the aptamer theoretically leads to a blockage of the processing sites and inhibits processing of the pre-miRNA. The addition of dox reverses the maturation stop as the inducer

molecule binds to TetR and induces a conformational change that relieves the pre-miRNA from the steric hindrance and the precursor is processed to mature miRNA, again.

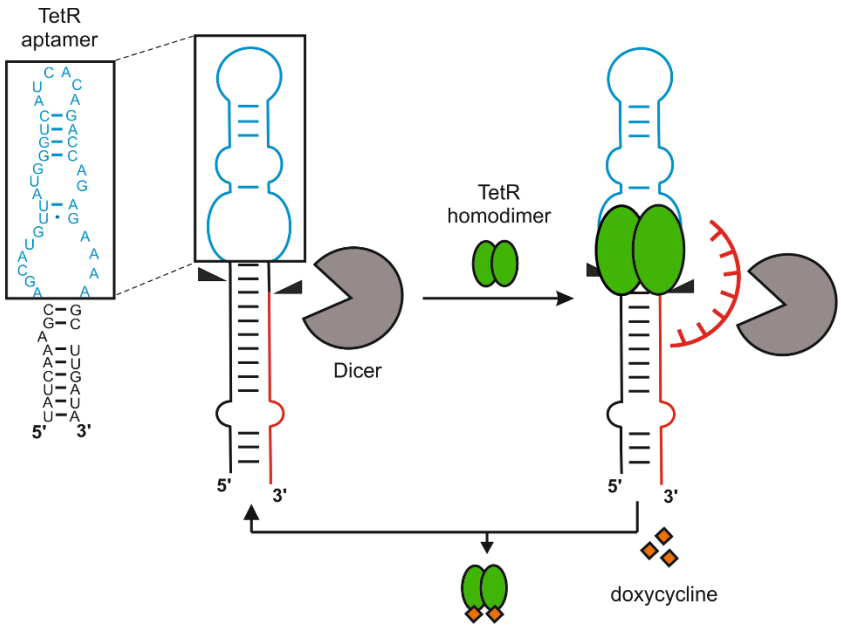

Figure 3.1 TetR aptamer dependent regulation of Dicer processing. As the sensor domain of the pre-miR switch, the TetR aptamer replaces the terminal loop region. In the absence of the TetR homodimer, Dicer cleaves the pre-miRNA at the indicated processing sites (arrows) leading to the emergence of mature miRNA. Upon expression of the protein, the TetR homodimer binds to the aptamer and blocks the cleavage sites. This in turn results in an impairment of Dicer cleavage. The addition of dox to the medium causes the dissociation of TetR from the aptamer leading to an unblocking of the processing sites. Thus, the pre-miRNA can be processed to mature miRNA, again.

The first pre-miR switches miR-126_NL, _2, _5 and _5l were designed based on the natural miR-126 precursor (Fig. 3.2 A). The aptamer was inserted into the miRNA precursor, replacing the natural terminal loop. To find an appropriate communication module, stem length and flexibility in the shared region between the aptamer and the precursor were varied. For the design of construct miR-126_NL the lower part of the natural terminal loop structure was retained in the transition area to mimic the precursor structure as close as possible. An additional C-G bp was attached to the natural structure to connect the aptamer to the precursor to further stabilize the aptamer closing stem. For a stepwise increase of stem stability the constructs miR-126_2, _5 and _5l were designed. Construct miR-126_2 was built with a shortened transition region to decrease the distance between the Dicer cleavage sites and the TetR binding site and nearly complete strand complementarity with the exception of one mismatched bp. For the generation of miRNA-126_5 stem stability was further enhanced, as the transition area displayed complete base pairing. The communication module was shortened by two bp to decrease the distance of the TetR binding site to the Dicer cleavage sites. Construct miR-126_5l represented the elongated form of miR-126_5 and was designed to further explore the influence of the proximity of the TetR binding site and the Dicer cleavage sites on the inhibitory capacity.

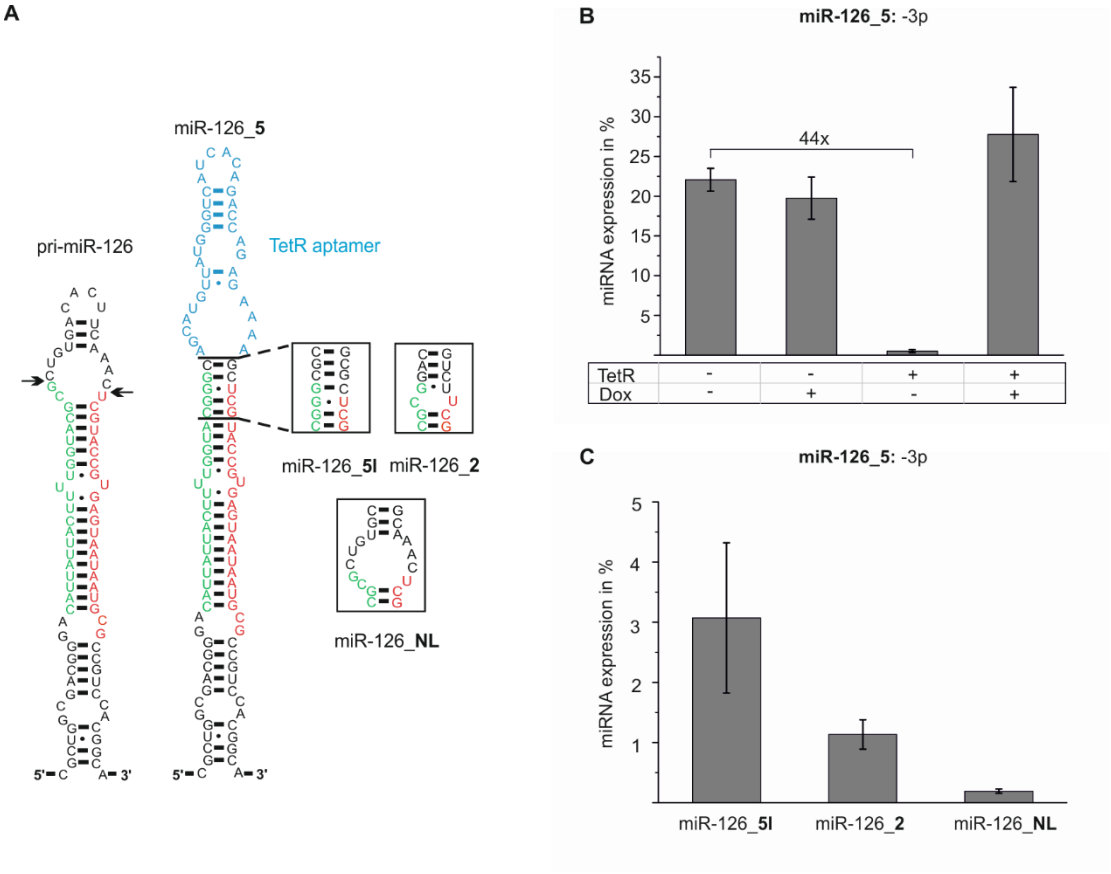

Figure 3.2 (A) Design scheme for the miR-126-based pre-miR switches. The predicted secondary structures of a part of the natural pri-miR-126 (left) and the modified pre-miR switches miR-126_5, _5l, _2 and _NL are shown. The TetR aptamer highlighted in blue replaces the natural terminal loop of the precursor. The communication modules between precursor stem and TetR aptamer were varied with regard to stem stability and length. The resulting differences in the transition areas between pre-miRNA and the aptamer are highlighted in boxes. In the precursor stem miRNA-126-5p is indicated in green, whereas red designates miRNA-126-3p. Arrows indicate the Dicer cleavage sites. **(B) TetR and dox-dependent regulation of mature miRNA-126 levels**. 1.4 x 10^5 HeLa cells were seeded into 12-well plates and transfected with a plasmid either harboring the natural miRNA precursor or the respective pre-miR switch and the TetR expression plasmid. 1 µg/ml dox was supplemented to the medium 3 h after transfection. The amount of mature miRNA-126 produced from the respective pre-miR switch was assessed in a quantitative PCR (qPCR) assay 24 h after transfection and normalized to the miRNA-126 amount derived from natural miRNA precursor construct. The measurements were performed in duplicates (n=3). **(C) Expression levels of mature miRNA-126.** 1.4 x 10^5 HeLa cells were seeded into 12-well plates and transfected with a plasmid either harboring the natural miRNA precursor or the respective pre-miR switch. 1 µg/ml dox was supplemented to the medium 3 h after transfection. The graph reveals the amount of mature miR-126 produced from the respective pre-miR switch normalized to the miRNA-126 amount derived from natural pre-miRNA processing determined in a qPCR assay 24 h after transfection. The measurements were performed in duplicates (n=2).

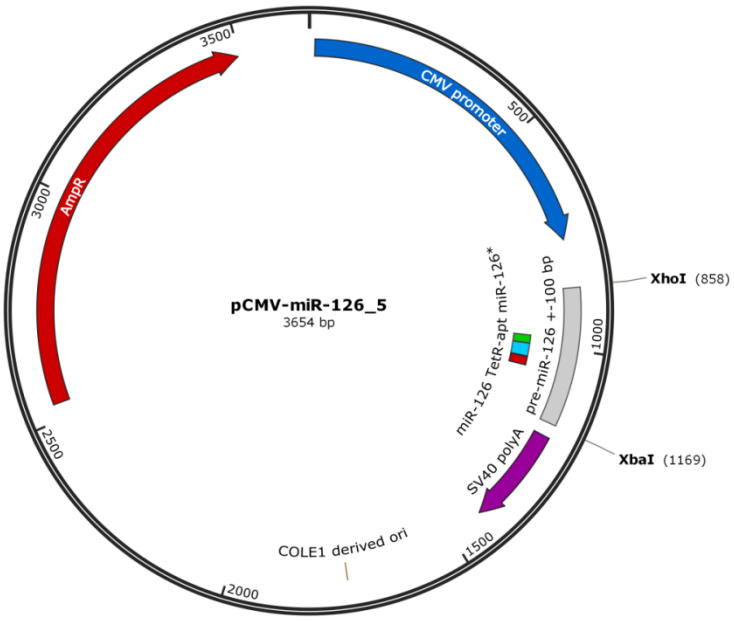

Figure 3.3 Plasmid map of pCMV-miR-126_5.
The plasmid map schematically shows the construction of the pre-miR switch miR-126_5 expression plasmid. The pre-miR switch construct is surrounded by 100 nt of natural context up- and downstream (grey) and expressed from a CMV promoter (blue). Within this natural context the miR-126 stem loop that harbors miR-126-5p (=miR-126*) highlighted in green and miR-126-3p (=miR-126) illustrated in red is located. In between the two miRNAs the TetR aptamer resides fused to the precursor through a communication module for the purpose of controlling miRNA processing in a ligand-dependent fashion. (Maps were created with SnapGene®)

To analyze the influence of the modification of the natural precursor on processing and the switching efficiency of the designed constructs, they were cloned into a plasmid pCMV-MS framed by 100 nt of the natural context up- and downstream to preserve precursor folding and putative recognition features essential for Drosha processing and expressed from a CMV promoter. The plasmid map pCMV-miR-126_5, depicted in Figure 3.3, exemplifies the composition of the plasmids used for the expression of the natural precursor and the pre-miR switch. TetR was co-expressed from the plasmid pCMV-TetR by a CMV promoter to accomplish high expression of the ligand of the TetR aptamer. For the experimental setup HeLa cells were used because of their low endogenous expression of almost all tested miRNAs with the exception of miRNA-92a that exhibits a relative strong endogenous expression profile in HeLa cells.

HeLa cells were transfected with the plasmids harboring the constructs or the natural miRNA precursors as a positive control for Dicer processing together with the TetR expression plasmid. 1 µg/ml dox was added to the medium 3 h after transfection to test the reversibility of TetR-induced inhibition of pre-miRNA processing. Total RNA was isolated 24 h after transfection and reversely transcribed with the respective stem loop primers. The amount of mature miRNA was then assessed by qPCR using the TaqMan method. In all TaqMan-based qPCR measurements the amount of mature miRNA of the predominant miRNA species after Dicer processing was assessed with the exception of miR-199a. For miR-199a the amount of both species, miR-199a-5p and -3p, was determined due to their biological interest.

The results of the qPCR measurements are depicted in Figure 3.2 B. In the absence of TetR and dox, the amount of mature miRNA-126 processed from construct miR-126_5 was detected at about 23% related to the amount of mature miR-126 naturally processed from the unmodified precursor. Co-expression of TetR resulted in a 44-fold reduction of mature miRNA, whereas the additional supplementation with dox allowed the total reversibility of the inhibitory effect. No significant influence on pre-miRNA-126_5 processing could be detected upon addition of exclusively dox. In contrast to miR-126_5, the maximal amount of mature miRNA of constructs miR-126_5l, _2 and _NL constituted merely 3% relative to the expression of mature miRNA derived from the unmodified precursor (Fig. 3.2 C).

Basically, the replacement of the terminal loop with the aptamer and the connection through a C-G bp attached to a completely complementary miRNA precursor stem negatively affected pre-miRNA processing. Nevertheless, processing was retained to a viable extent of 23% relative basal expression allowing the measurement of an effective and reversible switching activity of the pre-miR switch miR-126_5. Thus, the proximity of the aptamer as well as the resulting stem stability appeared to be suited to efficiently compromise processing by Dicer. However, the relative basal expression of the other constructs miR-126_5l, _2 and _NL turned out to be very weak. Due to the fact that the differences between these constructs and miR-126_5 consisted in variations of the transition area, the reasons for the strong reduction of pre-miRNA processing could be ascribed to either the stem length (communication module of three bp) or the stem flexibility (bulge, mismatch) of the respective constructs. According to their low processing efficiency the respective constructs were discarded from further analysis.

All in all, it can be concluded from the results that variations in the communication module affected processing as well as switching efficiency of the pre-miR switches. Using a short C-G bp communication module seemed to provide an adequate processing activity in the absence of TetR and efficient inhibition of miRNA processing in the presence of TetR.

3.2 Transfer of the pre-miR switch design to further miRNA precursors

To explore the involvement of miRNAs in cellular processes, the development of a universally applicable tool is desirable to confer control over the maturation of different miRNAs. For an assessment of the transferability of the design concept, the miRNA precursors of miR-34a, -199a, -92a and -101 were selected according to their structural variety as well as their clinical relevance and modified with the TetR aptamer. Due to the superior expression level provided by miR-126_5, its communication module was utilized to design further pre-miR switches. The communication module was further varied by either a removal of the connecting bp (Fig. 3.4, A, B, C, D miR-x_2 (con)) or an exchange of the C-G with an A-U bp (Fig. 3.4, A miR-34a_1) to test the flexibility of the communication module.

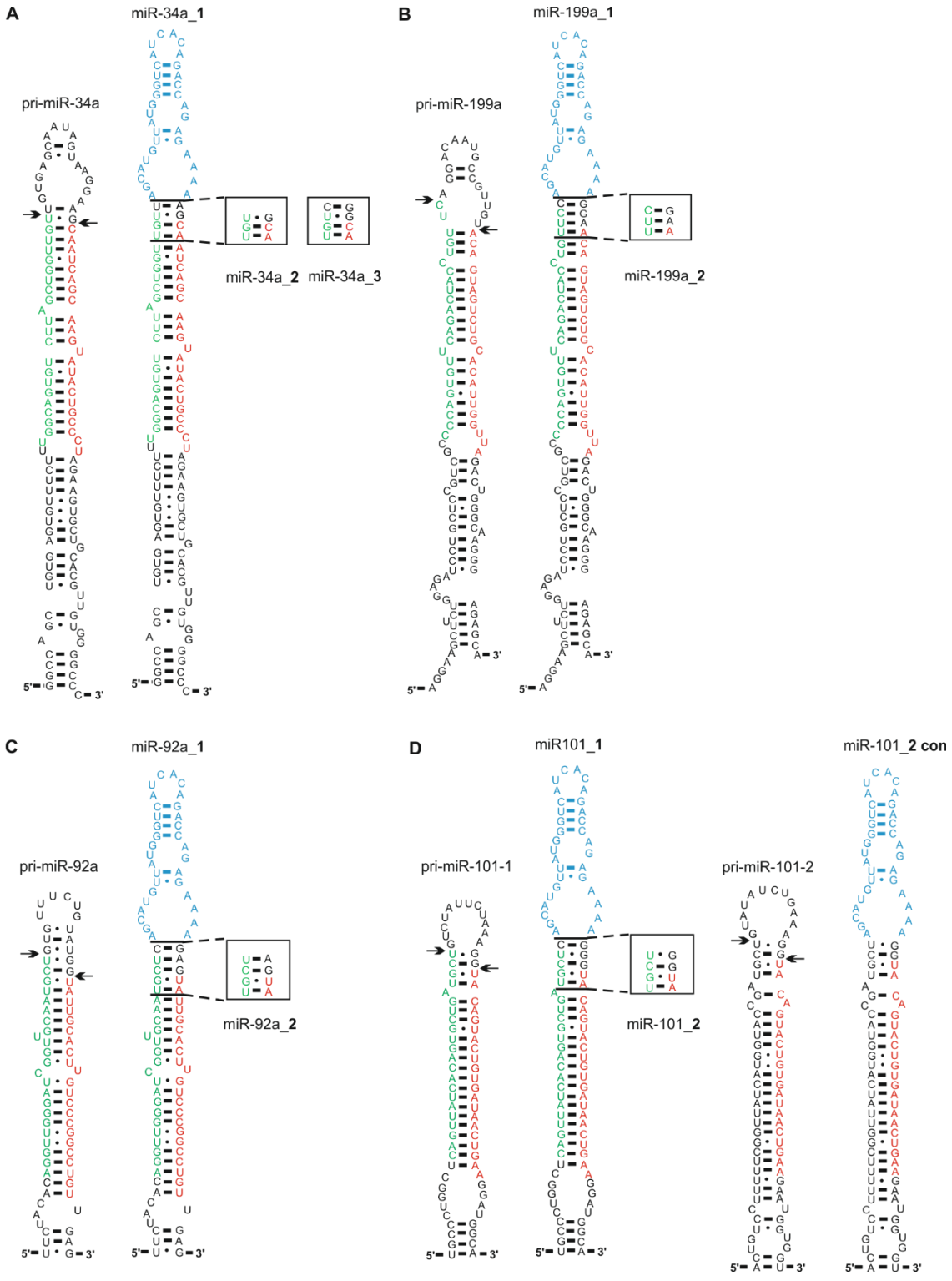

Figure 3.4 Transfer of the design concept for pre-miR switch miR-126_5 to the miRNA precursors of (A) miR-34a, (B) miR-199a, (C) miR-92a and (D) miR-101-1 and -2. The predicted secondary structures of parts of the natural pri-miRNAs (left) and the modified pre-miR switches (right) are shown. The TetR aptamer highlighted in blue replaces the natural terminal loop of the precursor. The communication modules between precursor stem and TetR aptamer were slightly varied. The resulting differences in the transition areas between miRNA precursor and aptamer are highlighted in boxes. In the precursor stem miRNAs-5p are indicated in green, whereas red designates miRNAs-3p. Arrows indicate the Dicer cleavage sites.

To analyze the miRNA expression levels as well as the switching efficiency of the novel pre-miR switch constructs, the same experiments were performed as for the miR-126-based constructs.

The results of the qPCR measurements testing the engineered miR-34a and -199a precursors are presented in Figure 3.5. Independent of the respective communication module, constructs based on the modified miR-34a precursor exhibited a comparable relative expression level of about 13% of mature miRNA compared to the unmodified precursor in the absence of TetR and dox. Furthermore, all construct designs for miR-34a displayed high dynamic ranges upon TetR expression. Whereas miR-34a_1 and _2 conferred a 33- and 41-fold reduction of miRNA processing, miR-34a_3 exhibited an outstandingly high dynamic range of about 400-fold. In contrast, only the former two designs of miR-34a enabled complete reversibility of the inhibitory effect by the supplementation with dox. The structural feature of miR-34a_3, distinguishing it from the other two constructs, is the C-G bp that served to couple the aptamer to the precursor structure. The additional stabilization of the stem turned out to be advantageous for aptamer functionality or to have an effect on the positioning of TetR in its bound state leading to the optimal proximity relative to the Dicer cleavage sites. As a consequence, an efficient inhibition of miRNA processing could be observed, since nearly no mature miRNA-34a accumulated in the presence of TetR.

In contrast to the pre-miR switches miR-34a_1, _2 and _3, the variations in the communication module of the modified precursors of miR-199a resulted in a different processing behavior. Construct miR-199a_2 that features a direct fusion of the aptamer to the miRNA precursor showed a distinct increase of about 10% of mature miRNA expression for both miRNAs compared to miR-199a_1 in the absence of ligand and inducer molecule. In that case, a direct connection of the aptamer to the precursor seemed to enhance pre-miRNA processing. Constructs miR-199a_1 and _2 revealed a 38- and 67-fold reduction of mature miRNA-199a-5p in the presence of TetR. Here, the increase of the dynamic range observed for miR-199a_2 could be mainly attributed to the higher expression level of mature miRNA in the absence of TetR, since the reduced level of mature miRNA-199a-5p was almost equal for both constructs upon TetR expression. Analyzing the dynamic ranges for processing regulation of miR-199a-3p, much higher repression factors were yielded, as it is displayed in Figure 3.5 B. This could be ascribed to the fact, that the relative reduction of mature miRNA in the presence of TetR was more distinct for miR-199a-3p compared to miR-199a-5p, in turn resulting in a much higher dynamic range. The addition of dox completely reactivated pre-miRNA processing for both constructs (Fig. 3.5). Compared to the miR-34a based pre-miR switches, the pre-miR switches of miR-199a exhibited an inherently more stable closing stem that possibly rendered the additional C-G bp dispensable for an efficient inhibition of pre-miR processing. Accordingly, miR-199a_2 could afford a higher expression level of mature miRNA-199a-5p and -3p and very efficient TetR-related inhibition of processing at the same time.

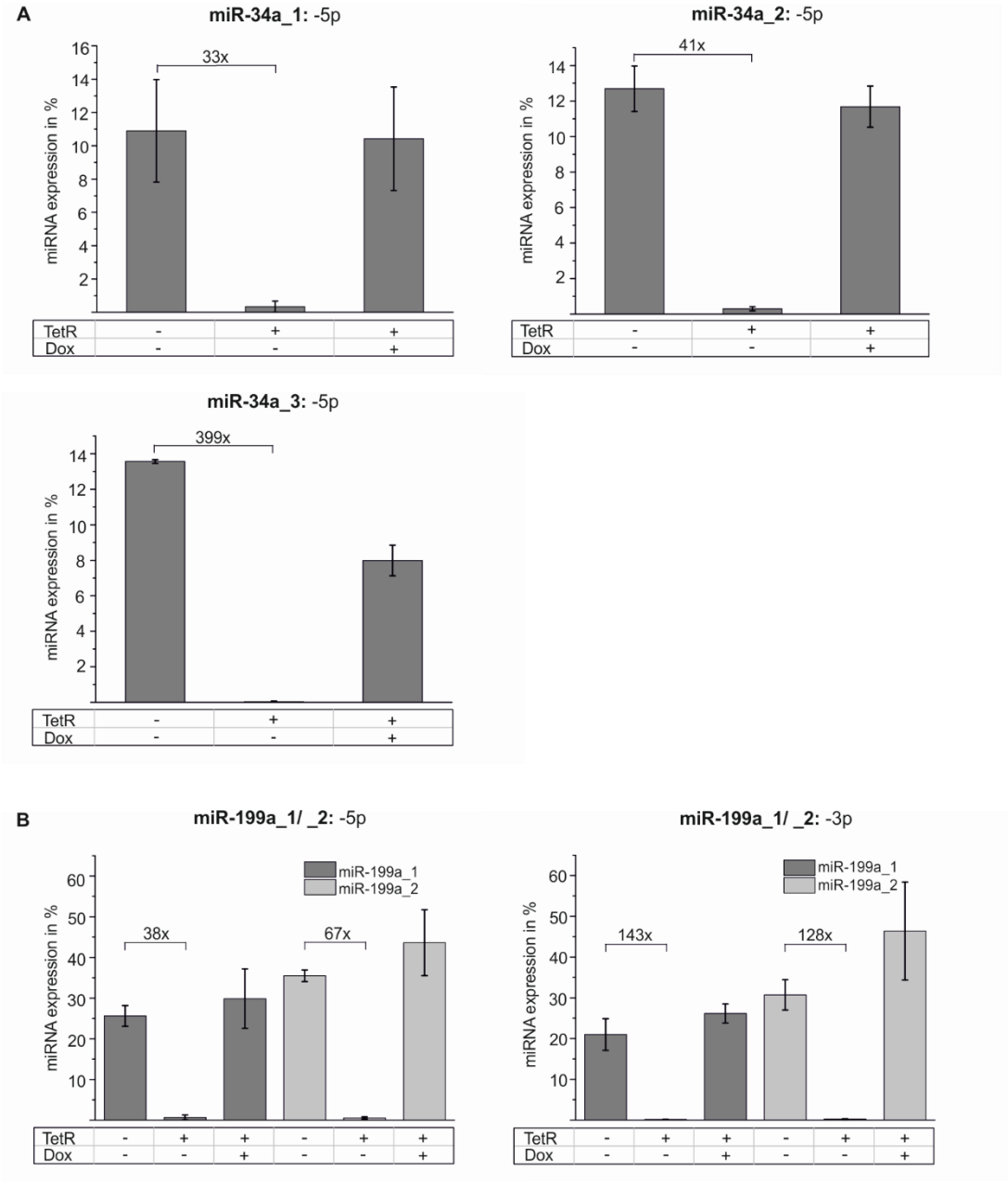

Figure 3.5 TetR- and dox-dependent regulation of mature miRNA-34a (A) and miR-199a (B) levels.
1.4 x 10^5 HeLa cells were seeded into 12-well plates and transfected with a plasmid either harboring the respective natural miRNA precursor or the pre-miR switch and the TetR expression plasmid. 1 µg/ml dox was supplemented to the medium 3 h after transfection. The amount of mature miRNA produced from the respective pre-miR switch was assessed in a qPCR assay 24 h after transfection and normalized to the miRNA amount derived from processing of the natural pre-miRNA. The measurements were performed in duplicates (n=3).

Figure 3.6 shows the overexpression factors of miRNA-92a-3p as well as the expression levels of mature miRNA-101-3p. As it is apparent from Figure 3.6 A, even the expression of the unmodified miR-92a precursor resulted in a merely 6-fold overexpression of the miRNA compared to the high background expression level of miRNA-92a in HeLa cells. Because an extensive structural modification is often paralleled with a reduction of expression, no overexpression was observed for the modified precursors miR-92a_1 and _2. Consequently, the amount of switchable miRNA-92a covered an extremely small percentage of total intracellular miRNA-92a concentration rendering the application of the miR-92a-based pre-miR switches useless in HeLa cells.

The expression level of mature miR-101-3p appeared to be very low with about 4% expression related to the unmodified miRNA-101 precursor for both designed constructs (Fig. 3.6 B). Similarly, for construct miR-101_2 con that was designed based on the miR-101-2 precursor structure, but gave rise to the identical sequence of miR-101-3p, no overexpression could be detected. Here, the modification of the miRNA precursors nearly abolished miRNA-101-1 and -2 precursor processing. Due to their low processing efficiency, the switching characteristic of these constructs was not further analyzed.

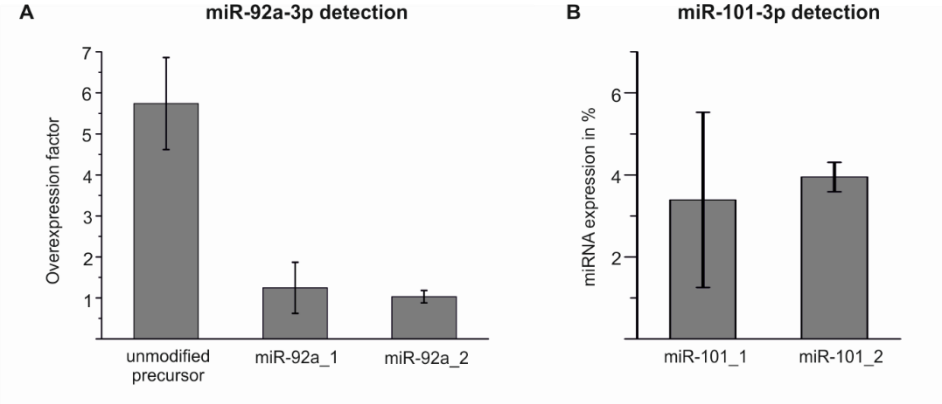

Figure 3.6 (A) Overexpression of the unmodified miR-92a precursor and pre-miR switches miR-92a_1, _2. 1.4 x 10^5 HeLa cells were seeded into 12-well plates and transfected with a plasmid either harboring the natural miRNA-92a precursor or the respective pre-miR switches. The graph shows the overexpression factor of mature miR-92a, resulting from overexpression of the respective pre-miR switch or the unmodified precursor, related to endogenous miR-92a expression in HeLa cells assessed in a qPCR assay 24 h after transfection. The measurements were performed in duplicates (n=2). **(B) Expression levels of mature miR-101-3p.** 1.4 x 10^5 HeLa cells were seeded into 12-well plates and transfected with a plasmid either containing the natural miRNA-101-1 precursor or the respective pre-miR switches. The graph reveals the amount of mature miR-101 produced from the respective pre-miR switch related to the miRNA-101 amount derived from natural pre-miRNA processing determined in a qPCR assay 24 h after transfection. The measurements were performed in duplicates (n=2).

In summary, the design concept proved to be transferable to the miRNA precursors of miRNA-34a and miRNA-199a. Here, the design yielded robust pre-miR switches that were able to efficiently inhibit miRNA processing and to reactivate miRNA biogenesis upon supplementation with dox. The endogenous expression of miRNA-92a in HeLa cells turned out to be too high to achieve a sufficient overexpression that in turn leaves room for an observable regulation. Processing to mature miRNA-101-3p was found to be nearly abrogated after replacing the natural terminal loop of the miR-101-1 and -2 precursors with the aptamer.

3.3 Proof of the functionality of the pre-miR switches in a reporter gene assay

The successful application of a pre-miR switch requires not only a robust functionality with regard to the control of mature miRNA levels, but also an efficient interaction with the miRNA target genes and regulatory function. Generally, a frequently used method to investigate the downstream effects of miRNA expression at the protein level is western blotting. However, it is not possible to distinguish between primary or secondary miRNA targets. Therefore, usually the predicted miRNA target sites of

the 3'UTR or the complete 3'UTR of a gene are used and introduced downstream of a firefly luciferase to elucidate the direct interaction of a regulatory miRNA with its target mRNA. In addition to the natural target sequences the perfect match target sites representing the perfect complement of the respective miRNA and therefore a positive control for miRNA binding and mRNA degradation are employed in such assays. Regardless of the mode of action of the respective miRNA, binding of the miRNA to the target sites can be visualized through a specific inhibition of reporter gene expression. Consequently, the level of luciferase expression also provides information about the intracellular level of mature miRNA.

In the reporter gene assays, the regulatory performance of the functional pre-miR switches miR-126_5, miR-34a_2 and miR-199a_2 was examined. A perfect match target site, the triplicate of a natural binding site or a full/ larger part of the 3'UTR of the respective target mRNA were cloned downstream of the firefly luciferase gene. The plasmid map of pMIR-perfect match miR-126 is presented in Figure 3.7. This map shows the perfect match target site for miR-126 that was inserted into the plasmid by the restriction sites for *SacI* and *SpeI*. Comparably, the triplicates of the natural miRNA binding site as well as the (part of the) 3'UTR of a target mRNA were inserted into the multiple cloning site (MCS) of the plasmid using the restriction sites for *XhoI*, *SpeI*, *SacI* and *HindIII*.

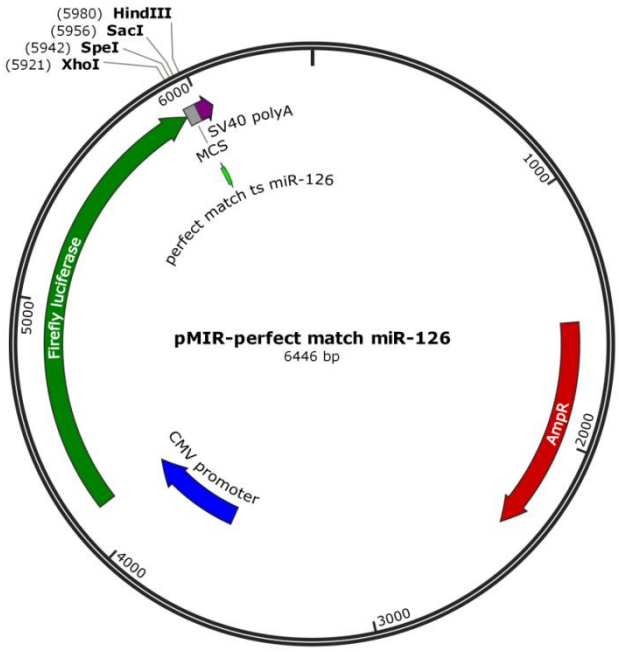

Figure 3.7 Plasmid map of pMIR-perfect match miR-126.
The plasmid map schematically shows the construction of a plasmid used for the reporter gene assay testing the binding of miR-126 to its perfect match target site (ts, light green) with regard to TetR and dox-dependent regulation. The firefly luciferase (green) is expressed under control of a CMV promoter (blue). The multiple cloning site (MCS, grey) of the plasmid was used to insert the perfect match target site for miR-126 using the restriction sites *SacI* and *SpeI*.

The respective targets of the miRNAs were selected according to a preceding validation by other groups. One known validated target of miRNA-126-3p is *SPRED1* that harbors three predicted binding sites for miRNA-126-3p [104]. For the analysis of the influence of miR-126_2 regulation on reporter gene expression, one predicted binding sequence was introduced as a triplicate downstream of the firefly

luciferase gene. To investigate the regulatory effect of pre-miR switch miR-34a_2 and miR-199a_2, a triplicate of one predicted miRNA target sequence of the 3'UTR of *E2F3,* a target of miR-34a-5p, of the 3'UTR of *DDR1*, constituting a target of miR-199a-5p and of the 3'UTR of *CAV2* validated as a target of miR-199a-3p, were cloned downstream of the reporter gene, respectively [79,111,113].

For the purpose of further investigating the influence of the pre-miR switches on luciferase gene expression, the complete natural 3'UTR of the miR-34a-5p target *MET* with three predicted binding sites was employed [85]. A larger part of the 3'UTR of the miR-199a-5p target *DDR1* with four predicted binding sites was used. Furthermore, a part of the 3'UTR of the miR-199a-3p target *CAV2* harboring two predicted miRNA binding sites as well as the two complete 3'UTRs of *MET* and *CD44* with three predicted miRNA binding sites for miR-199a-3p were used for the experiments [115].

HeLa cells were co-transfected with the plasmid containing the respective modified reporter gene and the plasmid bearing the pre-miR switch. In addition to this, the TetR expression plasmid and a plasmid harboring a *Renilla* luciferase that served to normalize the firefly luciferase values to the respective cell count as well as to account for experimental variations due to differences in transfection efficiency were co-transfected. The luminescence values were normalized to the respective controls that showed the reporter gene expression in the absence of the particular miRNA. To exclude off-target effects, control constructs were generated with a single or a triplicate random sequence. 1 µg/ml dox was added 3 h after transfection and luminescence values were measured 24 h after transfection.

The data of the reporter gene assay are presented in Figure 3.8 to Figure 3.11. Generally, the inhibition of pre-miRNA processing through TetR binding is reflected by an increase in reporter gene expression. The experiments that employed the perfect match binding sites of the miRNAs downstream of the reporter gene revealed an increase of relative reporter gene expression between 2.5- and 3.1-fold for the pre-miR switches miR-126_5 and miR-199a_2, whereas the increase of relative expression for construct miR-34a_2 with 1.7-fold turned out to be comparably moderate in the presence of TetR (Fig. 3.8). This difference in regulation efficiency could be ascribed to the lower expression level of mature miRNA-34a-5p compared to that of miR-126-3p and miR-199a-5p/-3p. Furthermore, all of the tested pre-miR switches appeared to nearly completely restore the relative expression value of one in the presence of dox. Accordingly, the dissociation of TetR from the aptamer resulted in a resumption of pre-miRNA processing that, in turn, diminished reporter gene expression. The random controls did not show an effect on relative expression due to the presence of the respective pre-miR switch, excluding either unspecific binding or a TetR- or dox-based effect.

The examination of the influence of the pre-miR switch-controlled miRNA expression on reporter gene regulation after insertion of the triplicates of the natural target sites showed an increase of expression of 1.5- to 1.9-fold that could be observed for miR-126-3p, miR-34a-5p and miR-199a-5p upon TetR expression (Fig. 3.9). A direct interaction of miR-199a-3p with the predicted target site of *CAV2* could not be detected, as no change in relative reporter gene expression occurred (Fig. 3.11 A). Possibly, the tested miRNA binding site is either falsely designated as a binding site of miR-199a-3p or it the merely contributes weakly to the regulation of gene expression.

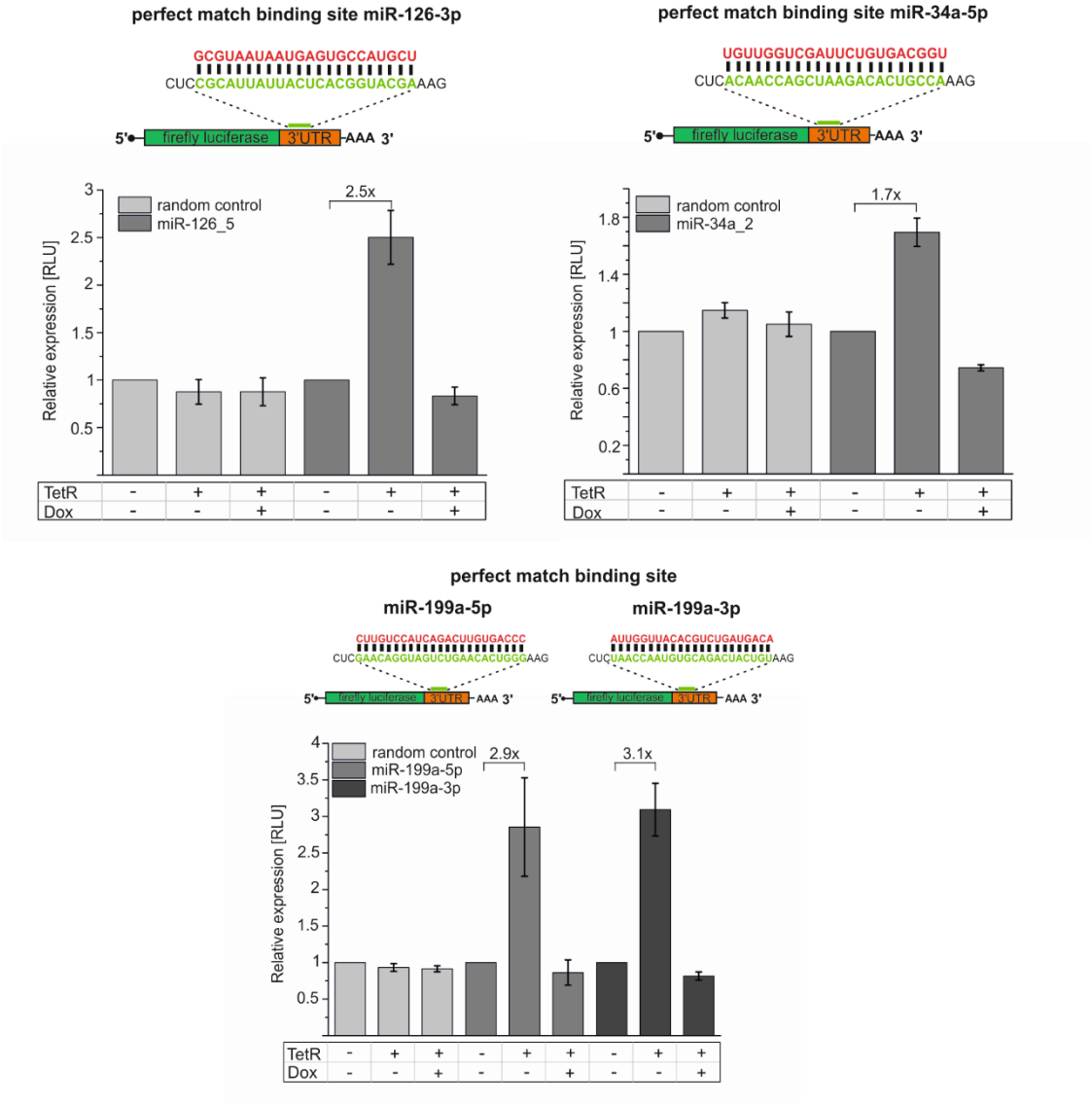

Figure 3.8 Effect of aptamer-controlled miRNA processing on reporter gene expression.
The respective perfect match binding site for testing miR-126-3p/ -34a-5p and miR-199a-3p/-5p binding were introduced downstream of a firefly luciferase gene. 0.55 x 10^5 HeLa cells were seeded into 24-well plates and transfected with a reporter gene plasmid either harboring the respective miRNA target sites or a random control site. Furthermore, the plasmids with the natural miRNA precursor or the pre-miR switch, a TetR expression plasmid as well as a *Renilla* luciferase expression plasmid for normalization were co-transfected (ratio of reporter gene plasmid:miRNA precursor or pre-miR switch expression plasmid:TetR expression plasmid:*Renilla* expression plasmid 4:7:7:2). 1 µg/ml dox was added to the medium 3 h after transfection. The luminescence measurements were performed in duplicates 24 h after transfection (n=3). The measured values related to *Renilla* luciferase expression were normalized to reporter gene expression in the absence of the respective miRNA expression plasmid followed by a second normalization to reporter gene expression in presence of the respective miRNA expression plasmid devoid of TetR or dox. Thus, graphs display the relative expression values as x-fold increase. Above the graphs the respective target sites are depicted that were introduced downstream of the firefly luciferase gene. The miRNA target sequences are shown in green, the miRNA sequences are highlighted in red. **RLU** Relative luminescence unit.

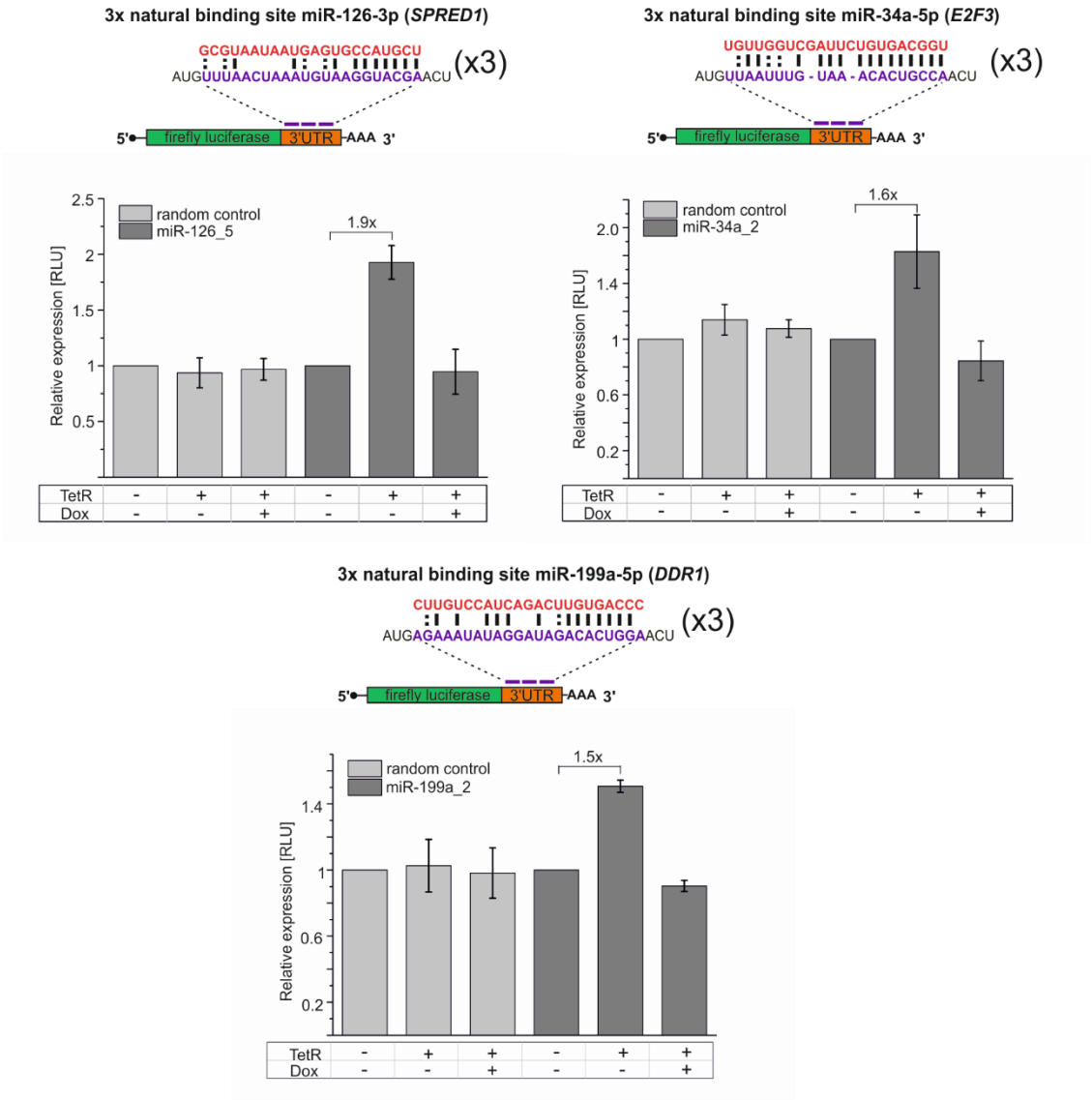

Figure 3.9 Effect of aptamer-controlled pre-miRNA processing on reporter gene expression.
The respective triplicate of one binding site derived from a natural target gene for testing miR-126-3p/ -34a-5p and miR-199a-5p binding were introduced downstream of a firefly luciferase gene. 0.55 x 10^5 HeLa cells were seeded into 24-well plates and transfected with a reporter gene plasmid either harboring the respective miRNA target sites or random control sites. Furthermore, the plasmids with the natural miRNA precursor or the pre-miR switch, a TetR expression plasmid as well as a *Renilla* luciferase expression plasmid for normalization were co-transfected (ratio of reporter gene plasmid:miRNA precursor or pre-miR switch expression plasmid:TetR expression plasmid:*Renilla* expression plasmid 4:7:7:2). 1 µg/ml dox was added to the medium 3 h after transfection. The luminescence measurements were performed in duplicates 24 h after transfection (n=3). The measured values related to *Renilla* luciferase expression were normalized to reporter gene expression in the absence of the respective miRNA expression plasmid followed by a second normalization to reporter gene expression in presence of the respective miRNA expression plasmid devoid of TetR or dox. Thus, graphs display the relative expression values as x-fold increase. Above the graphs the respective target sites are depicted that were introduced downstream of the firefly luciferase gene. The miRNA target sequences are shown in purple, the miRNA sequences are highlighted in red. **RLU** Relative luminescence unit.

The insertion of the complete 3'UTR of *MET*, harboring three different miRNA binding sites for miR-34a led to an increase of relative expression of 1.4-fold (Fig. 3.10 left), whereas the incorporation of a part of the 3'UTR of *DDR1* resulted in a 1.8-fold elevation of relative expression due to miR-199a-5p binding (Fig. 3.10 right). The reversibility of that effect was also observed upon the addition of dox. Comparing the effect resulting from insertion of the triplicate of a single miR-199a-5p binding

sequence derived from *DDR1* with that of the insertion of a larger part of the 3'UTR with several binding sites for one miRNA, it can be asserted that the interplay of the four predicted target sites in the 3'UTR led to a more effective inhibition of firefly luciferase expression.

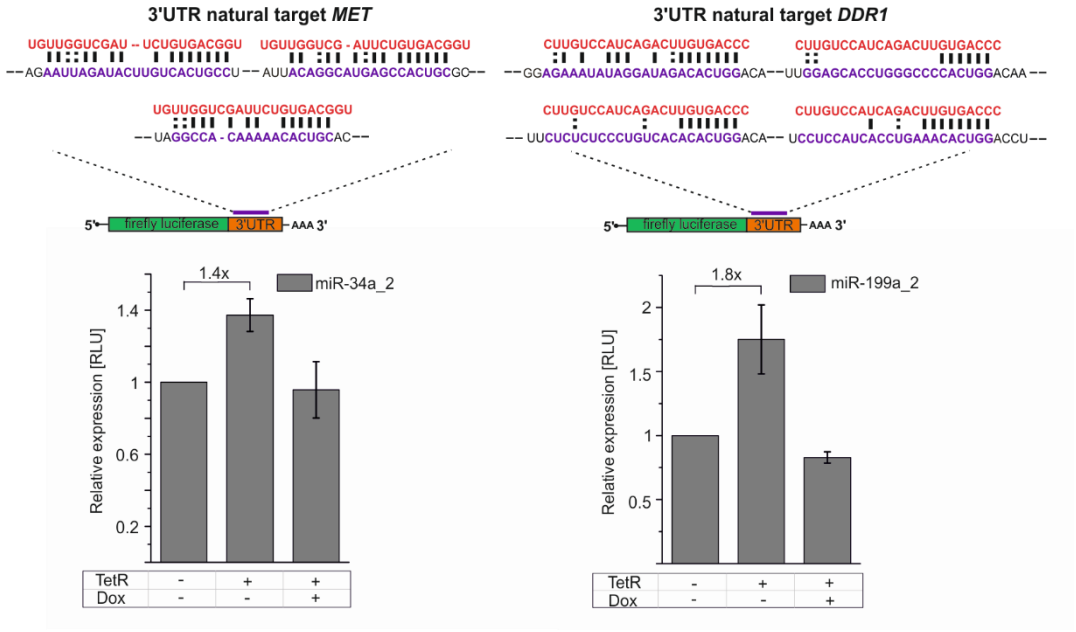

Figure 3.10 Effect of aptamer-controlled pre-miRNA processing on reporter gene expression.
A complete or a larger part of 3'UTR of a respective targets *MET* or *DDR1* for testing miR-34a-5p and miR-199a-5p binding were introduced downstream of a firefly luciferase gene. 0.55 x 10^5 HeLa cells were seeded into 24-well plates and transfected with a reporter gene plasmid harboring the respective (part of the) 3'UTR. Furthermore, the plasmids with the natural miRNA precursor or the pre-miR switch, a TetR expression plasmid as well as a *Renilla* luciferase expression plasmid for normalization were co-transfected (ratio of reporter gene plasmid: miRNA precursor or pre-miR switch expression plasmid:TetR expression plasmid:*Renilla* expression plasmid 4:7:7:2). 1 µg/ml dox was added to the medium 3 h after transfection. The luminescence measurements were performed in duplicates 24 h after transfection (n=3). The measured values related to *Renilla* luciferase expression were normalized to reporter gene expression in the absence of the respective miRNA expression plasmid followed by a second normalization to reporter gene expression in presence of the respective miRNA expression plasmid devoid of TetR or dox. Thus, graphs display the relative expression values as x-fold increase. Above the graphs the respective target sites within the target gene 3'UTR are depicted that were introduced downstream of the firefly luciferase gene. The miRNA target sequences are shown in purple, the miRNA sequences are highlighted in red. **RLU** Relative luminescence unit.

Although the complete 3'UTRs of the validated targets *CAV2*, *MET* and *CD44* were inserted downstream of the reporter gene, no regulatory effect hinting at a direct interaction of miR-199a-3p with these 3'UTRs could be inferred (Fig. 3.11). In consent with these findings, also no change in firefly luciferase gene expression could be determined when the miRNA was naturally processed from the unmodified precursor. It can be assumed that either the expression levels of miR-199a-3p were generally not sufficient to affect gene expression or the cellular context was not appropriate to facilitate a miRNA-target site interaction.

For all of the tested miRNAs with the exception of miR-199a-3p, a regulation of reporter gene expression based on pre-miR switch performance could be demonstrated dependent on the presence of TetR and dox. Thus, the results confirmed that the expression levels of the miRNAs as well as the regulation efficiency of the respective pre-miR switches notably influenced reporter gene expression and hence supported the data previously obtained by qPCR. The different extents of regulation were

constituted by the different amounts of mature miRNA dependent on the pre-miR switch as well as the various binding sites that all display individual interaction characteristics with the respective miRNAs.

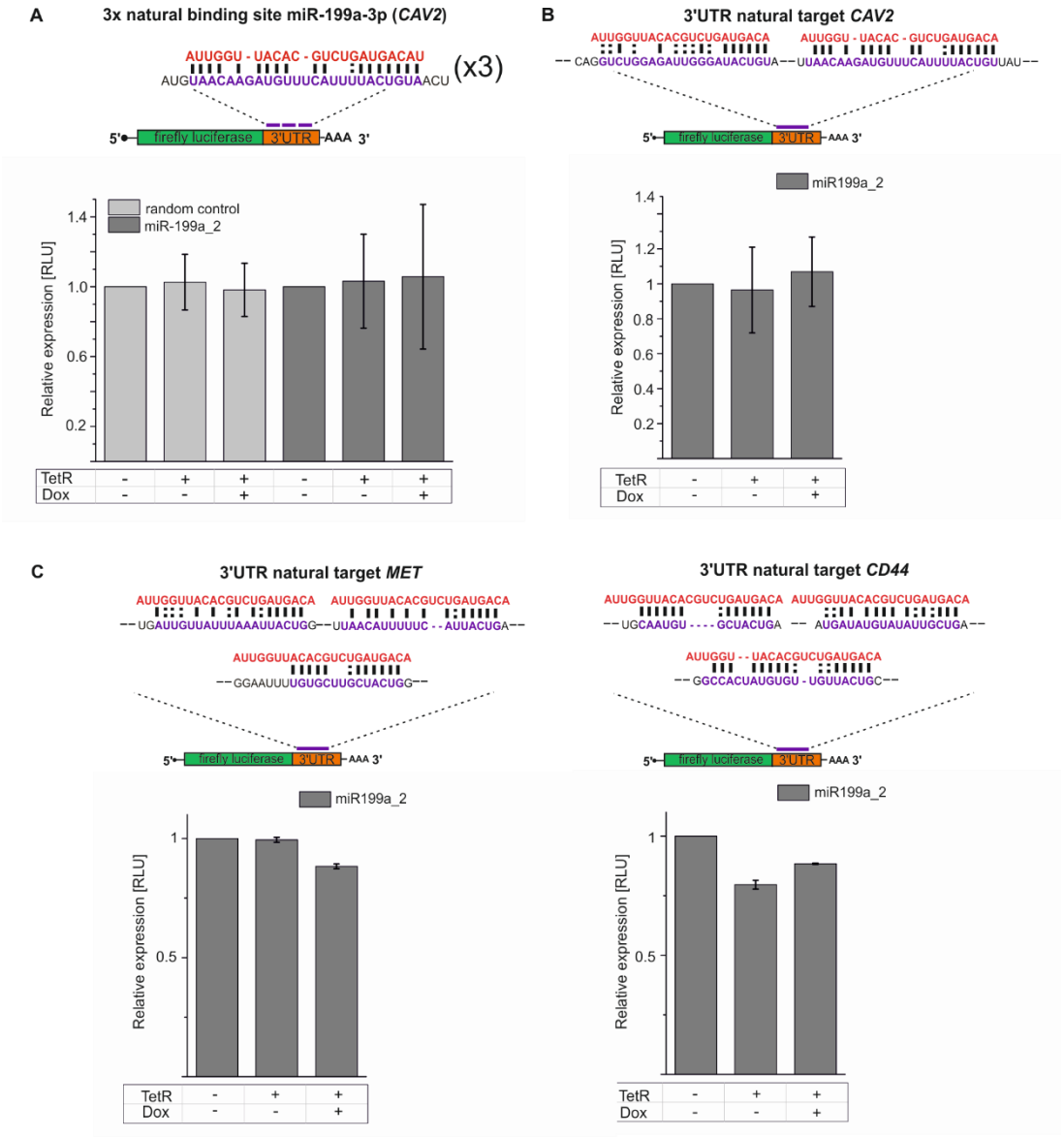

Figure 3.11 Effect of aptamer-controlled miR-199a-3p presence on reporter gene expression.
(A) A triplicate of one binding site of miR-199a-3p derived from the natural target *CAV2,* **(B)** a larger part of the 3'UTR of *CAV2* harboring two predicted miRNA binding sites and **(C)** the two complete 3'UTRs of *MET* and *CD44* featuring three predicted miRNA binding sites for miR-199a-3p were introduced downstream of a firefly luciferase gene. 0.55 x 10^5 HeLa cells were seeded into 24-well plates and transfected with a reporter gene plasmid either harboring the respective miRNA target sites or random control sites. Additionally, the plasmids with the natural miRNA precursor or the pre-miR switch, a TetR expression plasmid as well as a *Renilla* luciferase expression plasmid for normalization were co-transfected (4:7:7:2 ratio of reporter gene plasmid: miRNA precursor or pre-miR switch expression plasmid:TetR expression plasmid:*Renilla* expression plasmid). 1µg/µl Dox was added to the medium 3 h after transfection. The luminescence measurements were performed in duplicates 24 h after transfection (n=2). The measured values related to *Renilla* luciferase expression were normalized to reporter gene expression in the absence of the respective miRNA expression plasmid followed by a second normalization to reporter gene expression in presence of the respective miRNA expression plasmid devoid of TetR or dox. Thus, graphs display the relative expression values as x-fold increase. Above the graphs the respective target sites (within the target gene 3'UTR) are depicted. The miRNA target sequences are shown in purple, the miRNA sequences are highlighted in red. **RLU** Relative luminescence unit.

3.4 Determination of the pre-miR switch miR-199a_2 onset kinetics

The *in vivo* application of a pre-miR switch requires its operation at biological relevant time scales. Thus, a closer characterization of the onset kinetics of one pre-miR switch was pursued. With regard to the developed pre-miR switches the onset kinetics provided information on the time needed to respond to dox by a dissociation of TetR from the aptamer. Therefore the measured parameter was the continuation of miRNA processing that was constituted by the amount of mature miRNA.
Accordingly, time-course experiments were performed to elucidate the potential of pre-miR switch miR-199a_2. For that purpose, HeLa cells were transfected with the pre-miR switch miR-199a_2 containing plasmid and the TetR expression plasmid. The cells were treated with dox 24 h after transfection. To exclude effects arising from transient transfection, control cells were concomitantly transfected with the plasmid containing the pre-miR switch, omitting the TetR expression plasmid and dox supplementation, to monitor the processing of the pre-miRNA switch in the course of the experiment. The levels of mature miR-199a-5p were measured at 0, 2, 4, 8, 16 and 24 h after dox addition by qPCR. The results were shown normalized to the respective controls, because a reduction of absolute processing to the mature miRNA was observed over time that was probably caused by cell division (Fig. 3.12 B).

Figure 3.12 A displays the results of the time course experiments. A rapid increase of miRNA expression was recorded already after 1 h, restoring pre-miRNA processing to about 30%. Furthermore, a steep digressive expression profile between 0 to 4 h suggested a preceding accumulation of pre-miRNA that has been shielded from degradation probably due to an occupation with TetR protein before dox addition led to a dissociation of TetR from the aptamer. That effect might have superimposed the natural kinetics of the pre-miR switch resulting in the observed curve progression. Once, excess pre-miRNA was processed by Dicer, miRNA expression kinetics resumed a constant expression profile climaxing in the highest miRNA amount of 80% measured at about 16 h after dox addition.
From the experiment it can be deduced that pre-miR switch miR-199a_2 features fast onset kinetics. An almost complete restoration of miRNA processing was accomplished within 24 h. Hence, the developed pre-miR switch operates at biological relevant time scales highlighting its applicability as a robust and efficient regulator of miRNA biogenesis.

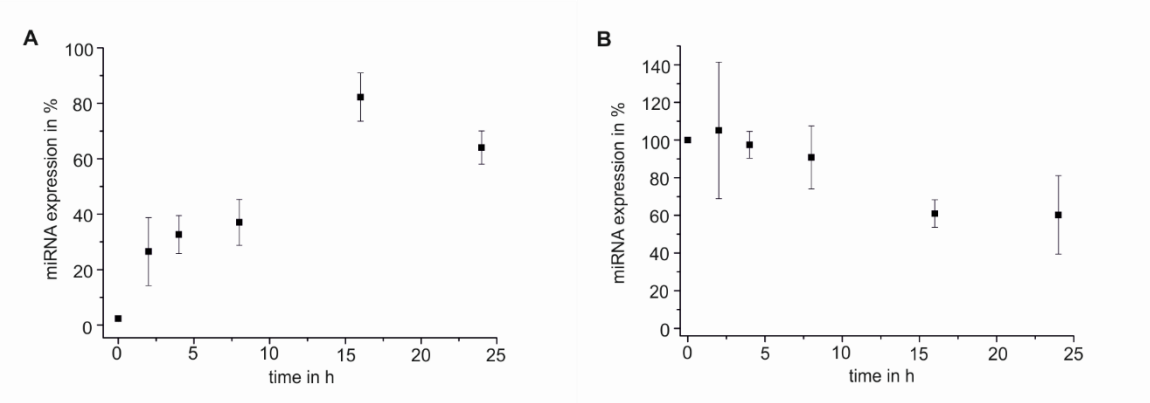

Figure 3.12 (A) Onset kinetics of pre-miR switch 199a_2. 1.4 x 10^5 HeLa cells were seeded into 12-well plates and transfected with a plasmid harboring pre-miR switch miR-199a_2 and the TetR expression plasmid. 24 h after transfection, 1 µg/ml dox was added to the medium and cells were harvested after 0, 2, 4, 8, 16 and 24 h after dox addition. The qPCR-based measurement was performed in duplicates for detection of mature miRNA-199a-5p (n=3). Shown is the amount of mature miRNA-199a-5p produced from the pre-miR switch related to the miRNA levels derived from controls transfected with the pre-miR switch in the absence of TetR or dox (shown in B). **(B) Pre-miR switch miR-199a_2 processing over 24h.** 1.4 x 10^5 HeLa cells were seeded into 12-well plates and transfected with a plasmid harboring pre-miR switch miR-199a_2. 24 h after transfection growth medium was exchanged and cells were harvested after 0, 2, 4, 8, 16 and 24 h after medium exchange. The qPCR-based measurement was performed in duplicates for detection of mature miRNA-199a-5p (n=3). Shown is the amount of mature miRNA-199a-5p normalized to the amount of mature miRNA-199a-5p present at time point 0 (=100%) in the absence of TetR or dox.

3.5 Regulatory function of the pre-miR switches targeting endogenous genes

3.5.1 Transient transfection of pre-miR switch miR-199a_2

MiRNAs are known to confer regulation of gene expression through degradation of mRNA or inhibition of translation. In most cases the mode of action of a certain miRNA-target pair has not been elucidated so far and therefore it is not predictable, whether the interaction leads to a change at the mRNA level, a visible effect at the protein level, or both. To detect potential regulatory effects on endogenous miRNA targets caused by the pre-miR switch application, qPCR as well as western blotting were performed. Based on previously published studies, that identified *SMAD4* and *DDR1* as target genes of miR-199a-5p, these two endogenous targets were screened for regulation by the pre-miR switch miR-199a_2 [110,111].

For qPCR measurements, HeLa cells were transfected with the plasmid harboring the pre-miR switch miR-199a_2 or the natural miRNA precursor as a positive control for Dicer processing together with a TetR expression plasmid. 1 µg/ml dox was added to the medium 3 h after transfection. 24 h after transfection total RNA was isolated and transcribed with random hexamers. The amount of respective target mRNA was then assessed using cDNA-specific primers in a qPCR assay. For the examination of the protein level by western blotting, cells were transfected with 1,000 ng of the empty plasmid pCMV-MS (MS), 500 ng of pCMV-MS together with 500 ng of the natural precursor harboring construct (MS+miR-199a) or 1,000 ng of the natural precursor (miR-199a) alone, to test for a general response to miR-199a presence. Cells were lysed 24 h after transfection and 20 µg of total protein

analyzed by sodium dodecyl sulfate (SDS)-polyacrylamide gel electrophoresis (PAGE). Then, total protein was blotted onto a PVDF membrane. The target proteins SMAD4 (60 kDa) and DDR1 (100 kDa: non-glycosylated; 125 kDa: glycosylated) were visualized using horseradish peroxidase (HRP)-conjugated secondary antibodies with a chemiluminescence substrate. As a loading control β-actin was used.

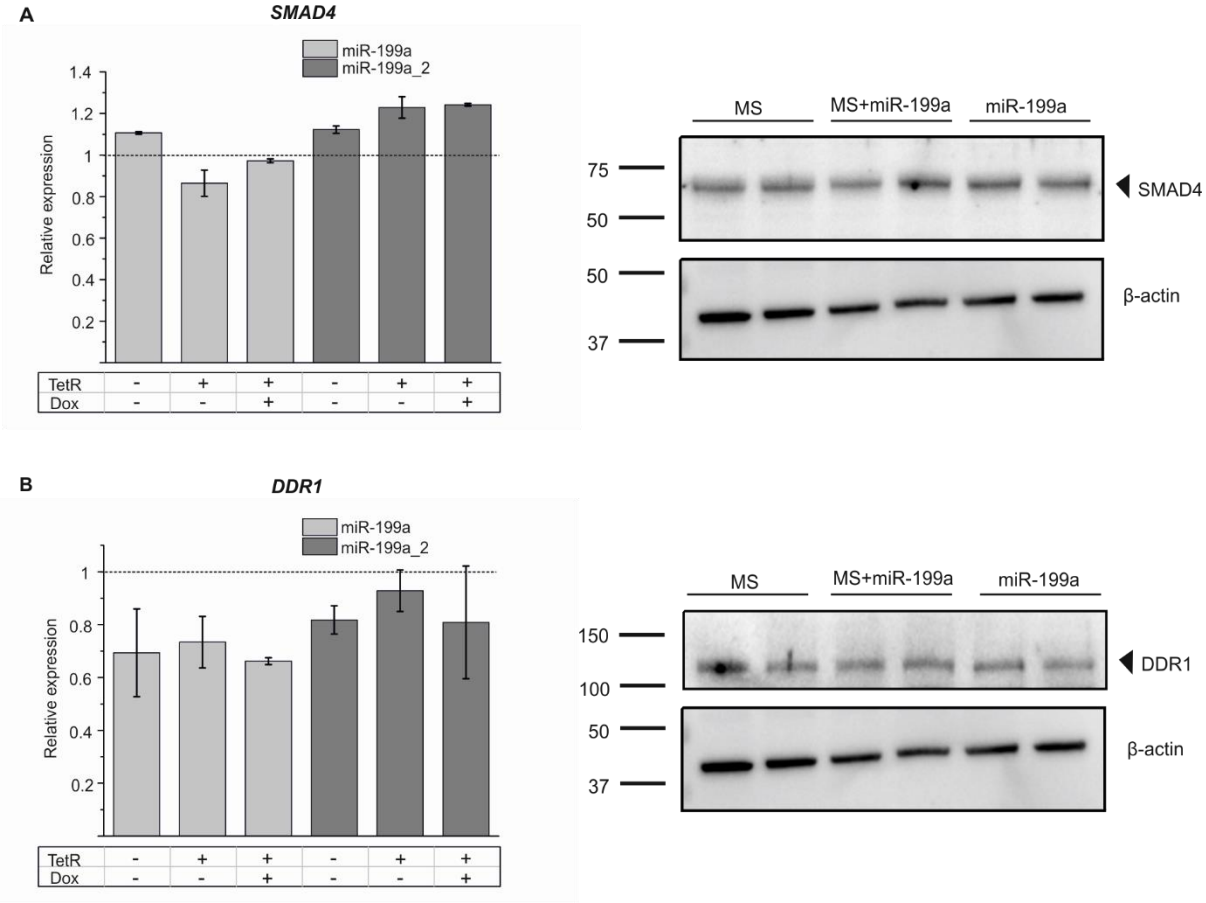

Figure 3.13 Influence of mature miR-199a levels on mRNA and protein level of (A) SMAD4 and (B) DDR1 after transient transfection. Shown are either the results from mRNA level determination using qPCR or the protein levels of the respective miR-199a target in a western blot. For qPCR assays, 1.4 x 10^5 HeLa cells were seeded into 12-well plates and transfected with the plasmid containing the natural miR-199a precursor or pre-miR switch miR-199a_2 and the TetR expression plasmid. 1 µg/ml dox was supplemented 3 h after transfection. Total RNA was isolated and the mRNA level measurements were performed in duplicates 24 h after transfection (n=2). The mRNA levels are shown normalized to the mRNA amount of HeLa cells transfected with empty plasmid. For the visualization of the target proteins SMAD4 and DDR1 in a western blot, 1.4 x 10^5 HeLa cells were seeded into 12-well plates and transfected with the either empty plasmid (MS), the natural miR-199a precursor bearing plasmid (miR-199a) or a 1:1 mixture of both (MS+miR-199a) in duplicates. Cells were lysed 24 h after transfection and 20 µg of total protein analyzed by an SDS-PAGE. Then total protein was blotted onto a PVDF membrane and the target proteins SMAD4 (60 kDa) and DDR1 (100 kDa, 125 kDa) were visualized using HRP-conjugated secondary antibodies with a chemiluminescence substrate. β-actin (42 kDa) was used as loading control. Protein sizes are indicated in kDa.

As it becomes evident from Figure 3.13 A, no relevant regulation of the mRNA level of *SMAD4* neither in the presence of miR-199a-5p derived from the natural precursor nor by miR-199a-5p stemming from the pre-miR switch miR-199a_2 was identifiable. In contrast to that, the presence of miR-199a processed from the unmodified precursor slightly diminished the mRNA amount of *DDR1* for about 30% compared to the mRNA expression in the absence of miR-199a (Fig. 3.13 B). In comparison, the

reduction of *DDR1* mRNA that could be associated with the pre-miR switch processing emerged to be less intense. Furthermore, a significant response of the mRNA levels to the presence of TetR or dox could not be deduced from the results.
Looking at the western blots of SMAD4 and DDR1, no changes at the protein level of both potential miR-199a-5p targets appeared due to miR-199a presence independent of the source of the miRNA. Also other cells (A549, HEK-293) were tested for a change at the protein level due to miR-199a presence but they equally yielded no visible regulation.
To sum up, for SMAD4 no regulation at the mRNA or protein level was observed. The small effect appearing at the *DDR1* mRNA level allowed the deduction of a small tendency regarding a response to the presence of the miRNA but was still far away from being significant. In case of *DDR1*, the detected decrease of the mRNA amount did not result in an apparent change at the protein level. Thus, it could not be excluded that the amount of miRNA-199a-5p provided by transient transfection was too weak to evoke significant changes on both, mRNA and protein level.

3.5.2 Genomic integration of pre-miR switch miR-199a_2

A genomic integration constitutes a valid approach to overcome an irregular distribution of the plasmid used for miRNA precursor expression within the cell population due to moderate transfection efficiencies and the capability of a cell to take up varying numbers of the transfected plasmid. Without a preceding selection the examination of the total RNA or the total protein after transient transfection implies mRNA and protein from both transfected as well as non-transfected cells. In contrast to that, genomic integration allows an assay performance with cells exhibiting a uniform genotype and thus comparable levels of miRNA.
For this reason, a stable integration of the pre-miR switch construct miR-199a_2 and the natural miR-199a precursor into the genome of HF1-3 cells was performed using the Flip-in® system. A plasmid was established for this purpose that harbored the respective constructs under control of an hCMV promoter and the Flp Recombination Target (FRT)-site that served as a recognition as well as cleavage site for the applied recombinase (Fig. 3.14). This FRT-site was located upstream of a hygromycin resistance conferring gene that lacked a promoter and a start codon. The promoter and the start codon were, in turn, integrated into the HF1-3 host cell genome and brought into correct proximity and frame with the hygromycin resistance gene upon genomic integration of the created plasmid at the FRT-site. Successful integration then conferred hygromycin resistance to the cells and enabled selection of the cells bearing the integrated constructs.
The respective plasmids containing either the natural miRNA precursor or the pre-miR switch and a plasmid for Flp recombinase expression were co-transfected into the HF1-3 host cells. Following transfection with the plasmids, cells were selected with 150 µg/µl hygromycin B for an integration of the constructs. After selection, cells with the integrated construct were additionally transfected with the TetR expression plasmid and 1 µg/ml dox was supplemented 3 h after transfection. To explore the expression level as well as switching characteristic of the chromosomally integrated pre-miR switch, total RNA was isolated, miR-199a-5p transcribed into cDNA and the amount of the mature miRNA-199a-5p was determined 24 h and 72 h after dox addition by qPCR. Concomitantly, the levels of

mRNA expression of *SMAD4* and *DDR1* were determined after 24 h in the presence of miR-199a derived from both the natural and the TetR aptamer-modified precursor in a qPCR assay.

To complete the dataset, a western blot was performed to reveal a possible regulation of DDR1 protein expression by miR-199a-5p. Therefore, a change from the previously used gradient SDS-PAGE gel to a 7.5% SDS-PAGE gel was conducted to obtain a better resolution of the two DDR1 bands.

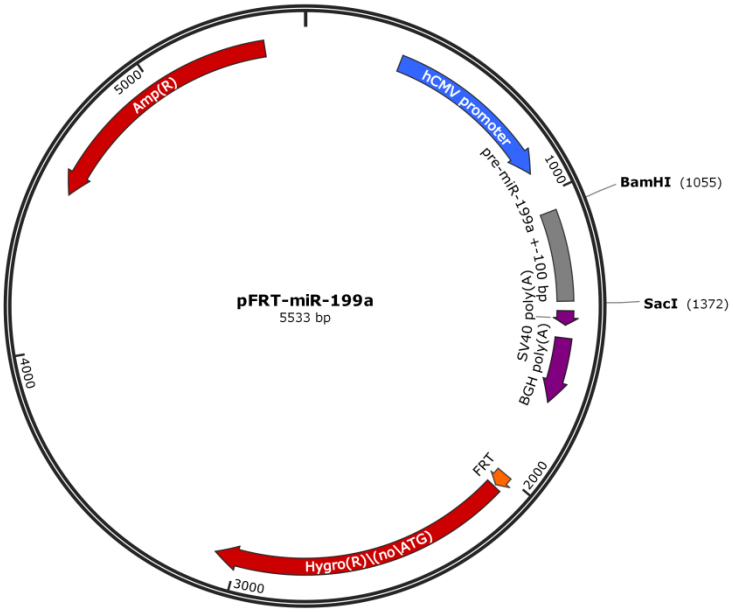

Figure 3.14 Plasmid map of pFRT-miR-199a.
The plasmid map schematically shows the construction of plasmid pFRT-miR-199a used for the genomic integration of the natural miRNA-199a precursor or pre-miR switch miR-199a_2. The constructs were expressed under control of an hCMV promoter (blue). *BamHI* and *SacI* restriction sites were employed for the insertion of the (un-)modified miRNA precursor surrounded by 100 nt of natural context up- and downstream (grey). The FRT-site (orange) for genomic integration is located upstream of the hygromycin B resistance gene (Hygro(R)\(no\ATG), red) that lacks a promoter and a start codon.

As Figure 3.15 A reveals, after 24 h the genomic integration of pre-miR switch miR-199a_2 resulted in 17% expression of mature miRNA-199a-5p compared to the natural precursor that was comparatively lower than for transient transfection. Unfortunately, the efficient inhibition of miRNA processing appeared to be strongly reduced to a factor of 1.4-fold. The addition of dox completely restored pre-miRNA processing to the primarily seen expression value. The measurements of the level of mature miR-199a-5p after 72 h revealed a reduction of miRNA expression to 10% compared to the natural precursor in the absence of TetR and dox, but the presence of TetR resulted in a slightly enhanced inhibitory effect compared to the results obtained after 24 h leading to a 3.2-fold reduction of pre-miRNA processing. Also here, a reversion of the inhibitory effect could be observed upon the supplementation with dox.

In summary, the qPCR measurements after 24 h uncovered a clear loss of efficient suppression of miRNA processing by TetR that was slightly improved after a longer incubation for 72 h. Possibly, this phenomenon can be ascribed to the genomic integration of the pre-miR switch without a parallel TetR integration that led to a continuous production of miRNA over a long period of time. As a consequence

of constitutive miRNA expression, preceding TetR expression, mature miR-199a-5p seemed to be accumulated in the cell. Thus, although the presence of TetR prevented the cell from processing new mature miR-199a through binding to the pre-miR switch, the measurements were falsified by the previously matured miRNA amount that therefore diminished the inhibitory effect. In that case, the effect caused by TetR binding might have been masked by the strong miRNA-199a background that persisted in the cell until miRNA degradation occurred. This theory was further supported by the results obtained from the 72 h measurements. They displayed a slightly improved dynamic range with regard to the suppression of pre-miR processing that hinted at the possibility that after a longer time of TetR induced suppression, the reduction of the miRNA amount became apparent due to the absence of *de novo* pre-miRNA processing. To exclude problems resulting from a defective expression of TetR, the presence of TetR (24 kDa) in the samples after 24 h and 48 h after transfection was verified in a western blot (Fig. 3.16 A). Regarding the cellular amount of TetR protein and the ratio of pre-miR switch and TetR no statements could be made.

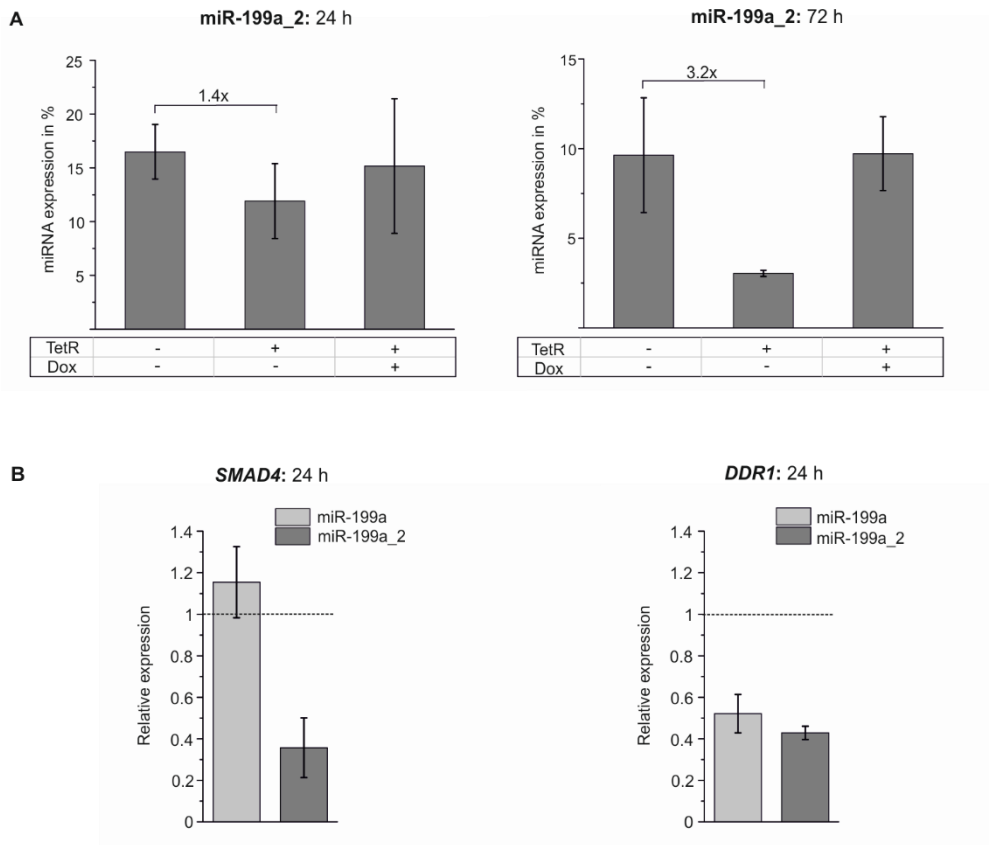

Figure 3.15 (A) TetR- and dox-dependent regulation of mature miRNA-199a after genomic integration of pre-miR switch miR-199a_2. To examine the switching efficiency after genomic integration, 0.9 x 10^5 HF1-3 cells exhibiting the natural miR-199a precursor or pre-miR switch miR-199a_2 integrated in their genome were seeded into 12-well plates, transfected with the TetR expression plasmid and 1 µg/ml dox was supplemented 3 h after transfection. Either 24 h (left) or 72 h (right) after transfection total RNA was isolated and the amount of mature miRNA-199a-5p determined in duplicates in a qPCR assay (n=3). The miR-199a-5p levels are presented normalized to the miRNA amount derived from natural pre-miRNA processing. **(B) Influence of miR-199a expression on mRNA level of *SMAD4* and *DDR1* after genomic integration.** To examine the effect of genomically expressed miR-199a on *SMAD4* and *DDR1* mRNA levels, 0.9 x 10^5 HF1-3 cells expressing the natural miR-199a precursor or pre-miR switch miR-199a_2 were seeded into 12-well plates and incubated for 24 h. Afterwards, total RNA was isolated and mRNA levels of the miR-199a target SMAD4 and DDR-1 were assessed in qPCR. The mRNA levels are shown normalized to the mRNA amount of non-integrated HF1-3 cells. The measurements were performed in duplicates (n=2).

Regardless of the loss of the efficient switching characteristic, the impact of a constant miRNA-199a overexpression on the mRNA level of *SMAD4* and *DDR1* in the cell was determined. The graph in Figure 3.15 B clearly shows that no decrease of the *SMAD4* mRNA level arose due to miR-199a presence for the control with the natural miRNA precursor (miR-199a), whereas miR-199a presence derived from the pre-miR switch (miR-199a_2) evoked a strong decline of the mRNA level to about 40% compared to the mRNA level provided by the untreated HF1-3 cells. In contrast to the inconsistent behavior seen for *SMAD4*, the chromosomal expression of miR-199a-5p from both integration HF1-3 cell lines elicited a comparable reduction of *DDR1* mRNA ranging from 50% to 40% of the mRNA level of the non-integrated cells.
It may be assumed, that *SMAD4* mRNA regulation was influenced by other unexpected factors. Since the expression level of miR-199a based on natural precursor processing usually excelled the miR-199a level derived of the pre-miR switch, a comparable or even stronger reduction of the mRNA level was to be expected. The expectations were met in case of *DDR1* where at least a similar decline of the mRNA level could be observed for miRNAs-199a-5p independent of the origin. Due to the emergence of that unknown factor that influenced *SMAD4* regulation, this miRNA target was abrogated from further analyses.

The western blot in Figure 3.16 B shows the DDR1 protein amount derived from the non-integrated HF1-3 cells (HF) and the cells harboring the natural precursor (199a) and the pre-miR switch (199a_2) chromosomally integrated into their genome, after 24 and 48 h. After 24 h a reduction of band intensity could be observed for the samples subjected to miR-199a-5p expression, supporting the findings from the measurement of *DDR1* mRNA levels. This effect was more distinct for the samples expressing miR-199a from the natural precursor. But also in sample 199a_2 the intensity of the DDR1 bands still exhibited a comparably lower band intensity compared to the untreated HF cells after 24 h. That tendency was also reflected in the western blot performed after 48 h. At least the protein amount in miR-199a-5p presence derived from the natural precursor seemed to be reduced, whereas the protein amount for the cells with the integrated pre-miR switch exhibited a DDR1 protein amount comparable to that of the HF cells despite of miR-199a-5p attendance.
These findings indicated a presumable interaction of miR-199a-5p, processed from both, the unmodified and the modified precursor, with *DDR1*. Considering the results from mRNA measurement and western blotting of DDR1, it could be deduced that the genomic integration accompanied by a constitutive expression of miR-199a was advantageous with regard to *DDR1* target regulation.

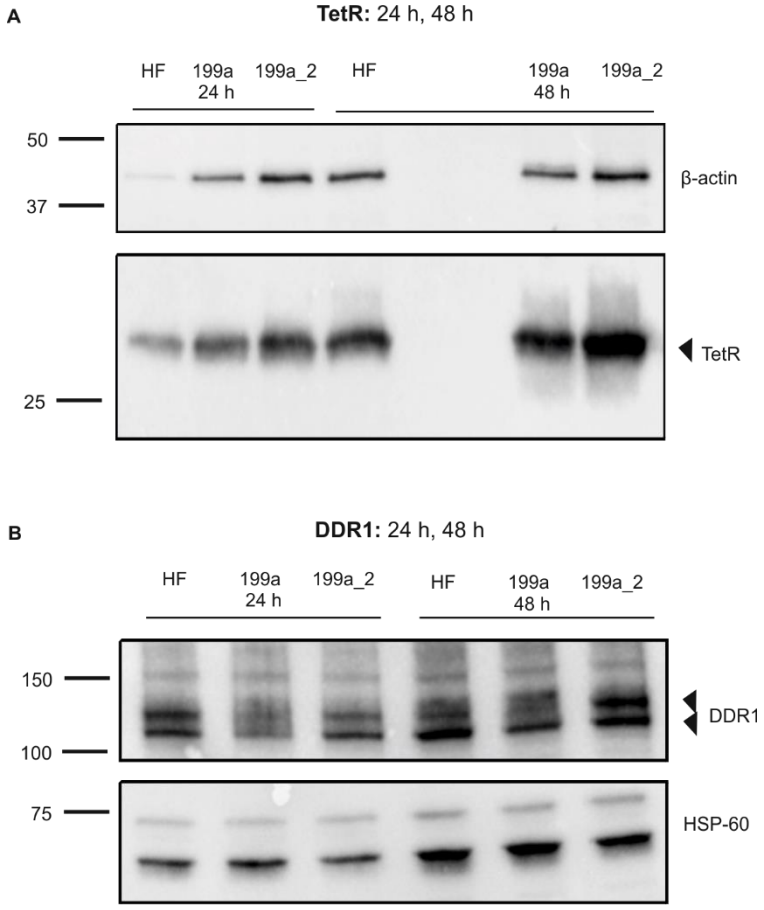

Figure 3.16 (A) TetR expression after transient transfection of HF1-3 cells. For the visualization of TetR in a western blot, 0.9 x 10^5 HF1-3 cells either carrying no construct (HF), the natural miR-199a precursor (miR-199a) or the pre-miR switch miR-199a_2 (miR-199a_2) integrated in the genome were seeded into 12-well plates and transiently transfected with the TetR expression plasmid. Cells were lysed 24 h or 48 h after transfection and 40 µg of total protein was analyzed in an SDS-PAGE. Total protein was blotted onto a PVDF membrane and TetR (24 kDa) visualized using HRP-conjugated secondary antibodies with a chemiluminescence substrate. β-actin (42 kDa) was used as loading control. Protein sizes are indicated in kDa. **(B) Influence of miR-199a construct integration on DDR1 protein level.** To test the influence on DDR1 protein expression, 0.9 x 10^5 of the non-integrated (HF) and the stably integrated HF1-3 cells (199a, 199a_2) were seeded into 12-well plates and incubated for either 24 h or 48 h. Afterwards, cells were lysed, 40 µg of total protein analyzed in an SDS-PAGE and blotted onto a PVDF membrane. DDR1 (100 kDa, 125 kDA) was visualized using HRP-conjugated secondary antibodies with a chemiluminescence substrate. HSP-60 (60 kDa) was used as a loading control. Protein sizes are indicated in kDa.

3.5.3 Genomic integration of pre-miR switch miR-199a_2 and TetR

A second genomic integration was performed where the natural precursor or the pre-miR switch were integrated together with TetR into the genome of HF1-3 cells. This approach aimed to prevent the constitutive expression followed by an accumulation of miR-199a-5p through a concurrent expression of the aptamer ligand TetR and the pre-miR switch miR-199a_2. Additionally, the cell was not under permanent influence of an endogenously absent miRNA that possibly changes cellular processes through unpredictable primary and secondary effects.

Genomic integration was performed as described earlier. The only variation consisted in the composition of the transfected integration plasmid that now additionally harbored the TetR expression gene under control of a SV40 promoter (Fig. 3.17). After selection, first, the dynamic range of the pre-

miR switch was examined after 24 h, 48 h and 5 d of dox incubation. Therefore, the selected and the control HF1-3 cells were seeded into 12-well plates and incubated with dox after 24 h. Cells were harvested after 24 h, 48 h and 5 d of dox incubation and total RNA was isolated, miRNA-199a-5p was reversely transcribed and qPCR measurements were performed to assess the amount of mature miR-199a-5p. In case of the 5 d incubation the medium was changed after two days and freshly supplemented with 1 µg/ml dox.

Furthermore, the expression of TetR was tested after genomic integration and visualized in a western blot. For this purpose, the cells expressing the natural miRNA-199a precursor (199a) or the pre-miR switch miR-199a_2 (199a_2) and non-integrated HF1-3 cells (HF) were seeded into 12-well plates and incubated for 24 h or 48 h at 37°C. Then, cells were lysed and 40 µg of total protein analyzed in an SDS-PAGE. Afterwards, total protein was blotted onto a PVDF membrane and TetR was detected using HRP-conjugated secondary antibodies with a chemiluminescence substrate. As a loading control β-actin was used.

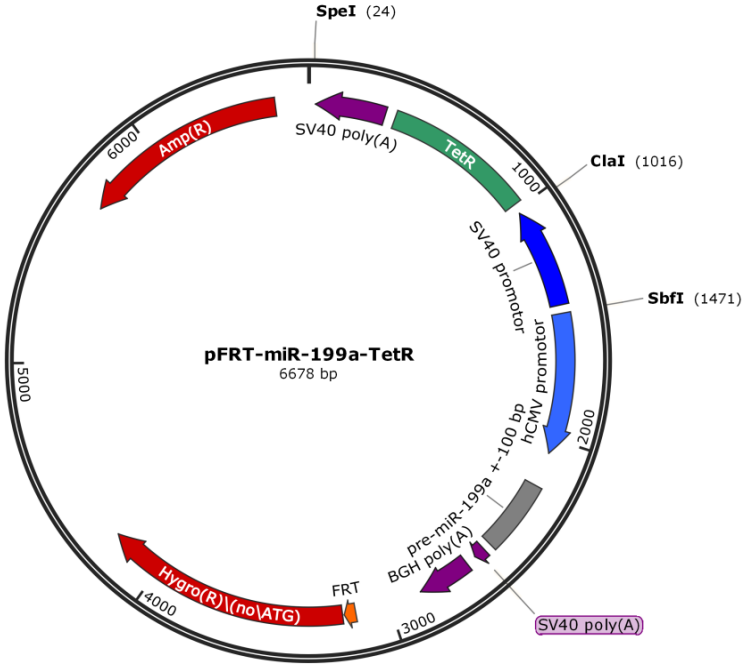

Figure 3.17 Plasmid map of pFRT-miR-199a-TetR.
The plasmid map schematically shows the composition of plasmid pFRT-miR-199a-TetR used for the genomic integration of the natural miRNA-199a precursor or pre-miR switch miR-199a_2 together with TetR. The constructs were expressed under control of an hCMV promoter (blue), whereas TetR expression was driven by an SV40 promoter (darker blue). The FRT-site (orange) for genomic integration is located upstream of the hygromycin B resistance gene (Hygro(R)\(no\ATG), red) that lacks a promoter and a start codon.

Figure 3.18 A clearly shows an efficient suppression of pre-miRNA processing to 1.4% of mature miRNA compared to the natural precursor-based miR-199a-5p expression according to the simultaneous expression of miR-199a_2 and TetR after genomic integration. The supplementation with dox resulted in a 12-fold increase of the amount of mature miRNA-199a-5p after 24 h up to 17%. This 17% of expression exactly agreed with the value obtained after the first genomic integration. The elevated miRNA expression level was also conserved after 48 h of dox incubation. Even after 5 d of incubation, a 9-fold elevation of the amount of the mature miRNA-199a-5p up to 15% in comparison to

the natural precursor appeared (Fig. 3.18 A right). These findings corresponded with the results obtained from time course experiments and confirmed that pre-miRNA processing was completely reconstituted within 24 h of incubation with dox. The western blot for TetR detection confirmed the successful integration and expression of TetR in the samples that derived from HF1-3 cells either harboring the natural precursor or the pre-miR switch integrated in their genome (Fig. 3.18 B).

Basically, the genomic integration including TetR restored the efficient switching characteristic of the pre-miR switch. Thus, repression due to TetR binding was reversible upon dox addition and found to be stable for at least 5 d. Supporting this observation, it could also be verified that TetR was present in all cells that were subject to genomic integration. But the genomic integration of the pre-miR switch resulted in a lower pre-miR switch expression and a strong loss of dynamic range compared to the effects seen after transient transfection.

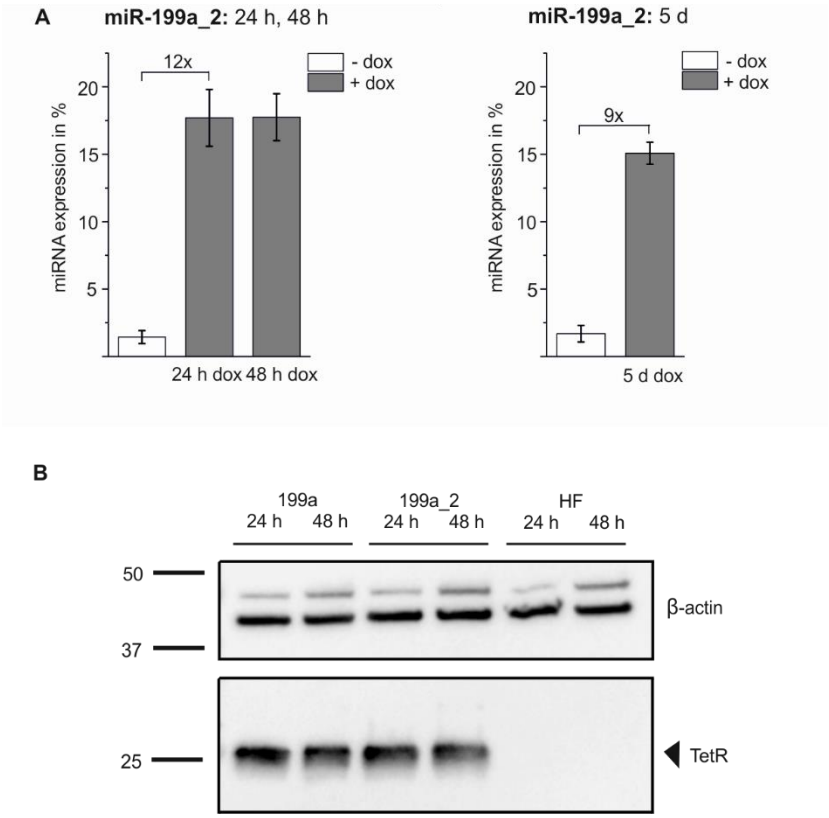

Figure 3.18 (A) TetR- and dox-dependent regulation of mature miRNA-199a after genomic integration of pre-miR switch miR-199a_2 and TetR. For identifying the switching efficiency after genomic integration of the constructs and TetR, 0.9 x 10^5 HF1-3 cells possessing the natural miR-199a precursor or pre-miR switch miR-199a_2 integrated in their genome were seeded into 12-well plates and treated with 1 µg/ml dox for either 24 h, 48 h (left) or 5 d (right). Then, total RNA was isolated and the amount of mature miRNA-199a-5p assessed in duplicates in a qPCR assay (n=3). The miR-199a-5p levels are presented normalized to the miRNA amount derived from natural pre-miRNA processing. **(B) TetR expression after genomic integration.** For verifying the successful integration of TetR into the genome at the protein level a western blot was performed. 0.9 x 10^5 HF1-3 cells harboring no construct (HF), the natural miR-199a precursor (miR-199a) or the pre-miR switch miR-199a_2 (miR-199a_2) together with TetR integrated in the genome were seeded into 12-well plates and incubated for 24 h or 48 h. Then, the cells were lysed and 40 µg of total protein analyzed in an SDS-PAGE. Total protein was blotted onto a PVDF membrane and TetR (24 kDa) visualized using HRP-conjugated secondary antibodies with a chemiluminescence substrate. β-actin (42 kDa) was used as loading control. Protein sizes are indicated in kDa.

After ascertaining that the pre-miR switch and TetR expression were functional after genomic integration, the effect of dox supplementation on DDR1 protein level was examined. Additionally, *CAV1* that constitutes another validated target of miR-199a-5p, was adjoined to explore the impact of pre-miR switch-controlled processing on CAV1 protein (22 kDa) expression. HF1-3 cells, either without integration (HF), expressing the integrated natural precursor (199a) or the pre-miR switch (199a_2) were treated with dox for 24 h, 48 h or 5 d. Then, cells were harvested, lysed and 40 µg of total protein were analyzed in an SDS-PAGE. Afterwards, total protein was blotted onto a PVDF membrane and DDR1 and CAV1 were detected using HRP-conjugated secondary antibodies with a chemiluminescence substrate. As loading controls either HSP-60 or β-actin were employed.

Basically, the western blots showing protein DDR1 revealed no significant reduction of the protein amount due to miR-199a-5p presence. For the samples 199a that expressed miR-199a-5p from the natural precursor, a weak reduction of the intensity of the upper band was observed in Figure 3.19 A and B compared to sample HF. This detected change at the protein level was completely abolished for the samples 199a_2 (A)/ _2 (B) with miR-199a-5p derived from the pre-miR switch miR-199a_2 hinting at too little amounts of mature miRNAs being processed under the present conditions. Comparing the band intensity of 199a_2 and 199a_2 24 h, no noticeable alteration of DDR1 protein levels was determined after 24 h of dox incubation. The western blot showing the samples after 48 h of dox incubation allowed no clear conclusion with regard to a potential dox effect due to the low band intensity revealed by the samples that were not treated with dox. The western blot, displayed in Figure 3.18 B, showed no relevant alteration in DDR1 protein amount as response to dox presence for samples _2 5 d.

Considering the results from the CAV1 protein expression, another interesting phenomenon was uncovered in Figure 3.20. The constitutive overexpression of miR-199a from the natural miRNA precursor consistently yielded a strong increase of CAV1 protein expression visible in samples 199a compared to all HF samples. Integration of the pre-miR switch, entailing a lower amount of mature miRNA-199a, showed a comparably weak increase of the amount of CAV1 protein for the samples _2 after 5 d. Equally to DDR1, no response to dox addition in form of an accompanying increase of miRNA-199a amount was reflected at CAV1 protein level neither after 24 h, 48 h nor even 5 d of incubation. Actually, the western blot for the samples after 5 d of incubation with dox was repeated four times with independently prepared samples, but for sample _2 and _2 5 d strong fluctuations in band intensity were determined prohibiting a clear statement to a potential, dox-related effect.

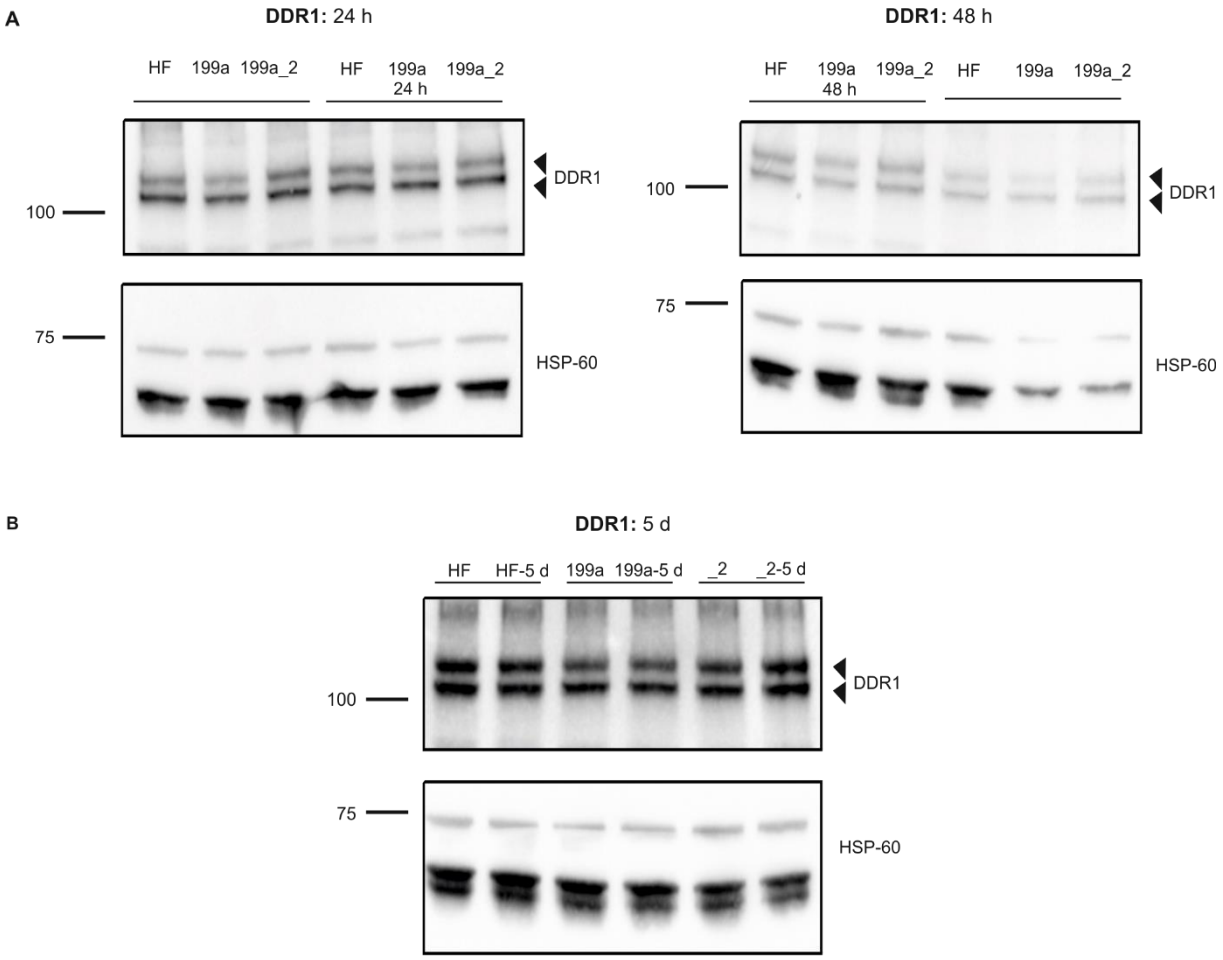

Figure 3.19 Influence of dox-dependent regulation of pre-miR switch miR-199a on DDR1 protein levels after 24 h and 48 h (A) or 5 d (B) of incubation. For monitoring the effect of pre-miR switch based regulation of miR-199a processing at the DDR1 protein amount a western blot was performed. 0.9 x 10^5 HF1-3 cells either carrying no construct (HF), the natural miR-199a precursor (miR-199a) or the pre-miR switch miR-199a_2 (miR-199a_2, (B) _2) together with the TetR expression sequence in the genome were seeded into 12-well plates and incubated with 1 µg/ml dox for 24 h, 48 h and 5 d. Subsequently, the cells were lysed and total protein was analyzed in an SDS-PAGE. Then, total protein was blotted onto a PVDF membrane and DDR1 (100 kDa, 125 kDa) was visualized using HRP-conjugated secondary antibodies with a chemiluminescence substrate. HSP-60 (60 kDa) was used as loading control. Protein sizes are indicated in kDa.

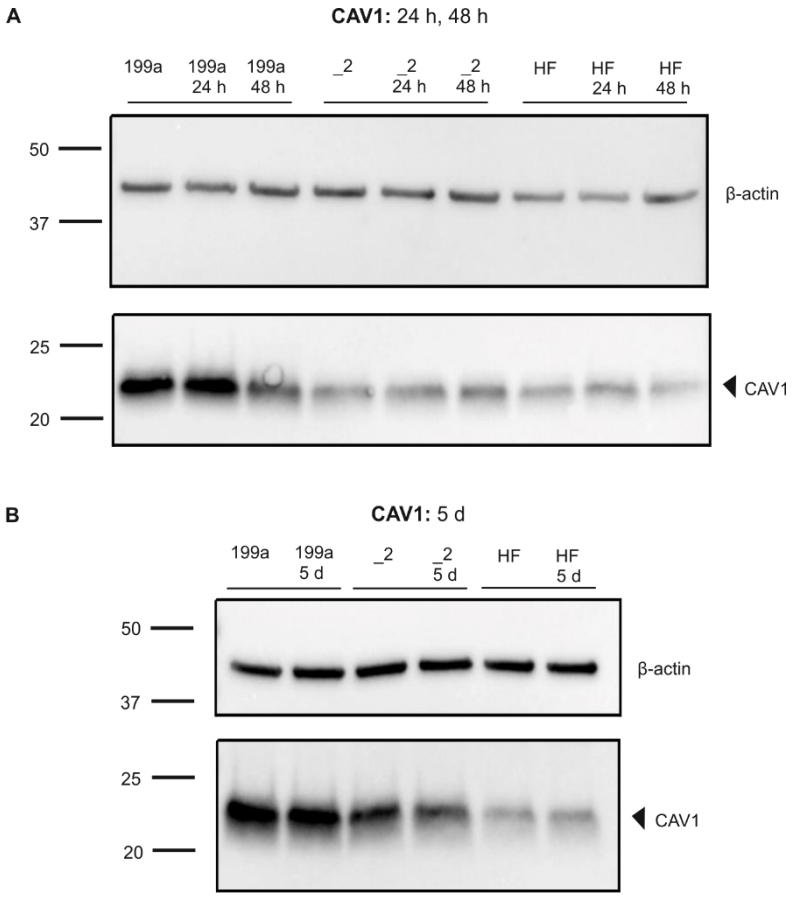

Figure 3.20 Influence of dox-dependent regulation of pre-miR switch miR-199a on CAV1 protein levels after 24 h and 48 h (A) or 5 d (B) of incubation. To check for an effect at the CAV1 protein level after genomic integration of the constructs and TetR a western blot was performed. 0.9 x 10^5 HF1-3 cells either featuring no construct (HF), the natural miR-199a precursor (miR-199a) or the pre-miR switch miR-199a_2 (_2) together with the TetR expression sequence in the genome were seeded into 12-well plates and incubated with 1 µg/ml dox for 24 h, 48 h and 5 d. Subsequently, the cells were lysed and 40 µg of total protein analyzed in an SDS-PAGE. Then, proteins were blotted onto a PVDF membrane and CAV1 (22 kDa) visualized using HRP-conjugated secondary antibodies with a chemiluminescence substrate. β-actin (42 kDa) was used as loading control. Protein sizes are indicated in kDa.

In parallel to the determination of protein levels, the mRNA levels of the miR-199a-5p targets *DDR1* and *CAV1* mRNA levels were monitored by qPCR (Fig. 3.21). Concordant with the results from western blotting, a weak diminishment of the amount of mRNA by 10-20% could be measured for *DDR1* in sample 199a after 24 h and 48 h of dox incubation (Fig. 3.21 A left). In contrast, the mRNA amount determination of the samples stably expressing pre-miR switch 199a_2 disclosed a weak increase of 10-20% in all measurements. After 5 d of dox incubation the mRNA levels of *DDR1* were comparable for the HF1-3 cells without integration, whereas the expression after the integration of pre-miR switch miR-199a_2 was elevated for about 40% compared to the expression of HF1-3 cells (Fig. 3.21 A right).

The assessment of *CAV1* mRNA level supported the results obtained at the protein level (Fig. 3.21 B). The presence of miR-199a-5p derived from the natural miRNA precursor led to a 2-fold increase after 24 h and 48 h and an up to 4-fold increase in mRNA observed after 5 d of dox incubation. No change of the mRNA amount of *CAV1* was present for the sampled expressing the pre-miR switch miR-199a_2 after 24 h and 48 h. Merely, a weak increase of the mRNA level of about 10% became

obvious for the samples that genomically expressed the pre-miR switch miR-199a_2. Also *CAV1* mRNA levels remained unaffected by the presence of dox.

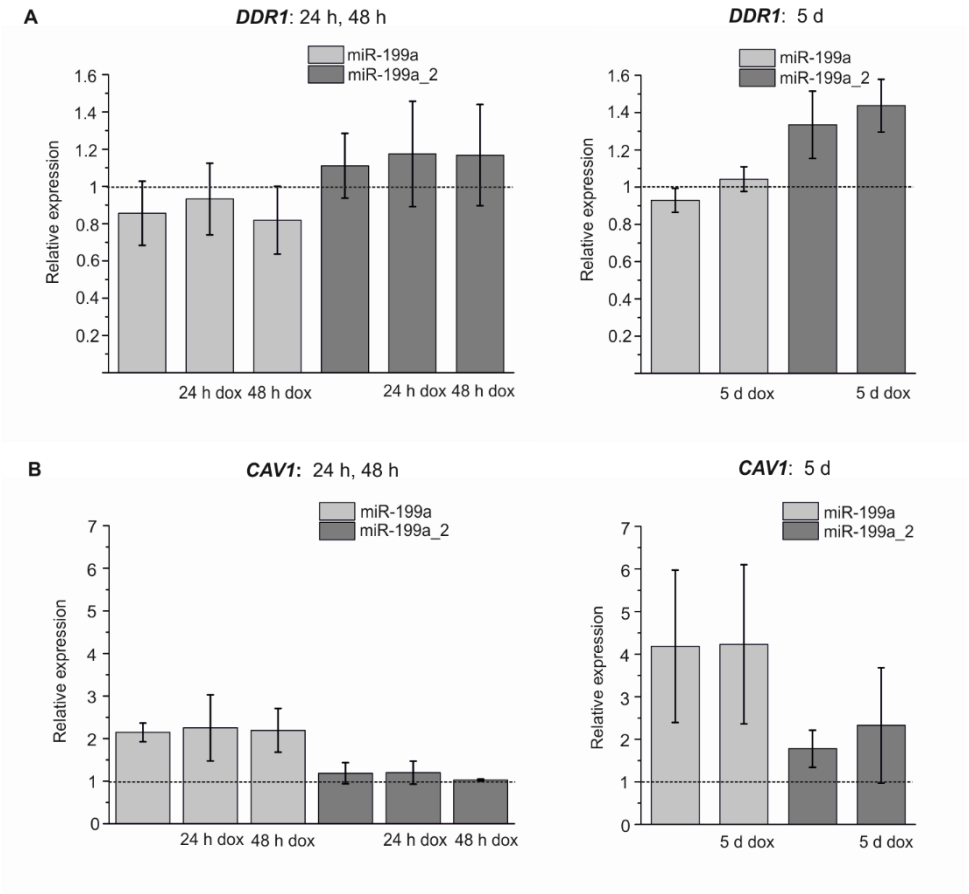

Figure 3.21 Influence of stable miR-199a expression on mRNA level of *DDR1* (A) and *CAV1* (B) after 24 h, 48 h and 5 d of dox incubation. To explore the effect of genomically expressed miR-199a at the *DDR1* and *CAV1* mRNA level, 0.9 x 10^5 HF1-3 cells harboring the natural miR-199a precursor or pre-miR switch miR-199a_2 were seeded into 12-well plates and incubated for 24 h, 48 h or 5 d with 1 µg/ml dox. Afterwards, total RNA was isolated and mRNA levels of the miR-199a target *DDR1* and *CAV1* were assessed in qPCR. The mRNA levels are shown normalized to the mRNA amount of *DDR1* and *CAV1* of non-integrated HF1-3 cells. The measurements were performed in duplicates (n=3, n=2 for (A) right and (B) left).

At last, an experiment was performed to check whether a relation between a constitutive expression of miR-199a and the strongly elevated mRNA and protein level of CAV1 exists. For that purpose, a transient co-transfection of HeLa cells with either an empty plasmid (MS), the natural miRNA precursor (199a) or pre-miR switch miR-199a_2 (199a_2) together with the TetR expression plasmid was performed. 1 µg/ml dox was supplemented 3 h after transfection. Cells were harvested 24 h after transfection, lysed and 40 µg of total protein was analyzed in an SDS-PAGE. Then, proteins were blotted onto a PVDF membrane and the protein amount of CAV1 visualized on a western blot using HRP-conjugated secondary antibodies with a chemiluminescence substrate. β-actin was used as loading control.

Looking at the western blot presented in Figure 3.22, no relevant alteration of the CAV1 protein level regardless of the presence of miR-199a-5p, TetR or dox occurred 24 h after transient transfection. This, in turn, strengthened the assumption that the strong increase of *CAV1* mRNA and CAV1 protein arose as a consequence of the long-time exposure to miR-199a-5p.

To come to a conclusion for the experiments after genomic integration, the results hinted at a very weak response of *DDR1* and an intense, but unexpected response of *CAV1* to miR-199a-5p presence at both, the protein and the mRNA level. Apart from that, primarily the expression level of mature miR-199a-5p processed from the pre-miR switch seemed to be too low to cause a significant effect at the mRNA or/ and the protein level. Consequently, the efficient regulation of the miRNA-199a-5p level provided by the pre-miR switch could not be demonstrated in the present experimental setup.

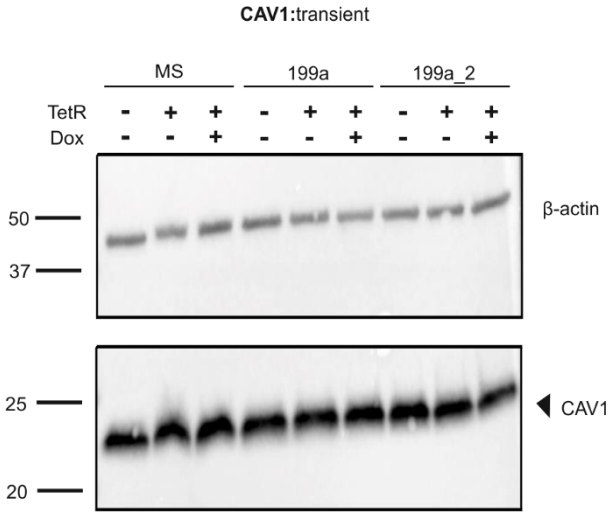

Figure 3.22 Influence of TetR-dependent regulation on CAV1 protein levels after transient transfection of the pre-miR switch miR-199a and TetR. For the visualization of a potential effect at the regulation of CAV1 protein level due to transient transfection of the pre-miR switch miR-199a_2 and the TetR expression plasmid, a western blot was prepared. Therefore, 1.4 x 10^5 HeLa cells were seeded into 12-well plates and transfected with either the empty plasmid (MS) or a plasmid containing the natural miR-199a precursor (199a) or the pre-miR switch miR-199a_2 (199a_2). Also, the TetR expression plasmid was co-transfected and 1 µg/ml dox was added 3 h after transfection. 24 h after transfection, the cells were lysed and total protein was analyzed in an SDS-PAGE. Afterwards, proteins were blotted onto a PVDF membrane and CAV1 (22 kDa) detected using HRP-conjugated secondary antibodies with a chemiluminescence substrate. β-actin (42 kDa) was used as loading control. Protein sizes are indicated in kDa.

4 Discussion

The elucidation of miRNA-related phenotypes requires an understanding of the particular cellular function of a certain miRNA. A disease-dependent, aberrant tissue-specific expression of a miRNA may yield first insights into its involvement in a specific disease pattern. In various cancer types and other human diseases, a distinct miRNA expression profile can often be observed that is directly linked to disease development (reviewed in [152]). The correlation between the potential target protein abundance and the respective miRNA level is investigated to get more detailed information about miRNA participation. Such experiments constitute a passive way to shed light on possible miRNA-target interactions and merely allow assumptions about how a given miRNA affects the cellular function, neglecting the detailed knowledge about the exact mode of miRNA action and the specific target.
A distinct exploration of miRNA function may be achieved through the directed overexpression or knockdown of the implied miRNA to observe the associated effects on cellular processes. A “gain-of-function” study is often implemented by using miRNA mimics, whereas a “loss-of-function” study is usually performed with modified antisense oligonucleotides that inhibit miRNA-target interactions through the sequestration of the miRNA. These chemically modified RNA-based oligonucleotides are easily to handle, but due to their modifications conferring enhanced stability, their half-life is often longer than the half-life of the naturally derived miRNAs, leading, in turn, to a non-physiological persistence and putative side effects.

In this work, a specific synthetic tool was developed that was intended to exploit controlled miRNA processing to explore miRNA function under more physiological conditions, bypassing the issues summarized previously. As such, a design concept for an RNA-based switch was pursued that would account for the structure of the natural precursor and the substrate recognition features of the cellular machinery required for miRNA maturation. The design was thus focused on the modification of the pre-miRNA to render its processing dependent on a reversible, external effector system. Ultimately, the miRNA precursor was linked to the TetR aptamer, restricting access to the Dicer cleavage sites in presence of its cognate ligand, TetR. Dox was then used to prevent TetR binding to the aptamer and, hence, to restore miRNA processing to the original activity.

4.1 Evaluation of design and functionality of the pre-miR switches

A design concept based on the direct or one bp fusion of the aptamer to the miRNA precursor stood out due to its characteristics of adequate precursor processing, efficient processing inhibition and complete reversibility. The design of pre-miR switch miR-126_5 turned out to be completely transferable to another two miRNA precursors, yielding comparable results with regard to the performance of the switch.

Evaluating the basic strategy of the pre-miR switch design and the selection of the insertion site for the TetR aptamer into the natural precursor, the Dicer cleavage sites could be successfully occupied in

the presence of TetR, leading to a nearly complete inhibition of processing. Consequently, the stability of the respective closing stem of the aptamer that was formed by the communication module and the stem region of the natural precursor seemed to be sufficient to serve as stabilizing scaffold for the TetR binding pocket and, thus, to facilitate ligand binding for all functional pre-miR switches. In a comparable approach to manipulate Dicer processing of shRNAs, Saito and coworkers exploited either protein-binding motifs for the human U1A protein and the snoRNA binding protein L7Ae or the p50-binding aptamer integrated into the loop region of the shRNA for regulating Dicer cleavage [153]. Similar to the present study, they chose the terminal loop to introduce their sensor elements into the shRNA and were able to regulate shRNA processing by imposing steric hindrance on the processing machinery. Although they employed different proteins and binding modes compared to the presented system, they demonstrated that the interference with the processing machinery poses a valuable opportunity to control small ncRNA levels. Furthermore, the protective binding of human Dicer to the terminal loop was demonstrated in an enzymatic probing experiment with the S1 nuclease [154]. The fact that Dicer seems to directly interact with the terminal loop further supports the basic idea of the design approach developed in this study.

In this context it should be noted that the modifications intended to regulate Dicer processing may have also influenced Drosha processing. Several substrate recognition features relevant for Drosha activity are known to reside in the terminal loop structure that was removed and replaced by the TetR aptamer in this study [54]. Here, northern blotting experiments could help to determine the amounts of present miRNA and pri-/pre-miRNA species and, thus, poses an adequate measure to provide evidence for a selective inhibition of Dicer processing as a consequence of TetR binding.

Generally, the replacement of the natural terminal loop structure with the TetR aptamer was observed to result in a distinct reduction of processing in comparison to the natural precursor, dependent on the used communication module. The variation of the communication module for coupling the miR-126 precursor with the TetR aptamer revealed that the replacement of the terminal loop was merely tolerated in combination with a very short C-G bp bridging the area between the aptamer and the precursor stem. It is a well-known effect in synthetic biology that the presence of a stable secondary structure like an aptamer strongly influences the level of gene expression (reviewed in [125]). Zeng and coworkers mutated the natural terminal loop of several miRNAs with regard to size and flexibility and found that Dicer prefers large flexible loop structures for processing [62]. As confirmed in an in-line probing by Hunsicker *et al*., the TetR aptamer constitutes a stable secondary structure that was inserted into the into the loop position of the precursor and therefore affected Dicer processing [136].

Furthermore, the terminal loop structure was shown to be highly conserved for some miRNAs and to harbor essential recognitions sites relevant for processing by Drosha and Dicer [155]. Michlewski *et al.* demonstrated that 14% of all pri-miRNAs possess terminal loops, which were well conserved throughout evolution [156]. In their experiments they identified a binding site of the heterogeneous nuclear ribonucleoprotein A1 (hnRNP A1) in the terminal loop region of pri-miR-18a. The interaction of hnRNP A1 with the miR-18a precursor loop was proven to cause a relaxation at the stem region that, in turn, creates a more favorable substrate structure for the processing by Drosha. What is more, the presence of a binding site for hnRNP A1 was also found to be located in the terminal loop of pri-miR-101-1 and a mutation analysis of the critical loop region appeared to almost completely abrogate

processing. A conserved terminal loop was also found to be existent in pri-miR-101-2. In this study, the replacement of the terminal loop structures of both miR-101 precursors also led to an abolishment of processing. Given this background, it is not surprising that a modification within a significant part of a natural miRNA precursor causes a reduction of processing efficiency.
Thus, the mentioned aspects could be related to the decrease or even the loss of precursor processing. Consequently, a restriction of modification to a particular set of miRNA precursors, including the precursors that are not reliant on their terminal loop structure for miRNA maturation, is conceivable.

The functionality of hybrid constructs, such as the pre-miR switch, strongly depends on the linker domains between the inherently different parts. According to this, one of the most challenging aspects in the design of a pre-miR switch was constituted by the adequate fusion of the TetR aptamer and the natural miRNA precursor through a communication module in a way that facilitated aptamer functionality and preserved miRNA biogenesis at the same time. Therefore, communication modules varying in length and stability were tested for the design of a pre-miR switch based on the miR-126 precursor. With the exception of a simple C-G bp, all communication modules impacted pre-miR switch processing to similar extents. Their introduction led to the abolishment of processing as they created non-cognate Dicer substrates either due to an improper stem length (three bp stem) or structural elements like mismatches or bulges. Considering the various structures of Dicer substrates, including miRNA precursors, it can be assumed that Dicer is very flexible with regard to its processing activity, but negative effects on Dicer cleavage due to lengthy or bulky structures have already been observed. Zhang and coworkers proposed a relation between Dicer processing efficiency and precursor stem length [155]. The Kay group demonstrated the dependence of Dicer cleavage accuracy on the position of loop structures in the precursor stem [157]. Taylor *et al.* also supported the hypothesis that the precursor length influences Dicer cleavage efficiency, since overlong substrates were supposed to disturb necessary conformational rearrangements of single domains within Dicer indispensable for adequate processing [158]. Nevertheless, due to the fact that the detailed Dicer mechanism still remains to be elucidated, a definitive correlation between miRNA precursor structure and enzyme activity cannot be stated yet.
During the design of further constructs based on the miR-34a and miR-199a precursors, the direct or one bp fusion of the aptamer to the precursor stem yielded an appropriate processing efficiency and pre-miR switch performance. Thus, the design concept revealed to be completely transferable to another two miRNA precursors. Similar to the findings presented in this work, Yokobayashi and coworkers designed a hybrid molecule composed of a theophylline aptamer and an shRNA with the purpose to control Dicer processing and observed that a direct fusion resulted in the best regulation of eGFP expression [129].

4.2 Regulation of reporter gene expression dependent on TetR and dox

Reporter gene assays are a frequently used method to investigate the direct interaction of a miRNA with the respective binding site of a target mRNA. In this work, the results obtained from reporter gene assays confirmed that the miRNA expression levels as well as the regulatory efficiency arising from

the pre-miR switch application are capable to notably influence reporter gene expression and thereby support the observations from qPCR.

The binding of a miRNA to its perfect complement does not resemble the natural mechanism in mammals and is therefore merely used as a positive control to confirm miRNA presence and binding to the sequences located downstream of the reporter gene. In the perfect match binding assay, the binding of all miRNAs derived from the respective pre-miR switch was shown to efficiently regulate gene expression. Due to perfect binding of the miRNA to the complementary target sequence, the maximal inhibitory effect under the given experimental conditions can be assessed. Thus, the regulatory factors exceeded the factors seen for their natural counterparts. Still, the interactions of all miRNAs originating from the processing of the pre-miR switch, except miR-199a-3p, with the natural target sites were successfully demonstrated. Considering the raw data with respect to regulatory activity, it is remarkable that the presence of TetR in parallel to the pre-miR switches resulted in firefly luciferase expression that was comparable with the reporter gene expression in the absence of the respective miRNA. This hints at a complete inhibition of the miRNA-target interaction by TetR and shows that the pre-miR switch is capable of tapping the full potential under the given conditions. Another interesting fact is that the regulatory efficiency of the miR-126 and -199a-derived pre-miR switches was 70-90% of the maximal, theoretical switching performance that could have been achieved with the miRNA amount obtained from the processing of the natural precursor. In contrast, about 45-50% of the maximal performance was observed for the miR-34a-dependent pre-miR switches. This can be attributed to the reduced processing efficiency (~12%) compared to the unmodified miR-34a precursor.

In general, a comparison between the dynamic ranges of different synthetic systems is often drawn to assess the value of the developed device. Here, a direct comparison of the performance of the developed pre-miR switches with other published regulatory tools is rather difficult due to alterations in the experimental setups. The Beckebaum group inserted a comparable part of the 3'UTR of *DDR1* also containing all four predicted target sites for miR-199a-5p downstream of a reporter gene and transfected HepG2 cells with chemically modified pre-miRNAs [111]. This arrangement yielded a 2.5-fold change of relative expression, which covers a similar range of efficiency as the factor determined for the *DDR1* 3'UTR insertion, testing the regulatory activity of pre-miR switch miR-199a_2. However, the particular results were obtained under a completely different experimental setup. Generally, the regulatory efficiency in a reporter gene assay strongly depends on factors concerning the experimental environment and target site selection itself. The transfection efficiency as well as the transfected amount of plasmid used for reporter gene and miRNA expression are crucial for the experimental outcome, as they directly determine the ratio of the miRNA and the cognate target site and, thus, also stochasticity of the miRNA-target interaction. With regard to this, the total number of plasmids used to transfect the cells is also essential for the same reason as mentioned before. Furthermore, the employed cell type and its transcriptional program are decisive and can affect specific miRNA-target interactions. Often, cancer cells reveal unexpected target modifications like point mutations or shortened 3'UTRs that can be accompanied by a loss of miRNA binding [159,160].

Additionally, the methods for miRNA target validation per se have to be seen critical. Most experiments are performed utilizing chemically modified miRNA mimics or precursors, often leading to

supra-physiological concentrations of miRNAs that is followed by non-specific alterations in gene expression and a saturation of the miRNA system [161]. A dramatic overexpression of a miRNA might directly influence the stoichiometric ratio of the miRNA-target site interaction and, thus, result in an occupation of not only all high- , but also many low-affinity binding sites. Consequently, false-positive results could be generated due to a shift of interaction that causes an inclusion of low-affinity binding sites normally not considered under natural conditions. Consequently, the currently applied methods are often far away from mirroring the naturally occurring miRNA-target interactions.
To gain confidence about the authenticity of a miRNA target and the exact target sites, a combination of functional assays and biochemical validation methods reflecting the physiological interactions between miRNA and target mRNA should be considered. An example of a powerful method to provide information about miRNA-target interaction under physiological conditions is a cross-linked immunoprecipitation followed by high-throughput sequencing (HITS-CLIP). This way, direct binding of the miRNA-RISC to a specific part of the target mRNA can be confirmed by cross-linking both components followed by sequencing analysis [162].

Although the miRNA-199a-3p targets *CAV2*, *MET* and *CD44* were validated by at least reporter gene assays, western blotting and RT-qPCR, a direct interaction with miR-199a-3p could not be confirmed in the reporter gene assays in this work. The presence of the mature miR-199a-3p was shown by qPCR and a regulatory effect on reporter gene expression was detected for the positive control. Analyzing the raw data obtained from the reporter gene assay, also no regulatory activity based on the naturally derived miRNA-199a-3p became apparent, although natural pre-miRNA processing led to demonstrably higher intracellular levels of mature miRNA than pre-miR switch processing. Accordingly, the reason for the missing regulation remains elusive.
As mentioned above, miRNA-target interactions can be strongly dependent on the cellular context and the experimental setup. Thus, the source and the quality of the 3'UTR bearing the respective miRNA binding sites could also be pivotal for miRNA binding. Due to the fact that the 3'UTRs were cloned from genomic HeLa DNA, it cannot be excluded that cell line-related point mutations or deletions have rendered the predicted target sites inactive. The importance of the employed cell type was highlighted by experiments from the Nares group that demonstrated the dependence of miRNA regulation strength on the respective cell line, thereby suggesting that different cell lines also exhibit varying levels of regulation [163]. Even the usually applied cell lines HEK-293 and HeLa revealed strong differences with regard to gene regulation in their experiments. Since all of the published luciferase assays investigating the interaction of miRNA-199a-3p and the respective target genes have been performed using either modified pre-miRNAs or miRNA mimics and different cell lines than HeLa, the experimental outcome may not show the same effect with regard to miRNA targeting.
At that point, evidence for the integrity of the HeLa cell-derived 3'UTR utilized in this work could be provided by conducting specific amplification and sequencing of the respective target sites. To exclude a potential influence of the cellular context, an alteration of the cell system should be considered to reassess the interaction between miR-199a-3p and the targets.

4.3 Regulation of endogenous miRNA-199a-5p targets with miR-199a_2

In a luciferase assay, the interaction between a miRNA und its potential target sequences is explored under unnatural conditions. Therefore, a positive outcome of such an assay can only serve as a positive indicator and the regulation has to be further investigated under more authentic cellular conditions. For testing the endogenous regulatory activity of pre-miR switch miR-199a_2, it was either expressed transiently or integrated into the genome. The validated targets *SMAD4*, *DDR1* and *CAV1* were employed to analyze the influence of the miR-199a_2 activity on regulating their mRNA and protein levels after different time points.

Although the first tested target, *SMAD4*, harbors three predicted target sites in its 3'UTR, no regulation either at the mRNA or the protein level that hints at a direct correlation between miR-199a presence and SMAD4 could be observed [164]. Until today, evidence of *SMAD4* being a direct target of miRNA-199a has only been provided by one group that conducted luciferase assays in NIH-3T3 cells to demonstrate the interaction between miRNA and *SMAD4* 3'UTR [110]. The performance of a luciferase assay, in which the natural precursor was transiently expressed from a CMV promoter, resulted in a regulation factor of about 1.3-fold, thereby demonstrating the suppression of the luciferase expression due to miRNA-199a presence. Furthermore, a reduction of SMAD4 protein expression as a consequence of transient transfection of miRNA-199a mimics could be visualized in a western blot in their experiments. However, the authors did not discuss why the suppression of the SMAD4 protein level was tested with miRNA mimics instead of the previously applied plasmid-based miRNA precursor expression. Possibly, the plasmid-derived level of miRNA expression was not sufficient to affect the SMAD4 protein amount. Alternatively, the distribution of the transfected miRNA mimics among the cells achieved by transient transfection could have been more homogenous compared to the miR-199a overexpression plasmid, thus leading to effective target regulation. Since the study presented in this work was also performed using plasmid-based miRNA expression under the control of a CMV promoter, the level of miRNA-199a-5p, derived from either the natural precursor or the pre-miR switch, might have been insufficient to cause an effect at the SMAD4 protein level. It is also conceivable that the conduction of transient transfection with Lipofectamine® 2000 led to an inhomogeneous miRNA expression profile within the HeLa cell population, which could have contributed to mask the miRNA-related regulatory effect.
As mentioned above, the regulatory effect of a miRNA often heavily depends on the cellular context. To rule out systematic errors caused by the use of the HeLa cell line and possibly shortened or mutated target sequences for miR-199a, RNA was isolated and the presence of the target regions was verified by sequencing. Nevertheless, the variation of the experimentally used cell line would be useful to gain more information about the suitability of the previously employed cell system.

Besides the miR-199a-based regulation of *SMAD4,* also the influence of miR-199a on *DDR1* mRNA and DDR1 protein level was examined, since an interaction of miR-199a-5p with the 3'UTR of *DDR1* has already been revealed in a reporter gene assay in this study. Further evidence for the direct relation between miRNA-199a-5p presence and DDR1 targeting was provided by Shen *et al.* [111].

After transient transfection, a slight reduction of 30% of *DDR1* mRNA level in the presence of miR-199a from the natural precursor could be seen, but nearly no regulation dependent on pre-miR switch processing. The apparent reduction at the mRNA level appeared to be too weak to demonstrably affect the DDR1 protein level.

To implement a consistent overexpression of miR-199a in the complete cell population, a genomic integration, omitting or including the simultaneous integration of TetR, was performed. The first genomic integration resulted in a strong reduction of 50% of *DDR1* mRNA level for HF1-3 cells, bearing either the integrated pre-miR switch or the natural miRNA precursor in comparison to the HF1-3 cells with an unmodified genome. This effect at the mRNA level led to a detectable reduction of DDR1 protein that was quite distinct for cells expressing the natural precursor and weak for the pre-miR switch expressing cells. Although unaltered basal levels of mature miRNA-199a-5p and *DDR1* mRNA were produced after the second genomic integration, the mRNA level as well as the protein amount of DDR1 merely showed a slight reduction in the presence of naturally processed miR-199a. In contrast to the results obtained after the first genomic integration, the significant reduction at the mRNA level due to the presence of the pre-miR switch was fully abolished.

The phenomenon observed after the second genomic integration might be directly linked to the selection procedure. Whereas the cells tested after the first integration originated from one single clone with a unique genotype, the second generation of cells was derived from a mixed pool of up to ten single clones. Thus, it cannot be excluded that the deterioration of regulation activity can be attributed to a mixture of genotypes, leading to varying gene expression profiles that possibly masked the effect caused by miR-199a. A re-selection of the second generation cells followed by a seeding for single cells should be performed to confirm this hypothesis.

Generally, the experimental conditions could also have influenced the results. Cell type specific effects on the regulation of *DDR1* mRNA levels through miR-199a expression were observed by Shen *et al.* [111]. In their study, they saw a differential regulation of the mRNA level of *DDR1* dependent on the cell type. A 5-fold reduction of the mRNA level was detected in HepG2 cells, whereas SNU-182 did not respond to the transfection of pre-miRNA at all, again underlining the influence of cell type specific effects. Thus, also in this case testing of the pre-miR switch in another cellular context could provide a good opportunity to assess the regulatory function of the tool developed in this study. At least, a lack of adequate miR-199a-5p target sites could be ruled out, as evidence for the presence of all of the predicted miRNA target sites was provided through sequencing and a response to miRNA-199a-5p presence was seen in the reporter gene assay.

In contrast to the results obtained for the regulation of endogenous *DDR1* during this study, the publication of Shen *et al.* demonstrated a great impact of miR-199a-5p on *DDR1* regulation. However, it must be considered that the effects seen in their experiments were based on the transfection with a chemically modified precursor. This presumably led to a more effective miR-199a-5p overexpression, exceeding the plasmid-based overexpression employed in this work. Thus, the concentration of miR-199a-5p resulting from plasmid expression of the pre-miR switch simply might have been too low to achieve a significant regulation of the *DDR1* target. Consequently, the pre-miR switching activity could not be demonstrated with regard to regulation of the endogenously expressed *DDR1.*

With *CAV1* a target of miR-199a-5p was selected that was validated using various methods according to the miRTarBase database [164]. After genomic integration a pronounced, yet unexpected increase of CAV1 protein as well as mRNA was detected for the cells with a persistently present miRNA-199a derived from the processing of the natural precursor. Such a distinct effect was not observed as a consequence of pre-miR switch miR-199a_2 expression due to a constitutive co-expression of TetR and the generally lower expression due to a modification of the miRNA precursor. So it can be assumed that the long-term expression of miR-199a-5p could be responsible for the observed effect, since transient transfection with the plasmid bearing the natural precursor or the pre-miR switch did not cause an increase at the CAV1 protein level. An effect related to the integration locus per se can be excluded since the pre-miR switch has been integrated at the same site as the natural miRNA precursor. Since miRNA-199a-5p is known to target many endocytosis-related proteins, the apparent increase could either be linked to an interference with factors related to the CAV1 pathway or other secondary effects caused by the constitutive miR-199a expression [165].

Regarding the publications of Cardenas *et al.* and Aranda *et al.*, a reduction of *CAV1* mRNA and CAV1 protein expression was to be expected as a response to miR-199a-5p [165,166]. In their works, they used chemically modified pre-miRNAs or miR-199a-5p mimics and demonstrated a regulation in reporter gene assays, RT-qPCR and western blotting in either HEK-293, hFL1, Huh7 or also HeLa cells. Accordingly, a correlation between the employed cell system and the failed regulation of *CAV1* mRNA and CAV1 protein can be ruled out. Considering also the results of the other tested endogenous targets of miR-199a, it can be assumed that the absence of *CAV1* regulation by miR-199a-5p after transient transfection is the consequence of either inhomogeneous transfection within the cell population or a comparably low amount of mature miRNA-199a-5p provided by plasmid-based miRNA expression.

4.4 Comparison between transient and genomic expression

Generally, transient transfection based on the uptake of lipoplexes suffers from two significant disadvantages that play a relevant role for the investigation of device activity on endogenous target regulation. On the one hand, not all cells of a population were comparably transfected with the miRNA expression plasmids. Thus, the target expression of non-transfected cells remains unaffected due to a lack of miR-199a and therefore falsifies the regulatory effect measured as an average from the overall cell population. On the other hand, different amounts of plasmid were probably incorporated into the cells with the applied method, resulting in varying levels of miRNA within the cells. The regulation of a miRNA target heavily depends on the amount of miRNA, target mRNA and the respective target sites [167]. Thus, the induced changes could be quite heterogeneous and cell-to-cell variations might have masked the efficiency of the miRNA-based regulatory performance.

Genomic integration was performed to gain independency of transfection efficiencies and to work with a homogenous cell population exhibiting narrowly distributed expression profiles with regard to the miRNA precursor. Also a contemporaneous integration of TetR turned out to be necessary, since the first integration led to a dramatic reduction of switching efficiency that was presumably caused by a high background of miRNA-199a produced before TetR expression.

Furthermore, the opportunity to extend the exposure to miR-199a in the system could have served to reveal a potential regulatory effect. All in all, a long-term persistence of miR-199a-5p did not achieve the desired effect for e.g. *DDR1* target regulation and significantly influenced the natural expression pattern of *CAV1.* Accounting for *CAV1* regulation, even an adverse effect arose as a consequence of genomic integration that recalls the fact that the endogenous miRNA-target interaction relies on complex fine tuning which cannot be simulated under the present experimental conditions.

Accounting for a lower copy number of the integrated constructs, their expression resulted in lower miR-199a-5p levels after genomic integration. Besides, also a deterioration of the pre-miR switch-based miRNA-199a-5p expression relative to natural precursor-based expression was assessed that was accompanied by a significant reduction of switching efficiency compared to transient transfection. Also after an incubation with dox for 5 d the observed effect remained stable and no further increase of relative miRNA expression could be achieved. As both the natural precursor and the pre-miR switch were expressed from the same hCMV promoter, differences concerning their relative abundance could be ruled out. Locus-specific effects are also not accountable for a switching factor reduction, since the same insertion site was employed for both constructs. The regulatory efficiency of the pre-miR switches is calculated by the ratio of the values obtained under active and inhibited processing states. Transiently transfected cells exhibited mature miRNA levels of 0.5% in the presence of TetR. In contrast, genomic integration yielded a value of 1.4% in the presence of constitutively expressed TetR, thus changing the regulatory factor for about 3-fold. The slightly lower inhibitory efficiency appearing after genomic integration could be related to a change of the CMV promoter to an SV40 promoter to drive *TetR* expression since the ratio of TetR and pre-miR switch are of the utmost importance for pre-miR switch functionality. A titration of the involved components dependent on promoter strength should be considered to optimize the performance of the pre-miR switch miR-199a_2 not only for transient transfection, but also for genomic integration.

4.5 Evaluation of the experimental setup to investigate endogenous regulation

As discussed earlier, the influence of the selected cell system is an important point to be considered. The experiments were performed in HeLa cells that do not endogenously express miR-199a. A lot of cancer cells are known to ectopically express specific miRNAs (reviewed in [152]). Often, the level of oncogenic miRNAs is increased in cancer cells and defects in miRNA biogenesis as well as global downregulation are often seen mechanisms. Also, several pathways are deregulated in cancer cell lines [168]. Another important requirement to the system used for the investigation of miRNA activity is that low endogenously expressed amounts of the examined miRNA are present to enable efficient switching of miRNA processing dependent on the developed construct.

In order to test a tool for the regulation of miRNA processing, the miRNA target should be chosen carefully. As demonstrated, the interaction of one specific miRNA with the 3'UTR of a potential target does not necessarily lead to a detectable outcome, since many transcripts are targeted by several miRNAs concertedly regulating target expression [168]. Besides, many different factors concerning the

experimental setup, mentioned before, play an important role and significantly influence the formation of a miRNA-target interaction.

The investigation of a whole cell population can also be seen problematic. By conducting single-cell measurements, Mukherji *et al* could show a high cell-to-cell variability of reporter gene expression although all targets were regulated by the same miRNA [167]. Theses variations are usually obscured in bulk measurements. Also pre-miR switch performance could have been masked due to large cell-to-cell variations. Therewith, single-cell studies that investigate the miRNA-target interaction and its effect based on an individual cell might be advantageous to test the influence of pre-miR switch regulation on a defined target.

Considering the expression system, transient transfection should be further enhanced by an alteration of the transfection method to achieve higher transfection efficiencies. Also, a pre-selection of transfected cells, e.g. by using FACS, could be advisable to exclude non-transfected cells from the measurements. Generally, to increase the amount of mature miRNA generated by the processing of the pre-miR switch, an exchange of promoter strength for construct expression is considerable, too.

4.6 Synthetic regulatory tools for controlling RNAi in mammals

Realizing the potential of RNAi as a general means for studying mammalian gene function, the first synthetic RNA-based tools were developed to control the abundance of small ncRNAs. So far, the majority of designs for RNAi-mediated gene silencing and functional studies concentrated on artificially modified shRNAs for tool development and implementation. The main differences between shRNA and miRNA-based tools lie in their targeting capabilities and the structural complexity of their precursors. Whereas siRNA activity is restricted to the regulation of one specific target site, a single miRNA is capable of targeting various mRNAs, facilitated by the tolerance of imperfect hybridization to their target sequences. In contrast to miRNA, shRNA precursors feature a perfectly hybridized stem connected by a short loop. This simple secondary structure is readily accessible to (i) a specific redesign matching virtually any target sequence and to (ii) an *in silico* prediction of the Dicer cleavage sites. Thus, issues accompanying the engineering of complex natural structures can be bypassed, because the modification of an shRNA structure does not require following the strict processing rules that apply to a miRNA precursor.

In an approach that also intended to interfere with Dicer processing, Yokobayashi and coworkers presented a fusion molecule composed of an *in vitro* selected theophylline aptamer inserted in the terminal loop of an shRNA [129]. Their construct design featured the integration of the Dicer cleavage sites into the aptamer structure. Consequently, theophylline binding resulted in the stabilization of the aptamer structure that masked the cleavage sites to prevent Dicer processing. With the shRNA-based construct they were able to control GFP silencing in mammalian cells with a regulatory factor of 2.7-fold in a ligand-dependent fashion. In an ensuing publication, the group demonstrated the adaptability of the developed shRNA technology in an approach to target endogenous human albumin in mammalian cells [170]. In their experiment they showed the specific modulation of the level of human serum albumin yielding a regulation factor of about 3.8-fold in the presence of 2 mM theophylline. The Smolke group modified an shRNA loop structure and integrated various aptamers as well as

competing strands affecting Dicer mediated processing of the shRNA [171]. Also a co-transfection with two engineered shRNAs either harboring a hypoxanthine- or a theophylline-binding aptamer was performed and the ligand-dependent regulating of processing to a GFP-binding siRNA resulted in a ~4-fold change of GFP expression in the simultaneous presence of both ligands. As mentioned before, Saito and coworkers inserted either protein-binding motifs for the human U1A protein and L7Ae or the p50-binding aptamer into the shRNA loop region for the purpose of controlling Dicer cleavage by employing protein-based sensor domains [135]. After exploring the optimal length of the modified shRNA with regard to the orientation of the U1A protein, a 4-fold regulation of eGFP expression could be achieved due to regulation of the siRNA amount. The introduction of the p50-binding aptamer resulted in a 3-fold regulation of eGFP expression. Also, miRNA precursors have been considered as valuable modification platforms for the integration of aptamers to enable ligand-dependent processing. Smolke and coworkers designed a synthetic precursor bearing an siRNA that targets GFP and integrated small molecule- or protein-binding aptamers into its basal segment. Mimicking a pri-miRNA, they targeted Drosha processing resulting in a genetic system that facilitated ligand control over the miRNA-mediated silencing of GFP expression. 2.4-fold regulation was observed for a theophylline-binding construct in the presence of 0.1 mM theophylline.

Since RNA interference experiences an increasing popularity as the method of choice for gene-silencing and functional analysis, there is also an increasing need for robustly working interference tools. So far, no modification of a natural miRNA precursor that resulted in an effective regulation of mature miRNA levels has been demonstrated. The RNA-based device developed in this study constitutes a flexible, reversible switching unit consisting of a synthetic aptamer as the ligand sensing domain coupled to a natural miRNA precursor and enables the efficient, ligand-controlled regulation of miRNA abundance. In contrast to the previously mentioned devices for controlling RNAi, the novel pre-miR switches are the first to provide a three-level regulatory system allowing the active reversion of inhibition of pre-miR processing.

4.7 Conclusion and perspectives

In this work, a robust pre-miR switch design was presented that allows the control of miRNA processing in a ligand-dependent fashion. Testing various communication modules revealed that either the direct fusion or the connection through a one base-pair communication module yields the best results with regard to miRNA precursor processing. The functionality of the designed pre-miR switches was asserted in qPCR and reporter gene assays, where the RNA-based tools led to the efficient regulation of luciferase expression. The regulation of validated endogenous targets of miR-199a could not be shown presumably due to an insufficient concentration of miRNA-199a present under the experimental conditions. To encounter the problem of the absence of endogenous target regulation, a revision of the experimental setup, including the adaptation of promoter strength to increase construct expression, should be taken into consideration. To exclude effects arising from large cell-to-cell variabilities, single-cell measurements could provide an adequate approach to gain information on the regulatory nature of the pre-miR switches concerning the endogenous regulation.

Whereas other publications demonstrated “one-way” switching devices for controlling the biogenesis of small ncRNAs, the design concept for the development of pre-miR switches is the first to enable the creation of a reversible and transferable system that accounts for ligand-dependent regulation of miRNA biogenesis. Thus, the system developed during this work poses the perfect basis for the generation of a robust RNA-based tool to investigate the physiological function of specific miRNAs.

In conclusion, dedicated design guidelines for the successful development of a pre-miR switch can be deduced from this work. But, in order to assess the scope of the universality of the design rules, the investigation of a further set of modified miRNA precursors should be taken into consideration to confirm the robustness and universal transferability of the pre-miR switch design strategy.

5 Material and Methods

The materials and instruments that were utilized in this work are listed below. The following section contains the lists for chemicals and reagents (Table 5.1), instrumentation (Table 5.2), kits and commercially available systems (Table 5.3), enzymes and proteins (Table 5.4), protein standards and DNA ladders (Table 5.5), consumables (Table 5.6), antibodies (Table 5.7), cell strains (Table 5.8), buffers and solutions (Table 5.9), oligonucleotides (Table 5.10) and plasmids (Table 5.11).
All buffers and solutions were produced using ultrapure water. If necessary, buffers and solutions were autoclaved at 121°C and 2 bar for 20 min. Oligonucleotides were ordered from Sigma-Aldrich, Munich (desalted or RP1 purified).

5.1 Chemicals, instrumentation and consumables

Table 5.1 List of employed chemicals and reagents.

Chemicals and reagents	**Manufacturer**
2-Mercaptoethanol	Roth, Karlsruhe
Acetic acid	Roth, Karlsruhe
Agar	Oxoid, Heidelberg
Agarose peqGold Universal	Peqlab, Erlangen
Ammonium sulfate	Roth, Karlsruhe
Ampicillin	Roth, Karlsruhe
Bovine serum albumin	New England Biolabs, USA
Bromophenol blue	Roth, Karlsruhe
Chloroform, p.a.	Roth, Karlsruhe
Clarity™/ Clarity Max™ Western ECL Blotting Substrates	Bio-Rad, Munich
Deoxynucleotide triphosphate (dNTP)	Peqlab, Erlangen
Dimethyl sulfoxide	Peqlab, Erlangen
Doxycycline hydrochloride	Sigma-Aldrich, USA
Dulbecco's Modified Eagle Medium (DMEM)	Sigma-Aldrich, USA
Dulbecco's Phosphate buffered Saline (PBS)	Life Technologies, USA
ECL Prime Blocking Reagent	Amersham, USA
Ethanol absolute, p.a.	Merck, Darmstadt
Ethanol, denatured	VWR, Darmstadt
Ethidium bromide	Roth, Karlsruhe
Ethylenediaminetetraacetic acid (EDTA)	Roth, Karlsruhe
Fetal Bovine Serum (FBS)	Biochrom, Berlin

Formamide	Roth, Karlsruhe
Glycerol, p.a.	Roth, Karlsruhe
Glycine	Roth, Karlsruhe
GlycoBlue™	Invitrogen, USA
Hydrochloric acid (HCl)	Roth, Karlsruhe
Hygromycin B	Invivogen, France
IGEPAL CA-630	Sigma-Aldrich, USA
Isopropylic alcohol, p.a.	VWR, Darmstadt
Lipofectamine® 2000	Life Technologies, USA
$MgCl_2$ solution	Applied Biosystems, USA
Opti-MEM®	Life Technologies, USA
Penicillin/ Streptomycin	Life Technologies, USA
Protein Assay Dye Reagent Concentrate (5x)	Bio-Rad, Munich
Proteinase-inhibitor-cocktail (PIC)	Sigma-Aldrich, USA
RiboLock RNase inhibitor	Thermo Fisher Scientific, USA
Sodium carbonate	Roth, Karlsruhe
Sodium chloride (NaCl)	Roth, Karlsruhe
Sodium dodecyl sulfate (SDS), pellets	Roth, Karlsruhe
SYBR Green PCR Master Mix	Life Technologies, USA
TaqMan® Universal PCR Master Mix	Applied Biosystems, USA
Tris	Roth, Karlsruhe
TRIzol® reagent	Thermo Fisher Scientific, USA
Trypan blue	Bio-Rad, Munich
Trypsin/ EDTA (10x)	Life Technologies, USA
Tryptone	Oxoid, Heidelberg
Tween® 20	Roth, Karlsruhe
Universal ProbeLibrary #21	Roche, Switzerland
Urea	Roth, Karlsruhe
Xylene cyanole	Roth, Karlsruhe
Yeast extract	Oxoid, Heidelberg
Zeocin	Invivogen, France

Table 5.2 List of utilized instruments.

Instrument	Manufacturer
Accuracy weighing machine	Acculab, USA
Centrifuges	Heraeus Christ, Osterode
Electroporator MicroPulser™	Bio-Rad, Munich
Gel documentation with UV screen	INTAS, Göttingen
Heating block	VWR, Darmstadt
Incubation Shaker Multitron	Infors AG, Bottmingen
Incubator	Heraeus Christ, Osterode
Infinite® M200 plate reader	Tecan Trading AG, Switzerland
Magnetic stirrer IKA RET basic	IKA, Staufen
Milli-Q® water purification system with RNase filter	EMD Millipore, France
Mini-PROTEAN Tetra Cell electophoresis chamber	Bio-Rad, Munich
NanoDrop® ND-1000 spectral photometer	Peqlab, Erlangen
StepOnePlus Real-Time PCR cycler	Thermo Fisher Scientific, USA
Scale	Acculab, USA
T100™ Thermal Cycler	Bio-Rad, Munich
TC-10™ Automated Cell Counter	Bio-Rad, Munich
Thermomixer comfort	Eppendorf AG, Hamburg
Trans-Blot®Turbo™ Transfer System	Bio-Rad, Munich

Table 5.3 List of kits and commercially available systems.

Kits and commercially available systems	Manufacturer
DNeasy® Blood & Tissue Kit	QIAGEN, Hilden
Dual-Glo® Luciferase Assay System	Promega, USA
ECL Primer Blocking Reagent	Amersham, USA
Flp-In™ System	Life Technologies, USA
Mini-PROTEAN® TGX™ Precast Gel, any Kd and 7.5%	Infors AG, Bottmingen
QIAprep® Spin Miniprep Kit	QIAGEN, Hilden
QIAquick PCR Purification Kit	VWR, Darmstadt
Trans-Blot® Turbo™ Transfer Pack Mini, 0.2 µm PVDF	Heraeus Christ, Osterode
Zymoclean™ Gel DNA Recovery Kit	Zymo Research, USA

Table 5.4 List of employed enzymes and proteins.

Enzymes and proteins	**Manufacturer**
MuLV Reverse Transcriptase [50 U/µl]	Applied Biosystems, USA
Q5 High-Fidelity DNA Polymerase [2 U/µl]	New England Biolabs, USA
RiboLock™ RNase Inhibitor [40 U/ml]	Fermentas, USA
SuperScript II Reverse Transcriptase [200 U/µl]	Life Technologies, USA
T4 DNA Ligase [400 U/µl]	New England Biolabs, USA
T4 Polynucleotide kinase [10 U/µl]	New England Biolabs, USA
Taq DNA Polymerase [5 U/µl]	New England Biolabs, USA
TURBO DNase [2 U/µl]	Life Technologies, USA
Restriction endonucleases	
BamHI [20 U/µl]	New England Biolabs, USA
ClaI [10 U/µl]	New England Biolabs, USA
DpnI [20 U/µl]	New England Biolabs, USA
HindIII [20 U/µl]	New England Biolabs, USA
SacI-HF [20 U/µl]	New England Biolabs, USA
SpeI-HF [20 U/µl]	New England Biolabs, USA
XbaI [20 U/µl]	New England Biolabs, USA
XhoI [20 U/µl]	New England Biolabs, USA

Table 5.5 List of used protein standards and DNA ladders.

Protein standards/ DNA ladders	**Manufacturer**
peqGold Ultra Low Range DNA ladder II	PeqLab, Erlangen
peqGold 1 kB DNA ladder	PeqLab, Erlangen
Precision Plus Protein™ All Blue Prestained Protein Standard	Bio-Rad, Munich

Table 5.6 List of utilized consumables.

Consumables	**Manufacturer**
Cell culture flasks	Greiner, Nürtingen
Cellstar® cell culture plates, 12-well/ 24-well	Greiner Bio-One, Austria
Cuvettes, acrylic	Sarstedt, Nürnbrecht
Dispenser tips	Greiner, Nürtingen
Micro Pulser Electroporation Cuvettes, 0.1 cm gap	Bio-Rad, Munich
MicroAmp® Fast 96-Well reaction plate	Applied Biosystems, USA
MicroAmp™ optical adhesive film	Applied Biosystems, USA

Nitrile Gloves	Starlab, Hamburg
Nunc™ MicroWell™ white 96-well plates, polystyrene	Thermo Fisher Scientific, USA
Petri dishes, plastic	Greiner, Nürtingen
Pipette tips, plastic	Greiner, Nürtingen Starlab, Hamburg Nerbe Plus, Winsen
Pipettes, plastic	Nerbe Plus, Winsen
Polyethylene tubes	Sarstedt, Nürnbrecht
Reaction tubes (1.5 ml, 2 ml)	Greiner, Nürtingen
Syringes	Becton Dickinson, Heidelberg

Table 5.7 List of employed antibodies.

Primary antibodies	**Host**	**Dilution**	**Manufacturer**
Anti-CAV1, sc-894	Rabbit	1:1,000	Santa Cruz Biotechnology, USA
Anti-DDR1, sc-532	Rabbit	1:1,000	Santa Cruz Biotechnology, USA
Anti-HSP60, ab-6530	Rabbit	1:2,000	Abcam, UK
Anti-SMAD4, sc-7154	Rabbit	1:1,000	Santa Cruz Biotechnology, USA
Anti-β-actin, AC-74	Mouse	1:7,000	Sigma-Aldrich, USA
Anti-TetR	Rabbit	1:5,000	Dr. Chris Berens, FAU Erlangen
Secondary antibodies	**Host**	**Dilution**	**Manufacturer**
Anti-mouse IgG (H+L)	Rabbit	1:7,000	Jackson Immunoresearch, USA
Anti-rabbit IgG (H+L)	Goat	1:7,000	Jackson Immunoresearch, USA

5.2 Prokaryotic and eukaryotic cell strains

Table 5.8 List of employed cell strains.

Cells	**Genotype/ Description**	**Reference**
Bacterial strains		
E. coli Top10	F- *mcrA* Δ(*mrr-hsd*RMS-*mcr*BC) Φ80*lac*ZΔM15 Δ *lac*X74 *rec*A1 *ara*D139 Δ(*araleu*)7697 *gal*U *gal*K *rps*L (StrR) *end*A1 *nup*G	Invitrogen, USA
Eukaryotic cell lines		
HeLa	Human epithelial cells derived from an epidermoid carcinoma of the cervix	DSMZ (ACC 57)
HeLa HF1-3	HeLa cell line with integrated FRT-site for a Flp-In™ system-based genomic integration	C. Berens [172]

5.3 Buffers and solutions

Table 5.9 List of buffers and solutions and their composition.

Buffer/ solution	Ingredients	Concentration
10x running buffer (SDS-PAGE)	Tris Glycine SDS pH 8.3	250 mM 1.9 M 1% (w/v)
10x TBS For 1x TBST	Tris NaCl pH 7.6 Tween™ 20	200 mM 1.5 M 0.1% (v/v)
2x RNA loading dye	EDTA Bromophenol blue Xylene cyanole In formamide (deionized)	25 mM 0.1% (w/v) 0.1% (w/v)
4x protein loading dye	Glycerol SDS 2-Mercaptoethanol Bromophenol blue	50% (v/v) 4% (w/v) 15% (v/v) 0.1% (w/v)
50x TAE	Tris Acetic acid EDTA pH 8.3	2 M 1 M 50 mM
6x DNA loading dye	Tris-HCl pH 7.6 EDTA Acetic acid Glycerol Bromophenol blue Xylene cyanole	40 mM 1 mM 20 mM 50% (v/v) Spatula point Spatula point
Ampicillin, stock solution	Ampicillin In 70% (v/v) EtOH	 100 mg/ml
LB medium For LB-Amp plates	Tryptone Yeast extract NaCl Agar Ampicillin	1% (w/v) 0.5% (w/v) 1% (w/v) 2% (w/v) 100 µg/ml
Lysis buffer	Tris-HCl, pH 8.0 EDTA NaCl	20 mM 2 mM 137 mM

	Glycerol IGEPAL CA-630 PIC	10% (v/v) 1% (v/v) 0.5% (v/v)
SOC-medium	Yeast Extract Tryptone NaCl KCl $MgCl_2$ MgSO4 Glucose	0.5% 0.2% 10 mM 2.5 mM 10 mM 10 mM 20 mM

5.4 Oligonucleotides

Table 5.10 List of oligonucleotides employed for reverse transcription, qPCR and cloning.

Oligonucleotide name	**Sequence (5' → 3')**
Reverse transcription	
Stem loop U48	GTTGGCTCTGGTGCAGGGTCCGAGGTATTCGCACCAGAGCCAACGGTCAG
Stem loop miR-126	GTTGGCTCTGGTGCAGGGTCCGAGGTATTCGCACCAGAGCCAACCGCATT
Stem loop miR-92a	GTTGGCTCTGGTGCAGGGTCCGAGGTATTCGCACCAGAGCCAACACAGGC
Stem loop miR-199a-5p	GTTGGCTCTGGTGCAGGGTCCGAGGTATTCGCACCAGAGCCAACGAACAG
Stem loop miR-199a-3p	GTTGGCTCTGGTGCAGGGTCCGAGGTATTCGCACCAGAGCCAACTAACCT
Stem loop miR-34a	GTTGGCTCTGGTGCAGGGTCCGAGGTATTCGCACCAGAGCCAACACAACC
Stem loop miR-101-1	GTTGGCTCTGGTGCAGGGTCCGAGGTATTCGCACCAGAGCCAACTTCAGT
qPCR, TaqMan assay	
Universal primer	GTGCAGGGTCCGAGGT
qPCR U48 fwd	GAGTGATGATGACCCCAGGTAA
qPCR miR-126 fwd	CGCGGTCGTACCGTGAGTAAT
qPCR miR-92a fwd	GCGGTATTGCACTTGTCCCG
qPCR miR-199a-5p fwd	GCGGCCCAGTGTTCAGACTAC
qPCR miR-199a-3p	CGGCGGACAGTAGTCTGCACAT

fwd	
qPCR miR-34a fwd	GCGTGGCAGTGTCTTAGCT
qPCR miR-101-1 fwd	GCGGTACAGTACTGTGATA
qPCR, SYBR Green assay	
SMAD4-qPCR_ 1130-1220-f	CCAGCTCTGTTAGCCCCATC
SMAD4-qPCR_ 1130-1220-r	TACTGGCAGGCTGACTTGTG
DDR1-qPCR_ 231-301-f	GAGAGGTGTCTGAAGGTGGC
DDR1-qPCR_ 231-301-r	GGCAGCATCTCTTGGCATTC
CAV1- qPCR 1_ 294-419-f	TACGTAGACTCGGAGGGACA
CAV1-qPCR_ 294-419-r	GGTTGACCAGGTCGATCTCC
Cloning	
CMV prom fwd	TAAGCAGAGCTCGTTTAGTG
SV40 polyA rev	CACTGCATTCTAGTTGTGG
pri-miR-34a_XhoI-f	cttctcCTCGAGTGCATCCTTTCTTTCCTCCCCAC
pri-miR-34a_XbaI-r	cttctcTCTAGACTTTCCCAGCCGCCCTCAC
pri-miR-101-1_XhoI-f	cttctcCTCGAGAGAAGGTGATCTTTTAGTCCTTCACTTCATGG
pri-miR-101-1_XbaI-r	cttctcTCTAGAGTAAGAGGGTTTCTGGGTCCCAGC
TetR5 p1-r	TCTGGTCTGTGATGACCCATAACATGCTGCCCGTACCAAAAGTAATAATG
TetR5 p2-f	TATGGGTCATCACAGACCAGAGAAAAGCTCGTACCGTGAGTAATAATGC
TetR2 p1-r	TCTGGTCTGTGATGACCCATAACATGCTGTCCGCGTACCAAAAGTAATAATG
TetR2 p2-f	TATGGGTCATCACAGACCAGAGAAAAGTCTTCGTACCGTGAGTAATAATGC
TetR5l p1-r	TCTGGTCTGTGATGACCCATAACATGCTGCGCCCGTACCAAAAGTAATAATGTCC
TetR5l p2-f	TATGGGTCATCACAGACCAGAGAAAAGCGCTCGTACCGTGAGTAATAATG
TetR NL1 p1-r	TCTGGTCTGTGATGACCCATAACATGCTGCACAGCGCGTACCAAAAG
TetR NL1 p2-f	TATGGGTCATCACAGACCAGAGAAAAGCAAACTCGTACCGTGAGTAATAATG
miR-199a-2-#1-1-r	TGGTCTGTGATGACCCATAACATGCTGGAACAGGTAGTCTGAACAC
miR-199a-2-#2-1-r	TGGTCTGTGATGACCCATAACATGCTGAACAGGTAGTCTGAACAC
miR-199a-2-#1-2-f	GTTATGGGTCATCACAGACCAGAGAAAAGGAACAGTAGTCTGCACATTGG
miR-199a-2-#2-2-f	GTTATGGGTCATCACAGACCAGAGAAAAGAACAGTAGTCTGCACATTGG
miR-92a-1-#1-1-r	CTGGTCTGTGATGACCCATAACATGCTGAGCATTGCAACCGATCC
miR-92a-1-#2-1-r	CTGGTCTGTGATGACCCATAACATGCTAGCATTGCAACCGATCC
miR-92a-1-#1-2-f	TGGGTCATCACAGACCAGAGAAAAGAGTATTGCACTTGTCCCGGC

miR-92a-1-#2-2-f	TGGGTCATCACAGACCAGAGAAAAAGTATTGCACTTGTCCCGGC
miR-34a-#1_1-r	TTTTCTCTGGTCTGTGATGACCCATAACATGCTAACAACCAGCTAAGACAC
miR-34a-#2_1-r	TTTTCTCTGGTCTGTGATGACCCATAACATGCTACAACCAGCTAAGACAC
miR-34a-#3_1-r	TTTTCTCTGGTCTGTGATGACCCATAACATGCTGACAACCAGCTAAGACAC
miR-34a-#1_2-f	GCATGTTATGGGTCATCACAGACCAGAGAAAAAGCAATCAGCAAGTATACTGCC
miR-34a-#2_2-f	CATGTTATGGGTCATCACAGACCAGAGAAAAGCAATCAGCAAGTATACTGCC
miR-34a-#3_2-f	GCATGTTATGGGTCATCACAGACCAGAGAAAAGGCAATCAGCAAGTATACTGCC
miR-101-1-#1_1-r	TTTTCTCTGGTCTGTGATGACCCATAACATGCTGAGCATCAGCACTGTGATAAC
miR-101-1-#2_1-r	TTTTCTCTGGTCTGTGATGACCCATAACATGCTAGCATCAGCACTGTGATAAC
miR-101-1-#1_2-f	TGTTATGGGTCATCACAGACCAGAGAAAAGGGTACAGTACTGTGATAACTGAAG
miR-101-1-#2_2-f	GTTATGGGTCATCACAGACCAGAGAAAAGGTACAGTACTGTGATAACTGAAG
miR-101-2-con_1-r	TTTTCTCTGGTCTGTGATGACCCATAACATGCTAGCATCGGTACCATGATAAC
miR-101-2-con_2-f	TGTTATGGGTCATCACAGACCAGAGAAAAGGTACAGTACTGTGATAACTG
perfectmatch-miR-199a-3p-f	AGCTTACAGTAGTCTGCACATTGGTTAGAGCT
perfectmatch-miR-199a-3p-r	CTAACCAATGTGCAGACTACTGTA
perfectmatch-miR-199a-5p-f	AGCTTCCCAGTGTTCAGACTACCTGTTCGAGCT
perfectmatch-miR-199a-5p-r	CGAACAGGTAGTCTGAACACTGGGA
perfectmatch-miR-34a-5p-f	AGCTTTGGCAGTGTCTTAGCTGGTTGTGAGCT
perfectmatch-miR-34a-5p-r	CACAACCAGCTAAGACACTGCCAA
3xseed-miR-126_I-f	AGCTTTCGTACCTTACATTTAGTTAAAGAGCT
3xseed-miR-126_I-r	CTTTAACTAAATGTAAGGTACGAA
3xseed-miR-126_II-f	CTCGTACCTTACATTTAGTTAAAA
3xseed-miR-126_II-r	CTAGTTTTAACTAAATGTAAGGTACGAGAGCT
3xseed-miR-126_III-f	CTAGTTCGTACCTTACATTTAGTTAAACATCAC
3xseed-miR-126_III-r	TCGAGTGATGTTTAACTAAATGTAAGGTACGAA
3xseed-miR-199a-5p_I-f	AGCTTTCCAGTGTCTATCCTATATTTCTGAGCT
3xseed-miR-199a-5p_I-r	CAGAAATATAGGATAGACACTGGAA
3xseed-miR-199a-5p_II-f	CTCCAGTGTCTATCCTATATTTCTA
3xseed-miR-199a-5p_II-r	CTAGTAGAAATATAGGATAGACACTGGAGAGCT
3xseed-miR-199a-5p_III-f	CTAGTTCCAGTGTCTATCCTATATTTCTCATCAC
3xseed-miR-199a-5p_III-r	TCGAGTGATGAGAAATATAGGATAGACACTGGAA

3xseed-miR-199a-3p_I-f	AGCTTTACAGTAAAATGAAACATCTTGTTAGAGCT
3xseed-miR-199a-3p_I-r	CTAACAAGATGTTTCATTTTACTGTAA
3xseed-miR-199a-3p_II-f	CTACAGTAAAATGAAACATCTTGTTAA
3xseed-miR-199a-3p_II-r	CTAGTTAACAAGATGTTTCATTTTACTGTAGAGCT
3xseed-miR-199a-3p_III-f	CTAGTTACAGTAAAATGAAACATCTTGTTACATCAC
3xseed-miR-199a-3p_III-r	TCGAGTGATGTAACAAGATGTTTCATTTTACTGTAA
3xseed-miR-34a-5p_I-f	AGCTTTGGCAGTGTTTACAAATTAAGAGCT
3xseed-miR-34a-5p_I-r	CTTAATTTGTAAACACTGCCAA
3xseed-miR-34a-5p_II-f	CTGGCAGTGTTTACAAATTAAA
3xseed-miR-34a-5p_II-r	CTAGTTTAATTTGTAAACACTGCCAGAGCT
3xseed-miR-34a-5p_III-f	CTAGTTGGCAGTGTTTACAAATTAACATCAC
3xseed-miR-34a-5p_III-r	TCGAGTGATGTTAATTTGTAAACACTGCCAA
DDR1-UTR_SpeI-f	ctcttcACTAGTCCTCTCCACCCTCCTCTAGC
DDR1-UTR_HindIII-r	ctcttcAAGCTTGGGGTGACTGAGGGCTG
Cav2-UTR_SpeI-f	ctcttcACTAGTGAATACTTGGACCCCAGGTCTGGAG
Cav2-UTR_HindIII-r	ctcttcAAGCTTAAGCAATCTGATTAGAGCAACATTTATATTAACTACAAAATATAC
MET-UTR_SpeI-f	ctcttcACTAGTTAGTGCTAGTACTATGTCAAAGCAACAGTCC
MET-UTR_HindIII-r	ctcttcAAGCTTACAAGATGTTGCATCACTTTACTTTAATTGCATG
CD44-UTR_XhoI-f	ctcttcCTCGAGTGATGTGATGAGACAAGGAACCTGCAGAATGTG
CD44-UTR_HindIII-r	ctcttcAAGCTTTCTGTTTCCTTTAGTCTTTTAATGTTAGCCTTTTAATATTTTCC
perfmat-mut-miR199-3p-5p-126-f	AGCTTGACCGTGACCGTGACCGTGACCGAGCT
perfmat-mut-miR199-3p-5p-126-r	CGGTCACGGTCACGGTCACGGTCA
2_3xseed random-f	CGACCGTGACCGTGACCGTGACCA
2_3xseed random-r	CTAGTGGTCACGGTCACGGTCACGGTCGAGCT
3_3xseed random-f	CTAGTGACCGTGACCGTGACCGTGACCCATCAC
3_3xseed random-r	TCGAGTGATGGGTCACGGTCACGGTCACGGTCA
Genomic integration	
Gen.int.199a(#2)-BamHI-f	cttctcGGATCCAGTCAGCGCAGCAGAATTCAG
Gen.int.199a(#2)-SacI-r	cttctcGAGCTCCTGTGAAGAAAAACACTGGATATGAGATTC
SpeI-ins-f	GATCTCTCTGAACTAGTCTCTGAAT
SpeI-ins-r	CGATTCAGAGACTAGTTCAGAGA
TetR-polyA-SpeI-f	ctcttCACTAGTGCGTCCGGGGACCTTG

TetR-polyA-ClaI-r	ctcttCATCGATAATTCACCCCGGCCGC
SV40prom-ClaI-f	ctcttCATCGATTTGCAAAAGCCTAGGCCTCC
SV40prom-SbfI-r	ctcttCCCTGCAGGGCTGGCCTTTTGCTCACATGG

5.5 Plasmids

Table 5.11 List of plasmids employed in this work.

Plasmid name	Description	Reference
Plasmids for miRNA overexpression		
pCMV-MS	Constructed from pGL4.75 for protein overexpression; empty MCS, CMV_{prom}	J. Weigand, TU Darmstadt
pCMV-TetR	Vector for TetR expression; CMV_{prom}	Doctoral thesis J. Langner, TU Darmstadt
pCMV-miR-126	Contains 100 nt natural context up- and downstream of the natural stem loop of miR-126; CMV_{prom}	F. Nies, lab course, TU Darmstadt
pCMV-miR-126_2	Contains 100 nt natural context up- and downstream of the pre-miR switch miR-126_2; CMV_{prom}	Doctoral thesis J. Atanasov, TU Darmstadt
pCMV-miR-126_5	Contains 100 nt natural context up- and downstream of the pre-miR switch miR-126_5; CMV_{prom}	Doctoral thesis J. Atanasov, TU Darmstadt
pCMV-miR-126_5l	Contains 100 nt natural context up- and downstream of the pre-miR switch miR-126_5l; CMV_{prom}	Doctoral thesis J. Atanasov, TU Darmstadt
pCMV-miR-126_NL	Contains 100 nt natural context up- and downstream of the pre-miR switch miR-126_NL; CMV_{prom}	Doctoral thesis J. Atanasov, TU Darmstadt
pCMV-miR-92a	Contains 100 nt natural context up- and downstream of the natural stem loop of miR-92a; CMV_{prom}	F. Nies, lab course, TU Darmstadt
pCMV-miR-92a_1	Contains 100 nt natural context up- and downstream of the pre-miR switch miR-92a_1; CMV_{prom}	Doctoral thesis J. Atanasov, TU Darmstadt
pCMV-miR-92a_2	Contains 100 nt natural context up- and downstream of the pre-miR switch miR-92a_2; CMV_{prom}	Doctoral thesis J. Atanasov, TU Darmstadt
pCMV-miR-199a	Contains 100 nt natural context up- and downstream of the natural stem loop of miR-199a; CMV_{prom}	F. Nies, lab course, TU Darmstadt
pCMV-miR-199a_1	Contains 100 nt natural context up- and downstream of the pre-miR switch miR-199a_1; CMV_{prom}	Doctoral thesis J. Atanasov, TU Darmstadt
pCMV-miR-199a_2	Contains 100 nt natural context up- and downstream of the pre-miR switch miR-199a_2; CMV_{prom}	Doctoral thesis J. Atanasov, TU Darmstadt
pCMV-miR-34a	Contains 100 nt natural context up- and downstream of the natural stem loop of miR-34a; CMV_{prom}	Doctoral thesis J. Atanasov, TU Darmstadt
pCMV-miR-34a_1	Contains 100 nt natural context up- and downstream of the pre-miR switch miR-34a_1; CMV_{prom}	Doctoral thesis J. Atanasov, TU Darmstadt
pCMV-miR-34a_2	Contains 100 nt natural context up- and downstream of the pre-miR switch miR-34a_2;	Doctoral thesis J. Atanasov,

	CMV_{prom}	TU Darmstadt
pCMV-miR-34a_3	Contains 100 nt natural context up- and downstream of the pre-miR switch miR-34a_3; CMV_{prom}	Doctoral thesis J. Atanasov, TU Darmstadt
pCMV-miR-101-1	Contains 100 nt natural context up- and downstream of the natural stem loop of miR-101-1; CMV_{prom}	Doctoral thesis J. Atanasov, TU Darmstadt
pCMV-miR-101_1	Contains 100 nt natural context up- and downstream of the pre-miR switch miR-101_1; CMV_{prom}	Doctoral thesis J. Atanasov, TU Darmstadt
pCMV-miR-101_2	Contains 100 nt natural context up- and downstream of the pre-miR switch miR-101_2; CMV_{prom}	Doctoral thesis J. Atanasov, TU Darmstadt
Plasmids for the reporter gene assay		
pMIR-Report	Vector for firefly luciferase expression; CMV_{prom}	Thermo Fisher Scientific, USA
pRL-SV40	Vector for *Renilla* luciferase expression; $SV40_{prom}$	Promega, USA
pMIR-perfect match-miR-126	Contains the perfect match binding site for miR-126-3p downstream of the firefly luciferase; CMV_{prom}	F. Nies, lab course, TU Darmstadt
pMIR-perfect match-miR-199a-5p	Contains the perfect match binding site for miR-199a-5p downstream of the firefly luciferase; CMV_{prom}	Doctoral thesis J. Atanasov, TU Darmstadt
pMIR-perfect match-miR-199a-3p	Contains the perfect match binding site for miR-199a-3p downstream of the firefly luciferase; CMV_{prom}	Doctoral thesis J. Atanasov, TU Darmstadt
pMIR-perfect match-miR-34a	Contains the perfect match binding site for miR-34a-5p downstream of the firefly luciferase; CMV_{prom}	Doctoral thesis J. Atanasov, TU Darmstadt
pMIR-3xseed-miR-126	Contains the triplicate of a predicted miR-126-3p target site (5'-TTTAACTAAATGTAAGGTACGA-3') of the 3'UTR of *SPRED1* downstream of the firefly luciferase; CMV_{prom}	Doctoral thesis J. Atanasov, TU Darmstadt
pMIR-3xseed-miR-199a-5p	Contains the triplicate of a predicted miR-199a-5p target site (5'-AGAAATATAGGATAGACACTGGA-3') of the 3'UTR of *DDR1* downstream of the firefly luciferase; CMV_{prom}	Doctoral thesis J. Atanasov, TU Darmstadt
pMIR-3xseed-miR-199a-3p	Contains the triplicate of a predicted miR-199a-5p target site (5'-TAACAAGATGTTTCATTTTACTGTA-3') of the 3'UTR of *CAV2* downstream of the firefly luciferase; CMV_{prom}	Doctoral thesis J. Atanasov, TU Darmstadt
pMIR-3xseed-miR-34a	Contains the triplicate of a predicted miR-34a-5p target site of (5'-TTAATTTGTAAACACTGCCA-3') the 3'UTR of *E2F3* downstream of the firefly luciferase; CMV_{prom}	Doctoral thesis J. Atanasov, TU Darmstadt
pMIR-3'UTR-DDR1	Contains a part of the 3'UTR (position 264-582) of *DDR1* downstream of the firefly luciferase; CMV_{prom}	Doctoral thesis J. Atanasov, TU Darmstadt
pMIR-3'UTR-CAV2	Contains a part of the 3'UTR (position 1-665) of *CAV2* downstream of the firefly luciferase; CMV_{prom}	Doctoral thesis J. Atanasov, TU Darmstadt
pMIR-3'UTR-MET	Contains the 3'UTR of *MET* downstream of the firefly luciferase; CMV_{prom}	Doctoral thesis J. Atanasov, TU Darmstadt
pMIR-3'UTR-CD44	Contains the 3'UTR of *CD44* downstream of the firefly luciferase; CMV_{prom}	Doctoral thesis J. Atanasov, TU Darmstadt

pMIR-random	Contains one random site (5'GGTCACGGTCACGGTCACGGTC-3') downstream of the firefly luciferase; CMV_{prom}	Doctoral thesis J. Atanasov, TU Darmstadt
pMIR-3xrandom	Contains three random sites (3x 5'GGTCACGGTCACGGTCACGGTC-3') downstream of the firefly luciferase; CMV_{prom}	Doctoral thesis J. Atanasov, TU Darmstadt
Plasmids for the genomic integration		
pOG44	Vector for Flp recombinase expression; CMV_{prom}	Thermo Fisher Scientific, USA
pFRT-GFP	Contains the eGFP CDS behind the CMV_{prom} in the pFRT- vector for genomic integration	K. Beilstein[173]
pFRT-CD20	Contains the CD20 CDS behind the CMV_{prom} in the pFRT- vector for genomic integration	K. Beilstein, Goethe Universität, Frankfurt
pFRT-miR-199a	Contains the natural stem loop of miR-199a surrounded by 100 nt of natural context up- and downstream behind the CMV_{prom} in the pFRT- vector for genomic integration	Doctoral thesis J. Atanasov, TU Darmstadt
pFRT-miR-199a_2	Contains the pre-miR switch miR-199a_2 surrounded by 100 nt of natural context up- and downstream behind the CMV_{prom} in the pFRT- vector for genomic integration	Doctoral thesis J. Atanasov, TU Darmstadt
pFRT-miR-199a-TetR	Contains the natural stem loop of miR-199a surrounded by 100 nt of natural context up- and downstream behind the CMV_{prom} and the TetR CDS behind a $SV40_{prom}$ in the pFRT- vector for genomic integration	Doctoral thesis J. Atanasov, TU Darmstadt
pFRT-miR-199a_2-TetR	Contains the pre-miR switch miR-199a_2 surrounded by 100 nt of natural context up- and downstream behind the CMV_{prom} and the TetR CDS behind a $SV40_{prom}$ in the pFRT- vector for genomic integration	Doctoral thesis J. Atanasov, TU Darmstadt

5.5.1 Basic plasmids

All plasmids exhibiting the β-lactamase (bla) gene as a resistance marker for plasmid multiplication in bacteria also contain a bla promoter and an SV40 poly(A) signal downstream of the β-lactamase gene.

5.5.1.1 pCMV-MS

The plasmid pCMV-MS was used as the basic plasmid for the generation of the miRNA overexpression plasmids or as an empty plasmid for transfection. The plasmid map is presented in Figure 5.1. The plasmid contains a CMV promoter (including the CMV early enhancer) and a multiple cloning site (MCS) harboring restriction sites for *XhoI* and *XbaI* that were employed for the generation of the pre-miR switch constructs. The transcription start site (TSS) is located at the end of the CMV promoter. For transcription termination a SV40 poly(A) signal is present downstream of the MCS. Furthermore the plasmid encodes for a β-lactamase gene (AmpR) that confers ampicillin resistance to the bacterial host organism.

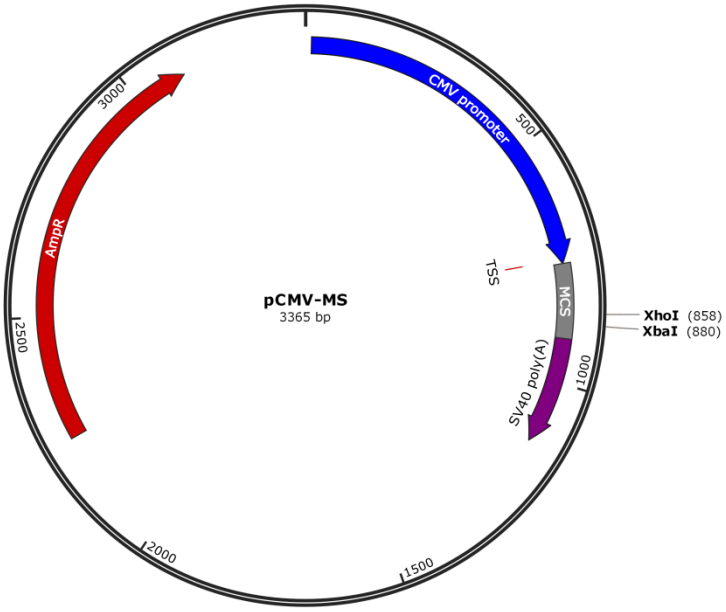

Figure 5.1 Plasmid map of pCMV-MS.
The plasmid map of pCMV-MS shows the CMV promoter (blue) located in front of the MCS (grey). Two restriction sites for *XhoI* and *XbaI* are present within the MCS. An SV40 poly(A) signal (purple) is placed downstream of the MCS. Additionally the plasmid harbors an ampicillin resistance gene (AmpR, red).

5.5.1.2 pCMV-TetR

The plasmid pCMV-TetR was used for the overexpression of TetR from a CMV promoter (including a CMV early enhancer). The plasmid map in Figure 5.2 shows the composition of the plasmid pCMV-TetR. The transcription of the TetR coding sequence (CDS) is terminated by an SV40 poly(A) signal. Furthermore the plasmid encodes for a β-lactamase gene that equips the bacterial host organism with an ampicillin resistance.

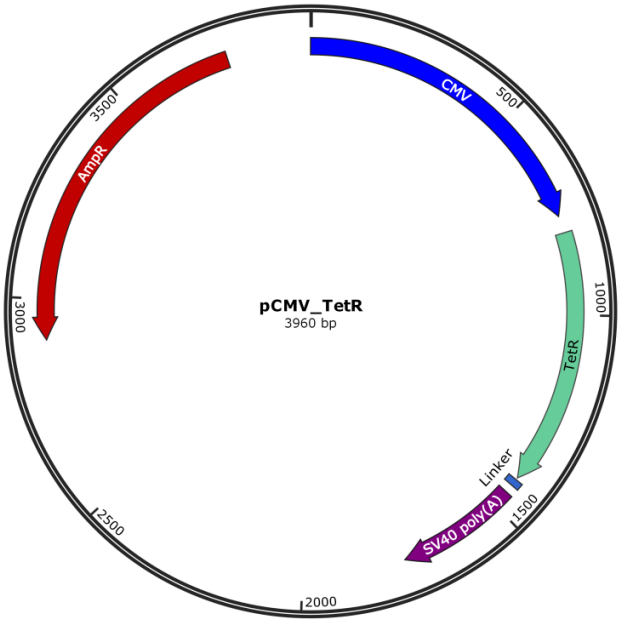

Figure 5.2 Plasmid map of pCMV-TetR.
Indicated are the CMV promoter (blue), the TetR CDS (light green) and the SV40 poly(A) signal (purple) for transcription termination (purple). A linker region (light blue) is present downstream of the TetR sequence. The ampicillin resistance conferring gene (AmpR) is shown in red.

5.5.1.3 pMIR-Report

The plasmid pMIR-Report was produced by Thermo Fisher Scientific for the insertion of putative miRNA binding sites to investigate the interaction of a miRNA with its target region. The related plasmid map is given in Figure 5.3. A MCS was positioned downstream of a firefly luciferase CDS that is expressed from a CMV promoter. For transcription termination an SV40 poly(A) signal is present downstream of the MCS region. Furthermore the plasmid encodes for a β-lactamase that confers ampicillin resistance to the bacterial host organism. The plasmid was employed for the construction of the plasmids for performing the reporter gene assay. The restriction sites *XhoI*, *SpeI*, *SacI* and *HindIII* located in the MCS were utilized for the insertion of either the perfect match target sites, triplicates of miRNA target sequences or (parts of) the 3'UTR of validated target genes.

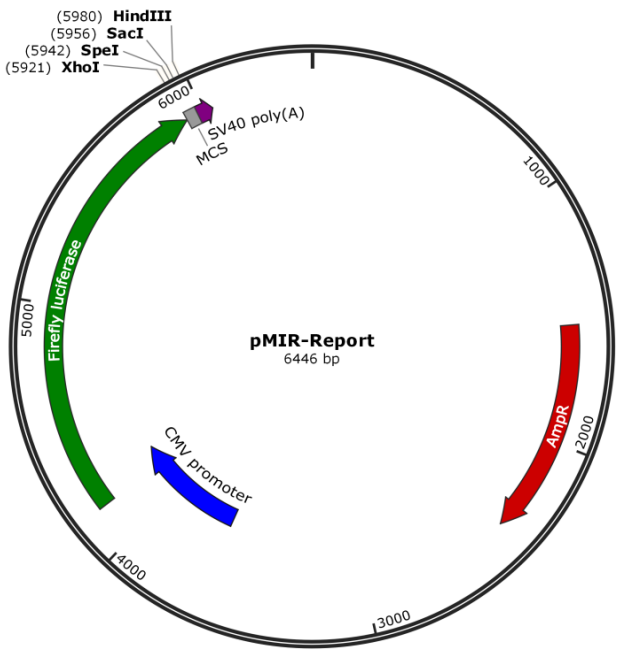

Figure 5.3 Plasmid map of pMIR-Report.
The plasmid pMIR-Report contains a CMV promoter (blue) upstream of the firefly luciferase CDS (green). An SV40 poly(A) signal (purple) is located downstream of the MCS (grey). In the MCS the restriction sites for *XhoI*, *SpeI*, *SacI* and *HindIII* are shown. Additionally, the plasmid harbors an ampicillin resistance gene (AmpR, red).

5.5.1.4 pFRT-CD20

Plasmid pFRT-CD20 was used as the basis for the generation of the plasmids used for genomic integration of the natural miR-199a precursor and the pre-miR switch miR-199a_2 (together with TetR). As shown in Figure 5.4, it contains an hCMV promoter in front of the CD20 CDS and an SV40 poly(A) and BGH poly(A) signal for transcription termination downstream of the CD20 CDS. An Flp Recombination Target (FRT)-site that serves as recognition and cleavage site for the Flp recombinase is present in the plasmid. The FRT-site is located upstream of a hygromycin resistance gene that lacks a promoter and a start codon. The required promoter as well as the start codon are, in turn, integrated into the host cell genome and are brought into correct proximity and frame with the hygromycin resistance gene upon genomic integration of the plasmid at the FRT-site. Successful integration then confers hygromycin resistance to the cells and enables selection of the cells bearing the integrated constructs. The restriction sites for *ClaI*, *SbfI*, *BamHI* and *SacI,* which were employed for the integration of the respective constructs and the TetR expression determinant, are also indicated in the map.

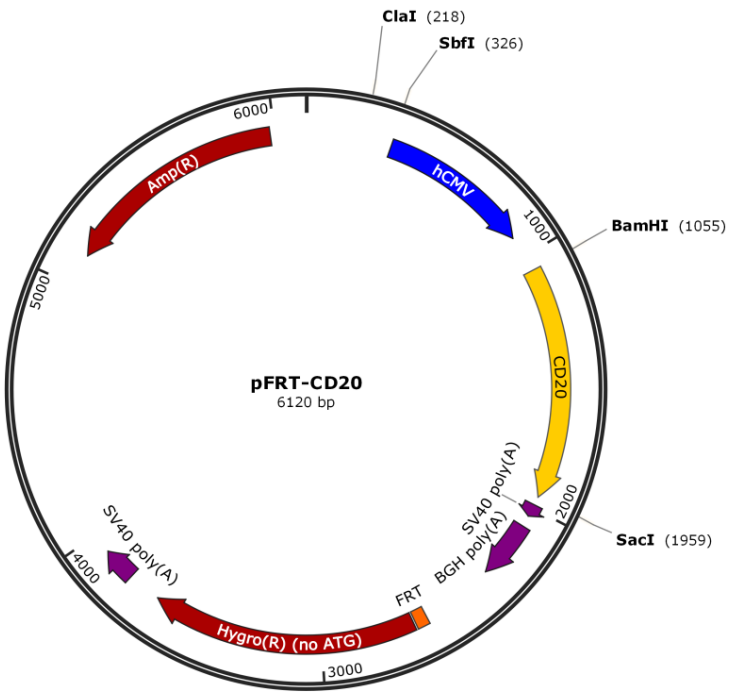

Figure 5.4 Plasmid map of pFRT-CD20.
The plasmid pFRT-CD20 contains an hCMV promoter (blue) in front of the CD20 CDS (yellow). An SV40 poly(A) signal (purple) and a BGH poly(A) (purple) is located downstream to the CD20 expression sequence. Furthermore the FRT site (orange) and a hygromycin resistance conferring CDS missing the start codon (Hygro(R) (no ATG), red) are indicated. A further SV40 poly(A) signal (purple) is provided downstream of the hygromycin resistance CDS to terminate transcription. Additionally, the plasmid harbors an ampicillin resistance gene (AmpR, red).

5.5.2 Construction of plasmids

All established constructs were precipitated with butanol after ligation and transformed into *E.coli* Top10. Then, the bacterial clones were tested in a colony-PCR and sequenced to confirm construct integrity. In the section below, one cloning history to generate a plasmid employed in a specific assay is exemplified, respectively. The other plasmids used in the same assay were created in analog to the presented example.

5.5.2.1 pCMV-miR-34a

Due to the fact that plasmid pCMV-miR-126, -199a and -92a were cloned by F. Nies, the construction of the plasmid pCMV-miR-34a is described here.

For the generation of a plasmid to express the natural miRNA-34a precursor, the miRNA-34a stem loop region surrounded by 100 nt of natural context was amplified from genomic HeLa DNA with the oligonucleotides pri-miR-34a_XhoI-f and pri-miR-34a_XbaI-r. The restriction sites for *XhoI* and *XbaI* together with an additional 5'-cttctc-3' sequence to enhance restriction efficiency were attached to the respective 5' ends of the oligonucleotides. After amplification, the PCR product was purified by gel extraction. Subsequently, the backbone plasmid pCMV-MS and the amplicon were digested with the restriction endonucleases *XhoI* and *XbaI* and the restricted backbone was purified through gel extraction, whereas the insert was purified via column purification. Then, the insert was ligated with the backbone resulting in plasmid pCMV-miR-34a (Fig. 5.5).

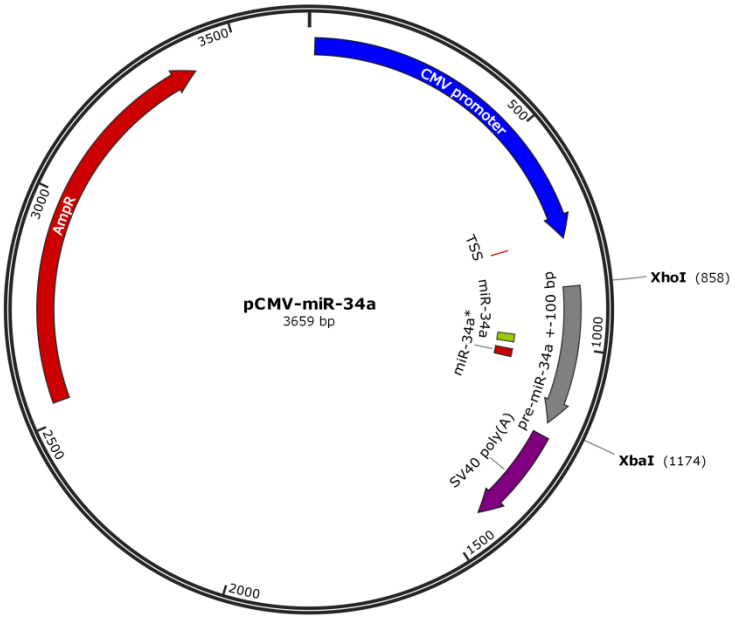

Figure 5.5 Plasmid map of pCMV-miR-34a.
The plasmid map schematically shows the composition of the expression plasmid pCMV-miR-34a. The natural miRNA-34a stem loop surrounded by 100 nt of natural context up- and downstream (grey) is expressed under control of a CMV promoter (blue). Within the miR-34a stem loop the miR-34a-5p (=miR-34a) highlighted in green and miR-34a-3p (=miR-34a*) illustrated in red are located. For transcription termination an SV40 poly(A) signal (purple) is present downstream of the natural miRNA precursor CDS. The restriction sites for *XbaI* and *XhoI* that were used for the insertion of the miRNA precursor surrounded by 100 nt of natural context are also shown.

5.5.2.2 pCMV-miR-34a_2

To generate pre-miR switch miR-34a_2 on the basis of plasmid pCMV-miR-34a, the replacement of the natural terminal loop with the TetR aptamer is illustrated below. A two-step overlap extension (OE) PCR was used to create the plasmid. The first PCR (pre-fusion PCR) was performed to amplify two PCR products each containing a part of the TetR aptamer from the template pCMV-miR-34a using the oligonucleotide combinations CMV prom fwd/miR-34a-#2_1-r and miR-34a-#2_2-f/SV40 poly(A) rev. For that purpose, a respective part of the TetR aptamer was attached to the 5' ends of the oligonucleotides miR-34a-#2_1-r and miR-34a-#2_2-f creating a 30 nt overlap of the TetR aptamer sequence (Fig. 5.6). After *DpnI* digestion of the template and column purification of the amplicons, the two PCR products and primers CMV prom fwd and SV40 polyA rev were used to perform the fusion PCR. Then, the produced amplicon was purified through gel extraction and digested together with the backbone plasmid pCMV-miR-34a using the restriction endonucleases *XhoI* and *XbaI*. After purification of the backbone using gel extraction and the column purification of the insert both parts were ligated resulting in plasmid pCMV-miR-34_2 (Fig. 5.7).

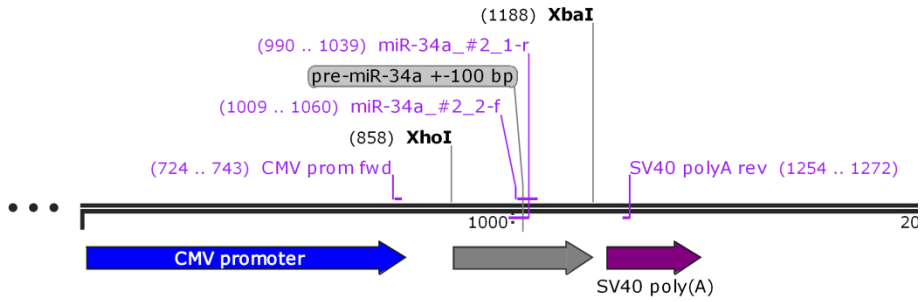

Figure 5.6 Schematic section of map pCMV-miR-34a_2.
The plasmid map schematically shows a section of plasmid pCMV-miR-34a_2. Indicated are the annealing positions of the respective primer pairs used to amplify the first two PCR products. The oligonucleotides miR-34a_#2_2-f and miR-34a_#2_1-r possess 5' overhangs containing parts of the TetR aptamer sequence, respectively. These overhangs produce a 30 nt overlap region necessary for overlap extension PCR.

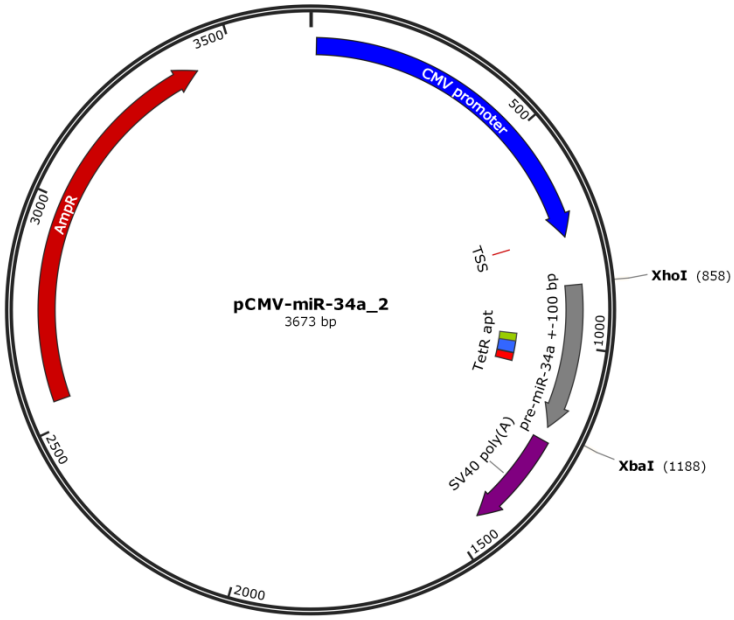

Figure 5.7 Plasmid map of pCMV-miR-34a_2.
The plasmid map schematically shows the composition of the pCMV-miR-34a_2 expression plasmid. The pre-miR switch miRNA-34a_2 construct is expressed under control of a CMV promoter (blue) and surrounded by 100 nt of natural context up- and downstream (grey). Within this natural context the pre-miR-34a stem loop that harbors miR-34a-5p highlighted in red and miR-34a-3p illustrated in green is located. The TetR aptamer (TetR apt, light blue) was inserted in between both miRNAs. For transcription termination an SV40 poly(A) signal (purple) is present downstream of the natural precursor CDS.

5.5.2.3 pMIR-perfect match-miR-199a-5p

For the construction of the reporter gene plasmids for performing the luciferase assay, plasmid pMIR-Report served as the basic plasmid. The MCS of pMIR-Report was used to insert either the perfect complementary sequence, a triplicate of a predicted target sequence or (a part of) the 3'UTR of a validated target gene.

To create pMIR-perfect match miR-199a-5p harboring the perfect match target site for miR-199a-5p the two oligonucleotides perfectmatch-miR-199a-5p-f and perfectmatch-miR-199a-5p-r equipped with the processed restriction ends of *HindIII* and *SacI* at both ends were ordered, 5'-phosphorylated and

hybridized. The plasmid pMIR-Report was digested employing the restriction enzymes *HindIII* and *SacI* and purified by gel extraction. After column purification, the insert was ligated with the pMIR-Report backbone resulting in the plasmid pMIR-perfect match miR-199a-5p (Fig. 5.8).

For the generation of plasmid pMIR-3xseed-miR-199a-5p bearing a triplicate of a target sequence downstream of the firefly luciferase CDS the respective primer pairs 3xseed-miR-199a-5p_I-f and 3xseed-miR-199a-5p_I-r, 3xseed-miR-199a-5p_II-f and 3xseed-miR-199a-5p_II-r as well as 3xseed-miR-199a-5p_III-f and 3xseed-miR-199a-5p_III-r were used. The oligonucleotides bearing the target sites were phosphorylated, hybridized and inserted stepwise into the backbone pMIR-Report employing the restriction sites for *XhoI* and *SpeI*, *SpeI* and *SacI* as well as *SacI* and *HindIII*.

The construction of plasmid pMIR-3'UTR-DDR1 that contains a larger part of the 3'UTR of *DDR1* downstream of the firefly luciferase CDS was accomplished using the primer pair DDR1-UTR_SpeI-f and DDR1-UTR_HindIII-r. This primer pair possesses the restriction sites for *HindIII* and *SpeI* at the respective 5' end and was used to amplify a part of the 3'UTR from genomic HeLa DNA. Then, the amplicon was purified through gel extraction and together with the pMIR-Report restricted using the restriction endonucleases *HindIII* and *SpeI.* Afterwards the prepared backbone and the insert were ligated.

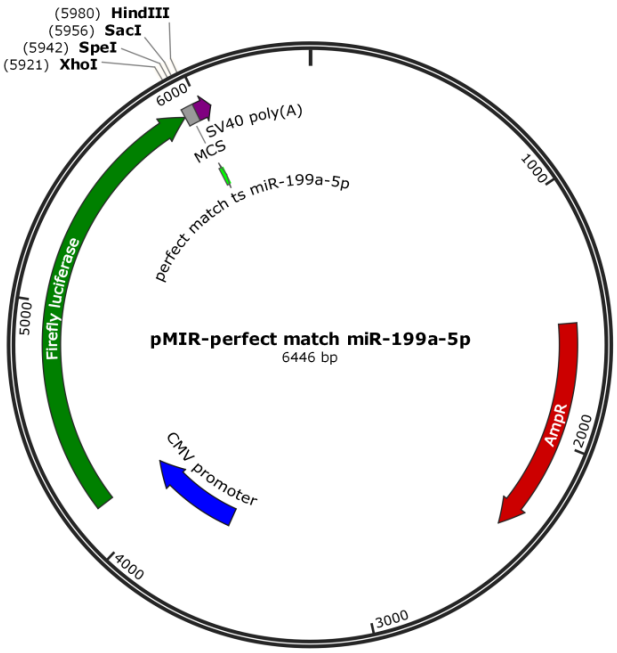

Figure 5.8 Plasmid map of pMIR-perfect match miR-199a-5p.
Indicated is the CMV promoter (blue) that regulates the expression of the firefly luciferase gene (green). Furthermore, the MCS (grey) containing the perfect match target site for miR-199a-5p binding (light green) and the SV40 poly(A) signal (purple) are shown. The plasmid contains the CDS of the β-lactamase (AmpR) that confers ampicillin resistance to the bacterial host organism. The restriction sites used for the insertion of all target regions are indicated within the MCS.

5.5.2.4 pFRT-miR-199a

To generate plasmid pFRT-miR-199a for the first genomic integration, the primer pair Gen.int.199a(#2)-BamHI-f and Gen.int.199a(#2)-SacI-r was used to amplify the natural pre-miR-199a surrounded by 100 nt of natural context from the template plasmid pCMV-miR-199a. The primers contained the restriction sites for *BamHI* or *SacI* attached to the 5' ends to enable the insertion of the amplified sequence into the backbone. After amplification, the insert was purified via column purification and backbone pFRT-CD20 and insert were restricted using the restriction endonucleases *BamHI* or *SacI.* After purification by gel extraction, both components were ligated to yield plasmid pFRT-miR-199a (Fig. 5.9).

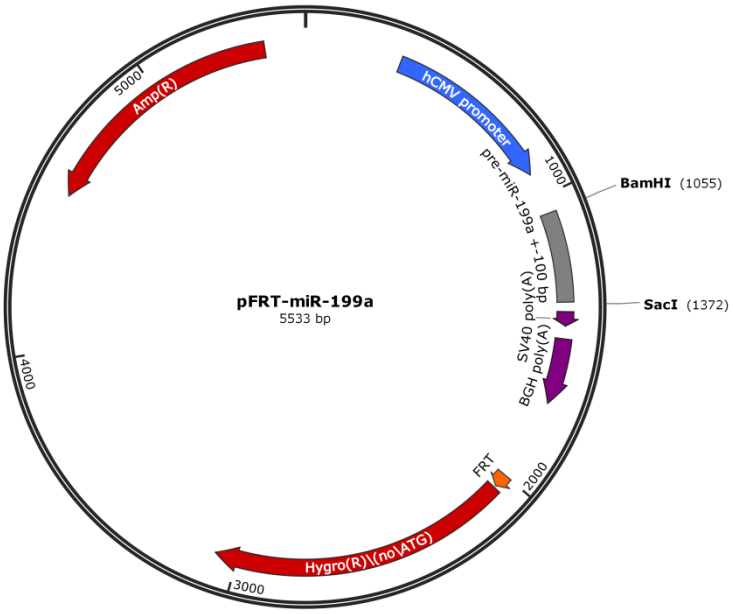

Figure 5.9 Plasmid map of pFRT-miR-199a.
The plasmid pFRT-miR-199a contains an hCMV promoter (blue) in front of the natural miR-199a precursor that is surrounded by 100 nt of natural context (grey). An SV40 poly(A) signal (purple) and a BGH poly(A) (purple) is located downstream of the pre-miR-199a expression sequence. Furthermore the FRT site (orange) and a hygromycin resistance conferring CDS missing the start codon (Hygro(R) (no ATG), red) are indicated. The plasmid harbors an ampicillin resistance gene (AmpR, red).

5.5.2.5 pFRT-miR-199a-TetR

In the second genomic integration, a co-integration of the natural miR-199a precursor surrounded by 100 nt natural context and a TetR expression determinant was performed. First, an additional restriction site for *SpeI* was inserted into the plasmid pFRT-miR-199a using the primer pair SpeI-ins-f and SpeI-ins-r that was later employed for the insertion of the TetR-poly(A) sequence.

The TetR-poly(A) sequence was amplified from the template plasmid pCMV-TetR using primers TetR-polyA-SpeI-f and TetR-polyA-ClaI-r. The SV40 promoter was amplified from the pRL-SV40 plasmid using SV40prom-ClaI-f and SV40prom-SbfI-r. After *DpnI* digestion and column purification, backbone pFRT-miR-199a as well as the inserts were restricted by *SpeI* and *ClaI* to insert the TetR-poly(A) as well as *ClaI* and *SbfI* to insert the SV40 promoter. After restriction digest, the single compounds were purified through gel extraction and ligated to produce plasmid pFRT-miR-199a-TetR (Fig. 5.10).

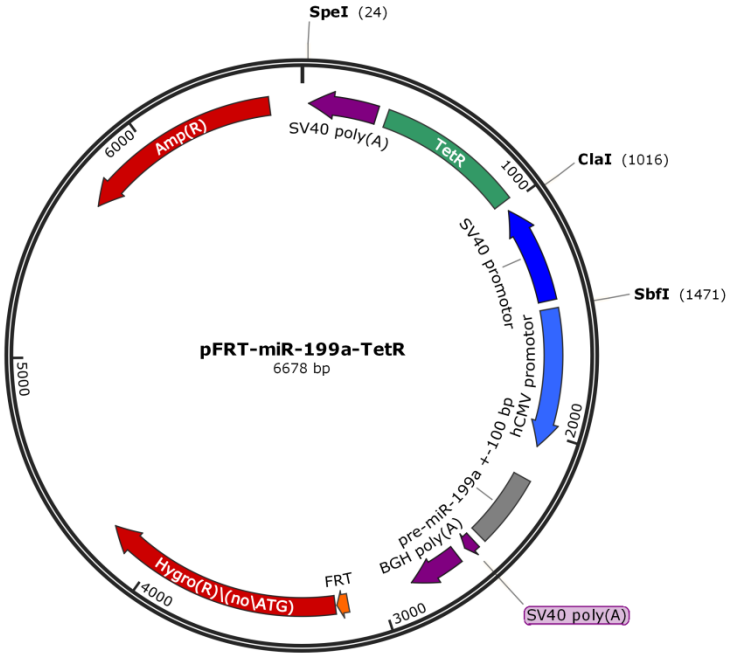

Figure 5.10 Plasmid map of pFRT-miR-199a-TetR.
The plasmid pFRT-miR-199a-TetR contains an hCMV promoter (blue) in front of the natural miR-199a precursor (grey) and an SV40 promoter (dark blue) in front of the TetR CDS (green). An SV40 poly(A) signal (purple) and a BGH poly(A) (purple) is located downstream of the pre-miR-199a expression sequence. Another SV40 poly(A) signal (purple) is located downstream of the TetR CDS. Furthermore the FRT site (orange) and a hygromycin resistance conferring CDS missing the start codon (Hygro(R) (no ATG), red) are indicated. The plasmid harbors an ampicillin resistance gene (AmpR, red).

5.6 Methods

5.6.1 Treatment of prokaryotic cells

5.6.1.1 Preparation of electrocompetent cells

One day before starting the preparation, two overnight cultures of 4 ml LB-medium containing tubes were inoculated with *E.coli* Top10 cells and grown at 37°C at 150 rpm overnight. At the following day, the overnight cultures were transferred to 600 ml of LB-medium in a 2 L baffle flask to yield a start OD_{600} of 0.1. The cell suspension was incubated at 37°C at 200 rpm. After reaching an OD_{600} between 0.6 - 0.8 cells were chilled on ice for 0.5 h on a slowly shaking rocking shaker, harvested by centrifugation for 20 min at 7,000 rpm and washed twice with 10% (v/v) of sterile glycerol. In the last step, all cells were suspended in 4 ml of 10% (v/v) of sterile glycerol and split into aliquots of 100 µl in 1 ml reaction tubes.

5.6.1.2 Electroporation of *E.coli*

Electroporation was used to transform *E.coli* cells. SOC-medium as well as cell culture plates were pre-warmed at 37°C, electroporation cuvettes pre-chilled and 50 µl of electrocompetent bacteria slowly thawed on ice. Then, 0.5 µl of DNA were gently mixed with the bacteria and the mixture transferred into the slit of the cuvette. The bacteria were electro-shocked with 1,800 V for 5 ms. Immediately after applying the electric field to the cells, cells were extracted from the cuvette and mixed with 450 µl SOC-medium. After a 10 min recovery phase at 37°C and 1,000 rpm in the shaker, 80 µl (re-transformation)-200 µl (ligation) of cells were plated onto agar plates containing ampicillin. Subsequently cells were incubated at 37°C overnight.

5.6.2 Treatment of eukaryotic cells

5.6.2.1 Cultivation, harvest and storage

For performing cell culture with human cells, a laminar flow cabinet was employed. HeLa cells and HeLa HF1-3 cells [172] were cultivated in Dulbecco's Modified Eagle Medium (DMEM) supplemented with 10% (v/v) fetal bovine serum, 100 U/ml penicillin, 100 µg/ml streptomycin and 1 mM sodium pyruvate. For the cultivation of HeLa HF1-3 cells, the medium was additionally supplemented with 100 µg/ml zeocin. For maintenance an incubator was adjusted to 37°C, 5% CO_2 and 100% humidity. 1 x 10^6 cells were seeded in 20 ml of medium into a T75 cell culture flask and splitted every 3 to 4 d. For splitting the cells, the medium was removed and cells were washed with 3 ml 1x PBS. Then, cells were detached from the flask surface through the addition of 3 ml of Trypsin/EDTA and incubation for 5 min at 37°C. Afterwards, 7 ml of medium were added and the cell count determined with the cell counter. For 12-well plates, 1.4 x 10^5 HeLa cells or 0.9 x 10^5 HF1-3 cells were seeded per well in 2 ml of medium. For 24-well plates, 0.55 x 10^5 HeLa cells were seeded per well in 1 ml of medium. For long-term storage, the harvested cells were centrifuged and re-suspended in DMEM supplemented with 10% (v/v) FBS, 100 U/ml penicillin, 100 µg/ml streptomycin, 1 mM sodium pyruvate and 10% (v/v) DMSO to yield a concentration of 1.5–2 x 10^6 cells/ ml. 1 ml of the cell suspension was then transferred into a cryo-vial and frozen in a 2-propanol containing freezing device at -80°C. After two

days, the cryo-vials were removed from the freezing device and stored in the liquid nitrogen phase of a container filled with liquid nitrogen.

5.6.2.2 Transient transfection

Cells were transiently transfected with Lipofectamine® 2000 according to the manufacturer`s protocol. For 12-well plates, 1.4 x 10^5 HeLa cells were seeded in 2 ml of medium one day before transfection. Cells were grown to 90-95% of confluency for transfection. A total amount of 800 ng DNA per well (ratio of miRNA precursor or pre-miR switch expression plasmid:TetR expression plasmid 1:1) was used for transfection. For each sample, 2 µl of Lipofectamine and 48 µl Opti-MEM were mixed and incubated for 5 min at room temperature. Furthermore, the DNA was diluted in 50 µl of Opti-MEM. The DNA- and Lipofectamine dilutions were mixed in a 1:1 ration and incubated for 20 min at room temperature. Meanwhile, the medium was removed from the cells and replaced with 500 µl Opti-MEM per well. Then, the DNA-Lipofectamine mixture was added to the cells and the cells were incubated for 3.5 h at 37°C. Afterwards, the lipofection medium was replaced with complete growth medium possibly supplemented with 1 µg/ml dox and cells were incubated at 37°C to the next day.

For 24-well plates, 0.55 x 10^5 HeLa cells per well were seeded in 1 ml of complete medium. A total DNA amount of 500 ng DNA per well (ratio of reporter gene plasmid: miRNA precursor or pre-miR switch expression plasmid:TetR expression plasmid:normalization plasmid 4:7:7:2) was used for transfection. For a 24-well-based transfection the respective amounts of Lipofectamine and Opti-MEM were scaled down: 1 µl of Lipofectamine was mixed with 24 µl of Opti-MEM per sample, and the DNA was diluted in 25 µl Opti-MEM.

5.6.2.3 Genomic integration

For genomic integration the Flp-In™ System in combination with HeLa HF1-3 cells harboring a single stably integrated FRT-site at a transcriptional active genomic locus was used. For the first integration, the miR-199a and miR-199a_2 constructs were cloned into the multiple cloning site of the pFRT-CD20 plasmid using *BamHI* and *SacI* and constitutively expressed from an hCMV immediate-early enhancer and promoter. For the second integration, the TetR expression sequence with an SV40 poly(A) tail as well as the SV40 promoter were additionally inserted into the plasmid pFRT-miR-199a(_2) using *ClaI* and *SpeI* and *ClaI* and *SbfI* in addition to the constructs miR-199a and miR-199a_2. The expression of miRNA and TetR from the integration plasmids was tested and after the confirmation of their functionality transfected into HF1-3 cells. As controls, a plasmid harboring no FRT-site for recombination constituting the negative selection control and a pFRT-GFP vector harboring the *GFP* gene for monitoring transfection and integration under the microscope were also transfected in parallel to the constructs. For transfection, 0.9 x 10^5 HF1-3 cells were seeded in 2 ml of complete medium without antibiotics per well in a 12-well plate. Then, 1,800 ng of the Flp-recombinase expression vector pOG44 and 200 ng of the construct vector or the control vectors (ratio 9:1) were transfected into the cells (5.6.2.2 transient transfection). After 4 h of incubation the lipofection mix was removed and 2 ml of complete medium without antibiotics were added to each well. At the following day, the medium was exchanged and the transfection efficiency was checked using fluorescence microscopy. The transfection efficiency was roughly approximated to be at 60-70%. After two days, the medium was removed and the selection medium supplemented with 150 µg/ml hygromycin B was added. During

the selection for integrated clones, the selection medium was exchanged all 2 to 3 d. After some weeks, the negative control cells were completely dead and, in case of the first integration, the successfully selected cells were split into single clones through dilution in 96-well plates. Cells derived from a single clone were raised and cultured in selection medium in T75 cell culture flasks. At the end of selection, cells were tested for miRNA and TetR expression and the integration sites were sequenced. For sequencing, the genomic DNA was isolated with the DNeasy® Blood & Tissue kit, the target sequence was amplified by PCR and the PCR product was sequenced.

5.6.2.4 Dual Luciferase reporter gene assay

For the performance of the dual luciferase assay, the pMIR-REPORT vector was used that constitutively expresses the firefly luciferase gene from the CMV promoter. The pRL-SV40 that provides constitutive expression of the wild-type *Renilla* luciferase gene through an SV40 promoter was co-transfected with the pMIR-REPORT vector and used as an internal control for normalization of the firefly luciferase reporter gene-derived luminescence values. The respective miRNA target sequences and control sequences or (larger parts of) the target gene 3'UTRs were introduced downstream of the firefly luciferase reporter gene. The plasmids were co-transfected into HeLa cells together with the respective pre-miR switch and TetR expression plasmids as well as the pRL-SV40 and cultivated in the absence or presence of 1 µg/ml dox. Luminescence measurements were performed 24 h post transfection with the Dual-Glo® Luciferase Assay System according to the manufacturer's protocol. Before cell lysis, the cells were washed twice with 1x PBS and 100 µl of complete medium without phenol red indicator were added to each well. Then, 100 µl of the Dual Glo® Luciferase reagent were mixed to each well and incubated for 10 min at room temperature. Afterwards, the 200 µl lysate was transferred into white, 96-well Nunc™ MicroWell™ plates and firefly luciferase luminescence was measured with the Infinite®M200 plate reader using one second integration time. After that, 100 µl of the freshly prepared Dual Glo® Stop&Glo® reagent were added, incubated for 10 min at room temperature and *Renilla* luciferase luminescence was monitored. For normalization, the ratio between *Renilla* and firefly luciferase values was calculated for each well. Then, mean values as well as standard deviation were calculated from duplicates and normalized to the value derived from the empty plasmid pCMV-MS.

5.6.2.5 Time course experiments

The time course experiments were performed using construct miR-199a_2 for transient transfection (5.6.2.2 transient transfection). To gain information about the processing of the modified precursor in the course of time, also additional control transfections were performed with the pre-miR switch bearing plasmid, but without the TetR expression plasmid or dox. After transfection, cells were incubated in complete medium for one day. At the next day, dox was added to the medium per wells and cells were harvested after 0, 4, 8, 16 and 24 h of incubation at 37°C. Then, RNA was isolated from the samples and the amount of mature miRNA was determined using qPCR. The amount of mature miRNA measured by qPCR was normalized to the amount of miRNA that was obtained from the above mentioned controls.

5.6.3 Treatment of proteins

5.6.3.1 Protein preparation from eukaryotic cells

After transfection and incubation, cells were washed with 1xPBS and harvested from 12-well plates or T75 cell culture flasks using either 500 µl or 3 ml of Trypsin/EDTA per well. After 5 min of incubation at 37°C, 1 ml or 7 ml of complete medium were added to each well or flask and the respective cell suspension was transferred to an either an 2 ml reaction tube or a 50 ml tube. Then, the cell suspensions were centrifuged at 9 x 10^3 rpm or 4.5 x 10^3 rpm for 5 min and the supernatant was removed. Subsequently, cells were re-suspended in 80 µl or 3 ml of protein lysis buffer and incubated for at least 30 min on ice. To separate supernatant and cell debris, the tubes were centrifuged for 5 min at 9 x 10^3 rpm and the supernatant was transferred into a fresh tube.

5.6.3.2 Protein concentration determination

For the determination of the protein concentration the Bradford protein assay was used. A standard curve was developed by using 0, 2, 6, 10, 15 and 20 µg of BSA. The amount of BSA was diluted with water ad 20 µl and 980 µl of a 1:5 dilution of the Bradford reagent were added, mixed and incubated for 10 min at room temperature. Then, the mixture was transferred into a cuvette and absorption was measured at 595 nm with a spectrophotometer.

2-3 µl of the protein extract were diluted with 17-18 µl of MQ and 980 µl of a 1:5 dilution of the Bradford reagent were added. The mixture was mixed and incubated for 10 min at room temperature. Afterwards, the measurement was performed the same way as described above. With the help of the standard curve, the concentration of each sample was determined and the required concentration was adjusted.

5.6.3.3 SDS-PAGE and western blotting

To investigate the effect caused by the miRNA switches at the protein level, western blotting was performed. For performing an SDS-PAGE, the Mini-PROTEAN® TGX Stain-Free™ precast gels with 10 wells or 8+1 wells and either any kDa or 7.5% dependent on protein size were employed. The protein amount was adjusted to 20-40 µg of protein per sample, mixed with 4x protein loading buffer and heated for 5–10 min to 95°C. The SDS-PAGE gels were run with 140 V in 1x running buffer.

For western blotting, the Trans-Blot® Turbo™ Transfer system was used according to the manufacturer`s protocol. The gel was removed from the gel chamber and washed with MQ water. Subsequently, the prepared stacks and the 0.2 µm PVDF membrane from the Transfer Pack were lifted from the tray and positioned in the centre of the cassette. The gel was placed onto the membrane and covered with the Top ion reservoir stack. After removing bubbles, the blotting cassette was closed and put into the Trans-Blot® Turbo™ apparatus. The transfer programs were chosen according to the size of the selected protein. For blotting the proteins SMAD4 with 65 kDa and DDR1 with 100–125 kDa, the “mixed MW” pre-programmed protocol was applied, whereas for blotting of CAV1 with 22 kDa the pre-programmed protocol “low MW” was used according to the manufacturer`s recommendations. After blotting the proteins onto the membrane, the membrane was blocked with either 2% (w/v) ECL-reagent (SMAD4, CAV1, TetR) or skimmed milk powder (DDR1) in 1x TBST for 1.5 h gently shaking on a rocking shaker at room temperature. Then, the membrane was incubated

with the first antibody for either 1-2 h (SMAD4) or overnight (DDR1, CAV1). The anti-SMAD4, anti-DDR1 and anti-CAV1 antibodies were diluted 1:1,000 with the respective blocking reagent for usage. The anti-TetR antibody was diluted 1:5,000, the anti-β-actin and anti-HSP-60 antibody 1:7,000 and 1:2,000 for application. Afterwards, the membrane was washed three times with 1x TBST for 15 min and the secondary antibody was added. The secondary antibodies were used in a 1:7,000 dilution with the respective blocking reagent and incubated for 1 h at room temperature. After washing the membranes three times for 15 min, the detection was performed with the Clarity™ and the Clarity Max™ Western ECL Blotting substrate dependent on signal intensity at the ChemiDoc™ MP system. For protein detection the Clarity Western Peroxid Reagent and the Clarity Luminol/Enhancer Reagent were mixed in a 1:1 ratio and incubated on the membrane for 5 min.

5.6.4 Treatment of nucleic acids

5.6.4.1 Agarose gel electrophoresis

The analysis of size and quality of DNA and RNA as well as the DNA fragment purification was performed through applying agarose gel electrophoresis. Dependent on fragment size, 1% - 3% (w/v) agarose gels were used. For their fabrication, the respective amount of agarose was dissolved in 1x TAE and dissolved by heating in the microwave. The samples were mixed with 6x DNA or 2x RNA loading dye, the gel was run in 1x TAE and an electric field strength of 6 V/cm. Afterwards, the gels were stained in 0.5 µg/ml ethidium bromide for 10 min and DNA or RNA was visualized under UV light. For analytical gels a wave length of 254 nm, for preparative gels a wave length of 366 nm was employed to prevent the extracted DNA from damage.

5.6.4.2 DNA precipitation with 1-butanol

To concentrate DNA, 10 volumes of 1-butanol were added to the DNA solution and the mix was vortexed for 10 s. Then, it was centrifuged for 10 min at 13,000 rpm, washed with 70% (v/v) ethanol and centrifuged for 5 min at 13,000 rpm, again. After removing the supernatant, the pellet was dried for 5 min at room temperature and subsequently dissolved in 8 µl water.

5.6.4.3 DNA purification

DNA purification was conducted by using column purification or gel extraction methods. To purify DNA from proteins, salt, RNA and small DNA fragments, the QIAquick PCR Purification kit was used. To isolate DNA fragments of defined size, the DNA sample was run on a gel and the band of interest was excised from the gel. Gel extraction was performed employing the Zymoclean® Gel DNA Recovery kit according to the manufacturer`s protocol. The pellet was dissolved in water instead of the recommended buffer. After purification, the concentration of the sample was determined with the NanoDrop® ND-1000 Spectrophotometer.

5.6.4.4 Determination of the concentration of nucleic acids

The concentration of DNA and RNA sample was determined at 260 nm wave length using the NanoDrop® ND-1000 Spectrophotometer. As reference the respective solvent was employed.

5.6.4.5 Plasmid preparation

For the propagation of a plasmid in bacteria, the cells containing the desired plasmid were inoculated in 4 ml of LB-medium supplemented with the respective antibiotic and grown at 37°C shaking at 150 rpm overnight. For plasmid isolation the QIAprep®Spin Miniprep kit was used according to the manufacturer`s protocol. The pellet was dissolved in water instead of the recommended buffer. After plasmid isolation, the concentration of the sample was determined with the NanoDrop® ND-1000 Spectrophotometer.

5.6.4.6 Polymerase Chain Reaction (PCR)

PCR was employed to delete, insert or amplify defined sequence parts and to screen for desired sequences. Here, plasmid- and genomic DNA, PCR amplicons or whole cells were applied as template.

For constructing the plasmids bearing the miRNA precursor, the respective miRNA stem loop structures flanked by 100 nt up- and downstream of the stem loop region were amplified from genomic HeLa DNA and introduced into the multiple cloning site of pCMV-MS. Afterwards, a two-step overlap extension-PCR was applied. The first PCR (pre-fusion PCR) served to introduce additional sequence parts that were attached to the 5' end of the respective primer into selected positions of the plasmid. By the creation of an overlap region in the PCR used to prime amplification, the second step (fusion PCR) was used to fuse the respective single fragments to one insert. The respective template amount was adjusted to result in equimolar amounts of template. The programs as well as the reaction mixtures for the two-step OE-PCR are depicted in Table 5.12-15.

Table 5.12 Reaction mixture for the performance of the pre-fusion PCR**.**

Concentration	Reagent	Reagent volume [µL]	End concentration
5x	Q5® Reaction Buffer	20	1x
10 µM	primer fwd	3	300 nM
10 µM	primer rev	3	300 nM
100%	DMSO	3	3%
25 ng/µL	template	4	1 ng/µl
10 mM	dNTPs	2	200 µM
2 U/µL	Q5® High-Fidelity DNA Polymerase	1	0.02 U/µl
	MQ	ad 100	
	total	100	

Table 5.13 PCR program applied for the pre-fusion PCR.

	Temperature [°C]	Time	
Initial denaturation	98	30 s	
Denaturation	98	7 s	35 cycles
Annealing	50	20 s	
Extension	72	20 s/kb	
Final extension	72	4 min	

Table 5.14 Reaction mixture for the performance of the fusion PCR**.**

Concentration	Reagent	Reagent volume [µL]	End concentration
5x	Q5® Reaction Buffer	20	1x
10 µM	primer fwd	3	300 nM
10 µM	primer rev	3	300 nM
100%	DMSO	3	3%
	template 1	x	50 – 150 ng
	template 2	x	50 – 150 ng
10 mM	dNTPs	2	200 µM
2 U/µL	Q5® High-Fidelity DNA Polymerase	1	0.02 U/µl
	MQ	ad 100	
	total	100	

Table 5.15 PCR program applied for the fusion PCR.

	Temperature [°C]	Time	
Initial denaturation	98	1 min	
Annealing	45	1 m	
Extension	72	20 s/kb	
Denaturation	98	10 s	30 cycles
Annealing	56	30 s	
Extension	72	20 s/kb	
Final extension	72	4 min	

The reaction mixture contents as well as the program for standard PCR amplification was absolutely conform to that of the Pre-Fusion-PCR. Merely, the annealing temperature was adapted to the melting temperature of the applied primers.

By means of colony-PCR, several bacterial clones were screened for harboring a plasmid with the correct insert by the amplification of a defined sequence. The band pattern obtained from PCR-based amplification was visualized on an agarose gel. The appearance of the desired band in the gel implied the correct insertion or deletion of a particular sequence in the plasmid. A bacterial colony was picked from an LB-plate and suspended in 50 µl of water. 1 µl was used for the analysis by PCR. The programs as well as the reaction mixture for colony PCR are shown in Table 5.16 and 5.17.

Table 5.16 Reaction mixture for the performance of the colony PCR**.**

Concentration	Reagent	Reagent volume [µL]	End concentration
10x	Taq DNA Buffer	10	1x
10 µM	primer fwd	0.3	300 nM
10 µM	primer rev	0.3	300 nM
	bacterial cell	1	
10 mM	dNTPs	0.2	200 µM
5 U/µL	Taq DNA Polymerase	0.2	0.1 U/µl
	MQ	6.8	
	total	10	

Table 5.17 PCR program applied for colony PCR.

	Temperature [°C]	Time	
Initial denaturation	95	10 s	
Denaturation	95	5 s	25 cycles
Annealing	50	30 s	
Extension	72	1 min/kb	
Final extension	72	4 min	

5.6.4.7 Oligonucleotide annealing and 5' end phosphorylation

To produce short oligonucleotide-based stretches without using a template for cloning, the complementary single strands were ordered pre-cut to match the restriction site of the target vector. For efficient sticky end ligation into a plasmid, the double-stranded products were phosphorylated at the 5' end. The reaction mix for 5' end phosphorylation is displayed in Table 5.18.

Table 5.18 Oligonucleotide-annealing reaction mix.

Concentration	Reagent	Reagent volume [µL]	End concentration
10x	T4-Polynucleotide Kinase Buffer	5	1x
100 µM	oligonucleotide fwd	1.5	3 µM
100 µM	oligonucleotide rev	1.5	3 µM
10 mM	ATP	5	1 mM
10 U/µL	T4-Polynucleotide Kinase (T4-PNK)	1	0.2 U/µl
	MQ	ad 50	
	total	50	

The mix without T4-PNK was incubated 2 min at 98 °C and then cooled with 0.1°C/s to 25°C. T4-PNK was added, the reaction mix was mixed and incubated at 37 °C for 1 h.

5.6.4.8 Restriction digest

For DNA restriction digest, type IIP restriction endonucleases were used with the manufacturer`s buffer systems according to the manufacturer`s recommendations. Up to 4 µg of DNA were applied for digestion in a volume of 50 µl. The reaction mixture for restriction digest is shown in Table 5.19.

Table 5.19 Reaction mix for restriction digest.

Concentration	Reagent	Reagent volume [µl]	End concentration
10x	buffer system	5	1x
20 U/µl	restriction enzyme	1-2	0.4-0.8 U/µl
	DNA	x	2-4 µg/50 µl
	H2O	ad 50	
	total	50	

The restricted plasmid backbones were purified by gel extraction, whereas the restricted PCR-products were purified through column purification, gel extraction or alcohol precipitation dependent on size.

5.6.4.9 DpnI digestion

After the amplification of a PCR product from a bacteria-derived plasmid, the PCR product was treated with 1 µl of *DpnI* for 45 minutes at 37°C to destroy the DNA template. Meanwhile, the amplified product stayed unaffected due to *DpnI*`s property to recognize and digest merely (hemi-)methylated DNA. Afterwards, the PCR product was purified by column purification.

5.6.4.10 Ligation

For ligation of backbone and insert a molar ratio of 1:6 was used. After 1-2 h of ligation at room temperature, the plasmid was precipitated using 1-butanol before transformation and the pellet was resupended in 8 µl of MQ water. The reaction mixture for ligation is depicted in Table 5.20.

Table 5.20 Reaction mixture for ligation.

Concentration	Reagent	Reagent volume [µl]	End concentration
10x	T4 DNA Ligase Buffer	2	1x
x ng/µl	backbone	x	25 ng/20 µl
x ng/µl	insert	x	x ng/20 µl
10 mM	ATP	2	1 mM
400 U/µl	T4 DNA ligase	1	400 U
	MQ	ad 20	
	total	20	

5.6.4.11 Total RNA extraction from human cells and digestion of DNA

The whole extraction process was performed on ice to prevent degradation of RNA through RNases. After transfection and incubation, cells were washed with 500 µl 1x PBS per well, respectively 400 µl of Trizol were added to the cells and the mixture was incubated for 5 min at room temperature. Then, the lyates were transferred to 2 ml reaction tubes and 80 µl of chloroform per sample were added, the samples were vortexed for 15 s and incubated for 3 min at room temperature. The samples were centrifuged for 15 min at 13,000 rpm and 4°C. Afterwards, the upper aqueous phase was transferred into a fresh 2 ml reaction tube and 200 µl of chloroform were mixed to the solution. Subsequently, the samples were vortexed for 15 s again and centrifuged for 15 min at 13,000 rpm and 4°C. Again, the upper aqueous phase was transferred into a fresh reaction tube and 0.75 µl of GlycoBlue™ as well as 200 µl of cold 2-isopropanol were added to the samples. After mixing, the samples were incubated for 10 min at room temperature and centrifuged for 45 min at 13000 rpm and 4°C. The supernatant was removed, samples were washed with 180 µl of 70% (v/v) ethanol and centrifuged for 10 min at 13,000 rpm and 4°C. The pellets were dried for 5 min at room temperature and dissolved in 35 µl of water.
To remove DNA from the samples, 4 µl of 10x TURBO DNase buffer and 0.5 µl TURBO DNase per sample were used. After 15 min incubation at room temperature, 4 µl of 3 M sodium acetate (pH=6.5) and 200 µl of cold 100% (v/v) ethanol were added for RNA precipitation and the samples were incubated for 45 min at - 80°C. Afterwards, RNAs were washed with 70% (v/v) ethanol and dried for 5 min at room temperature. The RNA pellets were dissolved in 20 µl of water, RNA concentration was determined by using the NanoDrop spectrophotometer and RNA integrity of each RNA sample was analyzed on a 1% (w/v) agarose gel. Isolated RNAs were stored at -80°C.

5.6.4.12 Reverse transcription

To transcribe the complete isolated RNA pool for qPCR detection with SYBR Green, random hexamer primers were employed. Random hexamer primers consist of a mixture of oligonucleotides representing all possible hexamer sequences. Random priming during cDNA generation results in a random coverage of all regions of the RNAs and generates cDNAs of different lengths. In total, 1 µg of RNA was transcribed into cDNA. The reaction mixture and the PCR program are depicted in Table 5.21 and 5.22.

Table 5.21 Reaction mix for reverse transcription with random hexamer primers.

Concentration	Reagent	Reagent volume [µL]	End concentration
25 mM	$MgCl_2$ Solution	8	5 mM
10x	PCR Buffer II	4	1x
100 mM	dNTPs	0.4	1 mM
20x	random hexamer primer	2	1x
40 U/µl	RiboLock RNase	1	0.025 U/µl
50 U/µL	MuLV Reverse Transcriptase	2	2.5 U/µl
	MQ	ad 40	
	total (with RNA)	40	

Table 5.22 PCR program for reverse transcription with random hexamer primers.

Temperature [°C]	Time
20	10 min
42	15 min
99	5 min
4	∞

Afterwards, the samples were filled with water ad 200 µl (1:5 dilution).

To rewrite miRNAs into complementary DNA (cDNA) for qPCR detection employing the TaqMan® method, sequence-specific stem-loop (SL) primers were used to make target-specific reverse transcription. In total, 100 ng of RNA were transcribed into cDNA. For normalization in qPCR, the small nucleolar RNA (snoRNA) U48 was co-transcribed to cDNA. In Table 5.23 and 5.24 the reaction mixture and the used PCR program are shown.

Table 5.23 Reaction mix for reverse transcription with SL-primers.

Concentration	Reagent	Reagent volume [µL]	End concentration
5x	First-Strand Buffer	2	1x
500 nM	SL-primer U48	1	50 nM
500 nM	SL-primer miR-X	1	50 nM
10 mM	dNTPs	0.25	0.25 mM
0.1 M	DTT	1	10 mM
25 ng/µl	RNA	4	100 ng/10 µl
200 U/µL	Super-Script™ II Reverse Transcriptase	0.25	5 U/µl
	MQ	0.5	
	total	10	

Table 5.24 PCR program for reverse transcription with SL-primers.

Temperature [°C]	Time	
16	30 min	
30	30 s	60 cycles
42	30 s	
50	1 min	
70	15 min	
4	∞	

After cDNA synthesis, the samples were diluted 1:5 with 40 µl of water.

5.6.4.13 qPCR

Quantitative Real-Time PCR (qPCR) was performed using the StepOnePlus™ Real-Time PCR System. During amplification of the target cDNA, the increase in amplification product is monitored by fluorescence measurement. The cycle threshold (Ct) value indicates the number of cycles that are required for the fluorescence signal to cross the threshold and constitutes a relative measure of the respective target concentration in the reaction sample.

During SYBR Green-based qPCR, the SYBR Green I dye efficiently intercalates into present ds DNA and fluoresces in that bound state. 5 µl of the diluted cDNA solution were employed for measurements and a primer mix of the respective two gene specific primers was mixed in advance. The reaction mix was pipetted into an optical 96-well reaction plate followed by the cDNA, the plate was covered with an optical membrane and shortly centrifuged at 1,500 rpm. The applied reaction mix and the qPCR program are depicted in Table 5.25 and 5.26.

Table 5.25 Reaction mix for reverse transcription.

Concentration	Reagent	Reagent volume [µL]	End concentration
2x	SYBR Green Master Mix	10	1x
10 µM each	Primer Mix	1	0.5 µM each
	cDNA	5	
	MQ	4	
	total	20	

Table 5.26 PCR program for SYBR Green-based qPCR.

Temperature [°C]	Time	
95	20 s	
95	3 s	40 cycles
60	30 s	
95	15 s	melting curve program
60	1 min	
95	15 s	

Each primer pair was tested to produce no unspecific by-products. Specific amplification was verified with melting curves and by visualization of the amplicon in an agarose gel.

All reactions for miRNAs and endogenous controls were run in duplicates. Relative gene expression was analyzed using the $2^{-\Delta\Delta Ct}$ method [174].

TaqMan qPCR was performed according to Chen *et al*. [175]. For this method, a TaqMan probe was used that harbors a fluorescence reporter dye at the 5' end as well as a quencher at the 3' end that quenches dye emission through its direct position next to the reporter dye. During amplification, the DNA polymerase cleaves the reporter dye from the quencher resulting in the reporter dye`s characteristic emission of the fluorescence signal. 5 µl of the cDNA mixture were used for qPCR. During cDNA synthesis, the applied SL-primer introduced a stem-loop structure which harbors a TaqMan probe binding site as well as a Universal Primer binding site required for qPCR. The presence of both binding sites enables the quantification of several miRNAs with one stem-loop sequence. The reaction mix was pipetted into an optical 96-well reaction plate followed by the cDNA, the plate was covered with an optical membrane and shortly centrifuged at 1,500 rpm. The composition of the reaction mix and the qPCR program are shown in Table 5.27 and 5.28.

Table 5.27 Reaction mixture for the TaqMan-based qPCR.

Concentration	Reagent	Reagent volume [µL]	End concentration
2x	TaqMan® Fast Universal Master Mix	10	1x
10 µM	Universal Primer	1	0.5 µM
10 µM	qPCR Primer fwd	1	0.5 µM
	Universal ProbeLibrary Probe #21	1	
	cDNA	5	100 ng/10 µl
200 U/µL	Super-Script™ II Reverse Transcriptase	0.25	5 U/µl
	MQ	2	
	total	20	

Table 5.28 PCR program for the TaqMan-based qPCR.

Temperature [°C]	Time	
50	2 min	
95	10 min	
95	15 s	40 cycles
60	1 min	

All reactions for miRNAs and endogenous control were run in duplicates. The ratio of two cDNAs was calculated through the exponential increase with the formula $2^{-\Delta Ct}$. The ΔCt value represents the difference between $Ct_{reference\ gene}$ and $Ct_{target\ gene}$.

6 Appendix

6.1 Abbreviations

Table 6.1 List of abbreviations.

Abbreviations		Abbreviations	
% (v/v)	% (volume/volume)	Prom	promoter
% (w/v)	% (weight/volume)	qPCR	quantitative PCR
Amp	ampicillin	rev/r	reverse
bp	base pair	RNA	ribonucleic acid
BSA	bovine serum albumin	RNAi	RNA interference
cDNA	complementary DNA	RISC	RNA induced silencing complex
CDS	coding sequence	SD	Shine-Dalgarno
CMV	cytomegalovirus	SDS	Sodium dodecyl sulfate
dNTP	deoxynucleoside triphosphate	shRNA	small hairpin RNA
DMSO	dimethylsufoxide	siRNA	small interfering RNA
DNA	deoxyribonucleic acid	SL	stem loop
dox	doxycycline	ss	single strand
ds	double stranded	SV40	Simian vacuolating virus 40
et al.	et alii	TBS	tris buffered saline
EtOH	ethanol	tc	tetracycline
FBS	fetal bovine serum	TF	transcription factor
fwd/f	forward	UTR	untranslated region
gDNA	genomic DNA	UTR	untranslated region
LB	lysogeny broth		
MCS	multiple cloning site		
miRNA/ miR	micro RNA		
mRNA	messenger RNA		
nt	nucleotides		
PAGE	polyacrylamide gel electrophoresis		
PBS	phosphate buffered saline		
PCR	polymerase chain reaction		
pre-miRNA	precursor miRNA		
pri-miRNA	primary miRNA		

6.2 Units

Table 6.2 List of units.

Units	
°C	degree Celsius
Da	Dalton
g	gram
h	hours
l	liter
M	molar
min	minutes
rpm	rounds per minute
sec	seconds
U	unit
V	volt
v/v	volume per volume
w/v	weight per volume

6.3 Prefixes

Table 6.3 List of used prefixes.

Dimensions	
k	kilo (10^{3})
m	milli (10^{-3})
µ	micro (10^{-6})
n	nano (10^{-9})
p	pico (10^{-12})

6.4 Nucleobases

Table 6.4 Abbreviations for nucleobases.

Nucleobases	
A	adenine
C	cytosine
G	guanine
T	thymine
U	uracil
N	A, C, G, T, U

7 References

(1) de Vriend, H. (2006) Constructing Life. Early social reflections on the emerging field of synthetic biology. The Hague: Rathenau Institute.

(2) Martin, V. J. J., Pitera, D. J., Withers, S. T., Newman, J. D., and Keasling, J. D. (2003) Engineering a mevalonate pathway in Escherichia coli for production of terpenoids. *Nat. Biotechnol. 21*, 796–802.

(3) Lindahl, A.-L., Olsson, M. E., Mercke, P., Tollbom, Ö., Schelin, J., Brodelius, M., and Brodelius, P. E. (2006) Production of the Artemisinin Precursor Amorpha-4,11-diene by Engineered Saccharomyces cerevisiae. *Biotechnol. Lett. 28*, 571–580.

(4) Ro, D.-K., Paradise, E. M., Ouellet, M., Fisher, K. J., Newman, K. L., Ndungu, J. M., Ho, K. A., Eachus, R. A., Ham, T. S., Kirby, J., Chang, M. C. Y., Withers, S. T., Shiba, Y., Sarpong, R., and Keasling, J. D. (2006) Production of the antimalarial drug precursor artemisinic acid in engineered yeast. *Nature 440*, 940–943.

(5) Berens, C., and Suess, B. (2015) Riboswitch engineering - making the all-important second and third steps. *Curr. Opin. Biotechnol. 31*, 10–15.

(6) van Steensel, B. (2011) Chromatin: constructing the big picture. *EMBO J. 30*, 1885–95.

(7) Brown, T. A. (2002) Genomes. 2nd ed. Wiley-Liss.

(8) Woodcock, C. L., and Ghosh, R. P. (2010) Chromatin Higher-order Structure and Dynamics. *Cold Spring Harb Perspect Biol 2*, 1–26.

(9) Li, B., Carey, M., and Workman, J. L. (2007) The Role of Chromatin during Transcription. *Cell 128*, 707–719.

(10) Iyer, B. V., Kenward, M., and Arya, G. (2011) Hierarchies in eukaryotic genome organization: Insights from polymer theory and simulations. *BMC Biophys. 4*, 8.

(11) Struhl, K. (1999) Fundamentally Different Logic of Gene Regulation in Eukaryotes and Prokaryotes. *Cell 98*, 1–4.

(12) Orphanides, G., Lagrange, T., and Reinberg, D. (1996) The general transcription factors of RNA polymerase II. *Genes Dev. 10*, 2657–83.

(13) Maston, G. a, Evans, S. K., and Green, M. R. (2006) Transcriptional regulatory elements in the human genome. *Annu. Rev. Genomics Hum. Genet. 7*, 29–59.

(14) Narlikar, G. J., Fan, H.-Y., and Kingston, R. E. (2002) Cooperation between complexes that regulate chromatin structure and transcription. *Cell 108*, 475–87.

(15) Purcell, O., Peccoud, J., and Lu, T. K. (2014) Rule-Based Design of Synthetic Transcription Factors in Eukaryotes. *ACS Synth. Biol. 3*, 737–744.

(16) Klug, A. (2010) The Discovery of Zinc Fingers and Their Applications in Gene Regulation and Genome Manipulation. *Annu. Rev. Biochem. 79*, 213–231.

(17) Khalil, A. S., Lu, T. K., Bashor, C. J., Ramirez, C. L., Pyenson, N. C., Joung, J. K., and Collins, J.

J. (2012) A synthetic biology framework for programming eukaryotic transcription functions. *Cell 150*, 647–658.

(18) Jankele, R., and Svoboda, P. (2014) TAL effectors: tools for DNA Targeting. *Brief. Funct. Genomics 13*, 409–419.

(19) Moscou, M. J., and Bogdanove, A. J. (2009) A Simple Cipher Governs DNA Recognition by TAL Effectors. *Science. 326*, 1501–1501.

(20) Zhang, F., Cong, L., Lodato, S., Kosuri, S., Church, G. M., and Arlotta, P. (2011) Efficient construction of sequence-specific TAL effectors for modulating mammalian transcription. *Nat. Biotechnol. 29*, 149–153.

(21) Morbitzer, R., Romer, P., Boch, J., and Lahaye, T. (2010) Regulation of selected genome loci using de novo-engineered transcription activator-like effector (TALE)-type transcription factors. *Proc. Natl. Acad. Sci. 107*, 21617–21622.

(22) Mercer, A. C., Gaj, T., Sirk, S. J., Lamb, B. M., and Barbas, C. F. (2014) Regulation of Endogenous Human Gene Expression by Ligand- Inducible TALE Transcription Factors. *ACS Synth. Biol. 3*, 723–730.

(23) Maeder, M. L., Linder, S. J., Cascio, V. M., Fu, Y., Ho, Q. H., and Joung, J. K. (2013) CRISPR RNA-guided activation of endogenous human genes. *Nat Methods 10*, 977–979.

(24) Gilbert, L. a, Larson, M. H., Morsut, L., Liu, Z., Gloria, A., Torres, S. E., Stern-ginossar, N., Brandman, O., Whitehead, H., Doudna, J. a, Lim, W. a, and Jonathan, S. (2013) CRISPR-Mediated Modular RNA-Guided Regualtion of Transcription in Eukaryotes. *Cell 154*, 442–451.

(25) Berg, J. M., Tymoczko, J. L., and Stryer, L. (2002) Biochemistry. W.H. Freeman.

(26) Keegan, L. P., Leroy, A., Sproul, D., and O'Connell, M. A. (2004) Adenosine deaminases acting on RNA (ADARs): RNA-editing enzymes. *Genome Biol. 5*, 209.

(27) Glisovic, T., Bachorik, J. L., Yong, J., and Dreyfuss, G. (2008) RNA-binding proteins and post-transcriptional gene regulation. *FEBS Lett. 582*, 1977–86.

(28) Palazzo, A. F., and Lee, E. S. (2015) Non-coding RNA: What is functional and what is junk? *Front. Genet. 5*, 1–11.

(29) Mattick, J. S., and Makunin, I. V. (2006) Non-coding RNA. *Hum. Mol. Genet. 15 Spec No*, 17–29.

(30) Carthew, Richard W. and Sontheimer, E. J. (2009) Origins and Mechanisms of miRNAs and siRNAs. *Cell 136*, 642–655.

(31) Lee, R. C., Feinbaum, R. L., and Ambros, V. (1993) The C. elegans heterochronic gene lin-4 encodes small RNAs with antisense complementarity to lin-14. *Cell 75*, 843–54.

(32) Mello, C. C., and Conte, D. (2004) Revealing the world of RNA interference. *Nature 431*, 338–342.

(33) Shabalina, S., and Koonin, E. (2008) Origins and evolution of eukaryotic RNA interference. *Trends Ecol. Evol. 23*, 578–587.

(34) Wilson, R. C., and Doudna, J. A. (2013) Molecular Mechanisms of RNA Interference. *Annu. Rev. Biophys 42*, 217–39.

(35) Seto, A. G., Kingston, R. E., and Lau, N. C. (2007) The Coming of Age for Piwi Proteins. *Mol. Cell 26*, 603–609.

(36) Meister, G. (2013) Argonaute proteins: functional insights and emerging roles. *Nat. Rev. Genet. 14*, 447–459.

(37) He, L., and Hannon, G. J. (2004) MicroRNAs: small RNAs with a big role in gene regulation. *Nat. Rev. Genet. 5*, 522–531.

(38) Hammond, S. M., Boettcher, S., Caudy, A. A., Kobayashi, R., and Hannon, G. J. (2001) Argonaute2, a Link Between Genetic and Biochemical Analyses of RNAi. *Science. 293*, 1146–1150.

(39) Friedman, R. C., Farh, K. K. H., Burge, C. B., and Bartel, D. P. (2009) Most mammalian mRNAs are conserved targets of microRNAs. *Genome Res. 19*, 92–105.

(40) Filipowicz, W., Bhattacharyya, S. N., and Sonenberg, N. (2008) Mechanisms of post-transcriptional regulation by microRNAs: are the answers in sight? *Nat Rev Genet 9*, 102–114.

(41) Lee, Y., Jeon, K., Lee, J.-T., Kim, S., and Kim, V. N. (2002) MicroRNA maturation: stepwisee processing and subcellular localization. *EMBO J. 21*, 4663–4670.

(42) Lewis, B. P., Burge, C. B., and Bartel, D. P. (2005) Conserved seed pairing, often flanked by adenosines, indicates that thousands of human genes are microRNA targets. *Cell 120*, 15–20.

(43) Kiriakidou, M., Nelson, P. T., Kouranov, A., Fitziev, P., Bouyioukos, C., Mourelatos, Z., and Hatzigeorgiou, A. (2004) A combined computational-experimental approach predicts human microRNA targets. *Genes Dev. 18*, 1165–1178.

(44) Kloosterman, W. P., Wienholds, E., Ketting, R. F., and Plasterk, R. H. A. (2004) Substrate requirements for let-7 function in the developing zebrafish embryo. *Nucleic Acids Res. 32*, 6284–6291.

(45) Huntzinger, E., and Izaurralde, E. (2011) Gene silencing by microRNAs: contributions of translational repression and mRNA decay. *Nat. Rev. Genet. 12*, 99–110.

(46) Fabian, M. R., Mathonnet, G., Sundermeier, T., Zipprich, J. T., Svitkin, Y. V, Rivas, F., Jinek, M., Doudna, J. A., Chen, C. A., Shyu, A., Yates, J. R., Hannon, G. J., Filipowicz, W., and Duchaine, T. F. (2010) Mammalian miRNA RISC Recruits CAF1 and PABP to Affect PABP- Dependent Deadenylation. *Mol cell. 35*, 868–880.

(47) Zdanowicz, A., Thermann, R., Kowalska, J., Jemielity, J., Duncan, K., Preiss, T., Darzynkiewicz, E., and Hentze, M. W. (2009) Drosophila miR2 Primarily Targets the m7GpppN Cap Structure for Translational Repression. *Mol. Cell 35*, 881–888.

(48) Wilczynska, A., and Bushell, M. (2015) The complexity of miRNA-mediated repression. *Cell Death Differ. 22*, 22–33.

(49) Bartel, D. P., and Chen, C.-Z. (2004) Opinion: Micromanagers of gene expression: the potentially widespread influence of metazoan microRNAs. *Nat. Rev. Genet. 5*, 396–400.

(50) Lee, Y., Ahn, C., Han, J., Choi, H., Kim, J., Yim, J., Lee, J., Provost, P., Rådmark, O., Kim, S., and Kim, V. N. (2003) The nuclear RNase III Drosha initiates microRNA processing. *Nature 425*, 415–419.

(51) Ma, H., Wu, Y., Choi, J.-G., and Wu, H. (2013) Lower and upper stem-single-stranded RNA junctions together determine the Drosha cleavage site. *Proc. Natl. Acad. Sci. U. S. A. 110*, 20687–92.

(52) Han, J., Lee, Y., Yeom, K., Kim, Y., Jin, H., and Kim, V. N. (2004) The Drosha – DGCR8 complex in primary microRNA processing. *Genes Dev.* 3016–3027.

(53) Zeng, Y., and Cullen, B. R. (2003) Sequence requirements for micro RNA processing and function in human cells. *RNA 9*, 112–23.

(54) Roden, C. A., Gaillard, J., Kanoria, S., Rennie, W., Barish, S., Cheng, J., Pan, W., Liu, J., Cotsapas, C., Ding, Y., and Lu, J. (2017) Novel determinants of mammalian primary microRNA processing revealed by systematic evaluation of hairpin-containing transcripts and human genetic variation. *Genome Res.* gr.208900.116.

(55) Lund, E., Güttinger, S., Calado, A., Dahlberg, J. E., and Kutay, U. (2004) Nuclear Export of MicroRNA Precursors. *Science. 303*, 95–98.

(56) Gregory, R. I., Yan, K., Amuthan, G., Chendrimada, T., Doratotaj, B., Cooch, N., and Shiekhattar, R. (2004) The Microprocessor complex mediates the genesis of microRNAs. *Nature 432*, 235–240.

(57) Basyuk, E., Suavet, F., Doglio, A., Bordonné, R., and Bertrand, E. (2003) Human let-7 stem-loop precursors harbor features of RNase III cleavage products. *Nucleic Acids Res. 31*, 6593–6597.

(58) Macrae, I. J., Zhou, K., Li, F., Repic, A., Brooks, A. N., Cande, W. Z., Adams, P. D., and Doudna, J. A. (2006) Structural Basis for Double-Stranded RNA Processing by Dicer. *Science. 311*.

(59) Park, J.-E., Heo, I., Tian, Y., Simanshu, D. K., Chang, H., Jee, D., Patel, D. J., and Kim, V. N. (2011) Dicer recognizes the 5’ end of RNA for efficient and accurate processing. *Nature 475*, 201–205.

(60) Tsutsumi, A., Kawamata, T., Izumi, N., Seitz, H., and Tomari, Y. (2011) Recognition of the pre-miRNA structure by Drosophila Dicer-1. *Nat. Struct. Mol. Biol. 18*, 1153–1158.

(61) Starega-Roslan, J., Galka-Marciniak, P., and Krzyzosiak, W. J. (2015) Nucleotide sequence of miRNA precursor contributes to cleavage site selection by Dicer. *Nucleic Acids Res. 43*, 10939–10951.

(62) Zhang, X., and Zeng, Y. (2010) The terminal loop region controls microRNA processing by Drosha and Dicer. *Nucleic Acids Res. 38*, 7689–7697.

(63) Bernstein, E., Caudy, A. A., Hammond, S. M., and Hannon, G. J. (2001) Role for a bidentate ribonuclease in the initiation step of RNA interference. *Nature 409*, 363–366.

(64) Daniels, S. M., Melendez-Peña, C. E., Scarborough, R. J., Daher, A., Christensen, H. S., El Far, M., Purcell, D. F. J., Lainé, S., and Gatignol, A. (2009) Characterization of the TRBP domain required for dicer interaction and function in RNA interference. *BMC Mol. Biol. 10*, 38.

(65) Lee, H. Y., and Doudna, J. A. (2012) TRBP alters human precursor microRNA processing in vitro. *RNA 18*, 2012–9.

(66) Fukunaga, R., Han, B. W., Hung, J.-H., Xu, J., Weng, Z., and Zamore, P. D. (2012) Dicer Partner Proteins Tune the Length of Mature miRNAs in Flies and Mammals. *Cell 151*, 533–546.

(67) Wang, H., Noland, C., Siridechadilok, B., Taylor, D. W., Ma, E., Felderer, K., Doudna, J. a, and Nogales, E. (2010) Structural insights into RNA Processing by the Human RISC- Loading Complex. *Nat Struct Mol Biol. 16*, 1148–1153.

(68) Hutvagner, G., and Simard, M. J. (2008) Argonaute proteins: key players in RNA silencing. *Nat. Rev. Mol. Cell Biol. 9*, 22–32.

(69) Wilson, R. C., and Doudna, J. A. (2013) Molecular Mechanisms of RNA Interference. *Annu. Rev. Biophys. 42*, 217–239.

(70) Schwarz, D. S., Hutvágner, G., Du, T., Xu, Z., Aronin, N., and Zamore, P. D. (2003) Asymmetry in the assembly of the RNAi enzyme complex. *Cell 115*, 199–208.

(71) O'Toole, A. S., Miller, S., Haines, N., Zink, M. C., and Serra, M. J. (2006) Comprehensive thermodynamic analysis of 3' double-nucleotide overhangs neighboring Watson-Crick terminal base pairs. *Nucleic Acids Res. 34*, 3338–3344.

(72) Johnston, R. J., Chang, S., Etchberger, J. F., Ortiz, C. O., and Hobert, O. (2005) MicroRNAs acting in a double-negative feedback loop to control a neuronal cell fate decision. *Proc. Natl. Acad. Sci. U. S. A. 102*, 12449–54.

(73) Chendrimada, T. P., Gregory, R. I., Kumaraswamy, E., Cooch, N., Nishikura, K., and Shiekhattar, R. (2010) TRBP recruits the Dicer complex to Ago2 for microRNA processing and gene silencing. *Nature 436*, 740–744.

(74) Viswanathan, S. R., and Daley, G. Q. (2010) Lin28: A MicroRNA Regulator with a Macro Role. *Cell 140*, 445–449.

(75) Kawahara, Y., Zinshteyn, B., Chendrimada, T. P., Shiekhattar, R., and Nishikura, K. (2007) RNA editing of the microRNA-151 precursor blocks cleavage by the Dicer-TRBP complex. *EMBO Rep. 8*, 763–9.

(76) Di Leva, G., Garofalo, M., and Croce, C. M. (2014) MicroRNAs in Cancer. *Annu. Rev. Pathol. Mech. Dis. 9*, 287–314.

(77) Mishra, P. J. (2014) MicroRNAs as promising biomarkers in cancer diagnostics. *Biomark. Res. 2*, 4–7.

(78) Thiery, J., Ralph, P., Häntzsch, M., and Leipzig, U. (2015) Zirkulierende MicroRNAs Neuartige Biomarker am Horizont ? *Medizin von Morgen 46*, 29–32.

(79) Welch, C., Chen, Y., and Stallings, R. L. (2007) MicroRNA-34a functions as a potential tumor suppressor by inducing apoptosis in neuroblastoma cells. *Oncogene 26*, 5017–22.

(80) Agostini, M., and Knight, R. A. (2014) miR-34 : from bench to bedside. *Oncotarget. 5*, 872–81.

(81) Tarasov, V., Jung, P., Verdoodt, B., Lodygin, D., Epanchintsev, A., Menssen, A., Meister, G., and Hermeking, H. (2007) Differential regulation of microRNAs by p53 revealed by massively parallel sequencing: miR-34a is a p53 target that induces apoptosis and G 1-arrest. *Cell Cycle 6*, 1586–1593.

(82) Hermeking, H. (2010) The miR-34 family in cancer and apoptosis. *Cell Death Differ. 17*, 193–9.

(83) Yamakuchi, M., and Lowenstein, C. J. (2009) MiR-34, SIRT1 and p53: The feedback loop. *Cell Cycle 8*, 712–715.

(84) Yamakuchi, M., Ferlito, M., and Lowenstein, C. J. (2008) miR-34a repression of SIRT1 regulates apoptosis. *Proc. Natl. Acad. Sci. 105*, 13421–13426.

(85) Li, N., Fu, H., Tie, Y., Hu, Z., Kong, W., Wu, Y., and Zheng, X. (2009) miR-34a inhibits migration and invasion by down-regulation of c-Met expression in human hepatocellular carcinoma cells. *Cancer Lett. 275*, 44–53.

(86) Tazawa, H., Tsuchiya, N., Izumiya, M., and Nakagama, H. (2007) Tumor-suppressive miR-34a induces senescence-like growth arrest through modulation of the E2F pathway in human colon cancer cells. *Proc. Natl. Acad. Sci. U. S. A. 104*, 15472–7.

(87) Concepcion, C. P., Bonetti, C., and Ventura, A. (2012) The MicroRNA-17-92 Family of MicroRNA Clusters in Development and Disease. *Cancer J. 18*, 262–267.

(88) Mitchell, P. S., Parkin, R. K., Kroh, E. M., Fritz, B. R., Wyman, S. K., Pogosova-Agadjanyan, E. L., Peterson, A., Noteboom, J., O'Briant, K. C., Allen, A., Lin, D. W., Urban, N., Drescher, C. W., Knudsen, B. S., Stirewalt, D. L., Gentleman, R., Vessella, R. L., Nelson, P. S., Martin, D. B., and Tewari, M. (2008) Circulating microRNAs as stable blood-based markers for cancer detection. *Proc. Natl. Acad. Sci. U.S.A. 105*, 10513–10518.

(89) Li, M., Guan, X., Sun, Y., Mi, J., Shu, X., Liu, F., and Li, C. (2014) MiR-92a family and their target genes in tumorigenesis and metastasis. *Exp. Cell Res. 323*, 1–6.

(90) Ohyagi-Hara, C., Sawada, K., Kamiura, S., Tomita, Y., Isobe, A., Hashimoto, K., Kinose, Y., Mabuchi, S., Hisamatsu, T., Takahashi, T., Kumasawa, K., Nagata, S., Morishige, K. I., Lengyel, E., Kurachi, H., and Kimura, T. (2013) MiR-92a inhibits peritoneal dissemination of ovarian cancer cells by inhibiting integrin alpha5 expression. *Am. J. Pathol. 182*, 1876–1889.

(91) Liao, W., Zhang, H., Feng, C., Wang, T., Zhang, Y., and Tang, S. (2014) Downregulation of TrkA protein expression by miRNA-92a promotes the proliferation and migration of human neuroblastoma cells. *Mol. Med. Rep. 10*, 778–784.

(92) Zhang, L., Zhou, M., Qin, G., Weintraub, N. L., and Tang, Y. (2014) MiR-92a regulates viability and angiogenesis of endothelial cells under oxidative stress. *Biochem. Biophys. Res. Commun. 446*, 952–958.

(93) Erdmann, K., Kaulke, K., Thomae, C., Huebner, D., Sergon, M., Froehner, M., Wirth, M. P., and Fuessel, S. (2014) Elevated expression of prostate cancer-associated genes is linked to down-regulation of microRNAs. *BMC Cancer 14*, 82.

(94) Zheng, F., Liao, Y. J., Cai, M. Y., Liu, T. H., Chen, S. P., Wu, P. H., Wu, L., Bian, X. W., Guan, X. Y., Zeng, Y. X., Yuan, Y. F., Kung, H. F., and Xie, D. (2015) Systemic delivery of microRNA-101 potently inhibits hepatocellular carcinoma in vivo by repressing multiple targets. *PLoS Genet. 11*, e1004873.

(95) Lei, Y., Li, B., Tong, S., Qi, L., Hu, X., Cui, Y., Li, Z., He, W., Zu, X., Wang, Z., and Chen, M. (2015) MiR-101 suppresses vascular endothelial growth factor C that inhibits migration and invasion and enhances cisplatin chemosensitivity of bladder cancer cells. *PLoS One 10*, 1–14.

(96) Liu, N., Xia, W.-Y., Liu, S.-S., Chen, H.-Y., Sun, L., Liu, M.-Y., Li, L.-F., Lu, H.-M., Fu, Y.-J., Wang, P., Wu, H., and Gao, J.-X. (2016) MicroRNA-101 targets von Hippel-Lindau tumor suppressor (VHL) to induce HIF1α mediated apoptosis and cell cycle arrest in normoxia condition. *Sci. Rep. 6*, 20489.

(97) Lin, C., Huang, F., Shen, G., and Yiming, A. (2015) MicroRNA-101 regulates the viability and invasion of cervical cancer cells. *Int J Clin Exp Pathol 8*, 10148–10155.

(98) Yan, D., Zhou, X., Chen, X., Hu, D. N., Dong, X. Da, Wang, J., Lu, F., Tu, L. L., and Qu, J. (2009) MicroRNA-34a inhibits uveal melanoma cell proliferation and migration through downregulation of c-Met. *Investig. Ophthalmol. Vis. Sci. 50*, 1559–1565.

(99) Sun, Y., Zhang, F., Bai, Y., and Guo, L. (2010) miR-126 modulates the expression of epidermal

growth factor-like domain 7 in human umbilical vein endothelial cells in vitro. *J South Med Univ 30*, 767–770.

(100) Fitch, M. J., Campagnolo, L., Kuhnert, F., and Stuhlmann, H. (2004) Egfl7, a novel epidermal growth factor-domain gene expressed in endothelial cells. *Dev. Dyn. 230*, 316–324.

(101) Meister, J., and Schmidt, M. H. H. (2010) miR-126 and miR-126*: New Players in Cancer. *Sci. World J. 10*, 2090–2100.

(102) Ebrahimi, F., Gopalan, V., Smith, R. A., and Lam, A. K. Y. (2014) MiR-126 in human cancers: Clinical roles and current perspectives. *Exp. Mol. Pathol. 96*, 98–107.

(103) Harris, T. A., Yamakuchi, M., Ferlito, M., Mendell, J. T., and Lowenstein, C. J. (2008) MicroRNA-126 regulates endothelial expression of vascular cell adhesion molecule 1. *Proc Natl Acad Sci U S A 105*, 1516–1521.

(104) Fish, J., Santoro, M., Morton, S., Yu, S., Yeh, R., Wythe, J., Ivey, K., Bruneau, B., Stainier, D., and Srivastava, D. (2008) miR-126 regulates angiogenic signaling and vascular integrity. *Dev Cell 15*, 272–84.

(105) Mizuno, S., Bogaard, H. J., Gomez-Arroyo, J., Alhussaini, A., Kraskauskas, D., Cool, C. D., and Voelkel, N. F. (2012) MicroRNA-199a-5p is associated with hypoxia-inducible factor-1 alpha expression in lungs from patients with COPD. *Chest 142*, 663–672.

(106) Gu, S., and Chan, W.-Y. (2012) Flexible and versatile as a chameleon-sophisticated functions of microRNA-199a. *Int. J. Mol. Sci. 13*, 8449–66.

(107) Jia, X. Q., Cheng, H. Q., Qian, X., Bian, C. X., Shi, Z. M., Zhang, J. P., Jiang, B. H., and Feng, Z. Q. (2012) Lentivirus-Mediated Overexpression of MicroRNA-199a Inhibits Cell Proliferation of Human Hepatocellular Carcinoma. *Cell Biochem. Biophys. 62*, 237–244.

(108) Rane, S., He, M., Sayed, D., Vashistha, H., Malhotra, A., Sadoshima, J., Vatner, D. E., Vatner, S. F., and Abdellatif, M. (2009) Downregulation of MiR-199a derepresses hypoxia-inducible factor-1 alpha and sirtuin 1 and recapitulates hypoxia preconditioning in cardiac myocytes. *Circ. Res. 104*, 879–886.

(109) Tsukigi, M., Bilim, V., Yuuki, K., Ugolkov, A., Naito, S., Nagaoka, A., Kato, T., Motoyama, T., and Tomita, Y. (2012) Re-expression of miR-199a suppresses renal cancer cell proliferation and survival by targeting GSK-3. *Cancer Lett. 315*, 189–197.

(110) Zhang, Y., Fan, K. J., Sun, Q., Chen, A. Z., Shen, W. L., Zhao, Z. H., Zheng, X. F., and Yang, X. (2012) Functional screening for miRNAs targeting Smad4 identified miR-199a as a negative regulator of TGF-ß signalling pathway. *Nucleic Acids Res. 40*, 9286–9297.

(111) Shen, Q., Cicinnati, V. R., Zhang, X., Iacob, S., Weber, F., Sotiropoulos, G. C., Radtke, A., Lu, M., Paul, A., Gerken, G., and Beckebaum, S. (2010) Role of microRNA-199a-5p and discoidin domain receptor 1 in human hepatocellular carcinoma invasion. *Mol. Cancer 9*, 1–12.

(112) Zhang, P., Cheng, J., Zou, S., D'Souza, A. D., Koff, J. L., Lu, J., Lee, P. J., Krause, D. S., Egan, M. E., and Bruscia, E. M. (2015) Pharmacological modulation of the AKT/microRNA-199a-5p/CAV1 pathway ameliorates cystic fibrosis lung hyper-inflammation. *Nat. Commun. 6*, 6221.

(113) Shatseva, T., Lee, D. Y., Deng, Z., and Yang, B. B. (2011) MicroRNA miR-199a-3p regulates cell proliferation and survival by targeting caveolin-2. *J. Cell Sci. 124*, 2826–2836.

(114) Kim, S., Ui, J. L., Mi, N. K., Lee, E. J., Ji, Y. K., Mi, Y. L., Choung, S., Young, J. K., and Choi, Y. C. (2008) MicroRNA miR-199a * regulates the MET proto-oncogene and the downstream extracellular signal-regulated kinase 2 (ERK2). *J. Biol. Chem. 283*, 18158–18166.

(115) Henry, J. C., Park, J. K., Jiang, J., Kim, J. H., Nagorney, D. M., Roberts, L. R., Banerjee, S., and Schmittgen, T. D. (2010) miR-199a-3p targets CD44 and reduces proliferation of CD44 positive hepatocellular carcinoma cell lines. *Biochem. Biophys. Res. Commun. 403*, 120–125.

(116) Winkler, W. C. (2002) An mRNA structure that controls gene expression by binding FMN. *Proc. Natl. Acad. Sci. 99*, 15908–15913.

(117) Tucker, B. J., and Breaker, R. R. (2005) Riboswitches as versatile gene control elements. *Curr. Opin. Struct. Biol. 15*, 342–348.

(118) Barrick, J. E., and Breaker, R. R. (2007) The distributions, mechanisms, and structures of metabolite-binding riboswitches. *Genome Biol. 8*, R239.

(119) Ellington, A. D., and Szostak, J. W. (1990) In vitro selection of RNA molecules that bind specific ligands. *Nature 346*, 818–822.

(120) Tuerk, C., and Gold, L. (1990) Systematic evolution of ligands by exponential enrichment: RNA ligands to bacteriophage T4 DNA polymerase. *Science 249*, 505–10.

(121) Darmostuk, M., Rimpelova, S., Gbelcova, H., and Ruml, T. (2015) Current approaches in SELEX: An update to aptamer selection technology. *Biotechnol. Adv. 33*, 1141–1161.

(122) Germer, K., Leonard, M., and Zhang, X. (2013) Review Article RNA aptamers and their therapeutic and diagnostic applications. *Int. J. Biochem. Mol. Biol. 4*, 27–40.

(123) Song, S., Wang, L., Li, J., Fan, C., and Zhao, J. (2008) Aptamer-based biosensors. *TrAC - Trends Anal. Chem. 27*, 108–117.

(124) Werstuck, G., and Green, M. R. (1998) Controlling Gene Expression in Living Cells Through Small Molecule – RNA Interactions. *Science. 282*, 296–298.

(125) Schneider, C., and Suess, B. (2016) Identification of RNA aptamers with riboswitching properties. *Methods 97*, 44–50.

(126) Weigand, J. E., Sanchez, M., Gunnesch, E.-B., Zeiher, S., Schroeder, R., and Suess, B. (2008) Screening for engineered neomycin riboswitches that control translation initiation. *RNA 14*, 89–97.

(127) Suess, B., Hanson, S., Berens, C., Fink, B., Schroeder, R., and Hillen, W. (2003) Conditional gene expression by controlling translation with tetracycline-binding aptamers. *Nucleic Acids Res. 31*, 1853–1858.

(128) Weigand, J. E., and Suess, B. (2007) Tetracycline aptamer-controlled regulation of pre-mRNA splicing in yeast. *Nucleic Acids Res. 35*, 4179–4185.

(129) An, C., Trinh, V. B., and Yokobayashi, Y. (2006) Artificial control of gene expression in mammalian cells by modulating RNA interference through aptamer − small molecule interaction Artificial control of gene expression in mammalian cells by modulating RNA interference through aptamer – small molecule i. *Rna 12*, 710–716.

(130) Wang, S., and White, K. A. (2007) Riboswitching on RNA virus replication. *Proc. Natl. Acad. Sci. 104*, 10406–10411.

(131) Suess, B., and Weigand, J. E. (2008) Engineered Riboswitches : Overview, problems and trends. *RNA Biol. 5*, 24–9.

(132) Desai, S. K., and Gallivan, J. P. (2004) Genetic Screens and Selections for Small Molecules Based on a Synthetic Riboswitch That Activates Protein Translation. *J. Am. Chem. Soc. 126*, 13247–13254.

(133) Suess, B., Fink, B., Berens, C., Stentz, R., and Hillen, W. (2004) A theophylline responsive riboswitch based on helix slipping controls gene expression in vivo. *Nucleic Acids Res. 32*, 1610–1614.

(134) Famulok, M., Hartig, J. S., and Mayer, G. (2007) Functional aptamers and aptazymes in biotechnology, diagnostics, and therapy. *Chem. Rev. 107*, 3715–3743.

(135) Kashida, S., Inoue, T., and Saito, H. (2012) Three-dimensionally designed protein-responsive RNA devices for cell signaling regulation. *Nucleic Acids Res. 40*, 9369–9378.

(136) Hunsicker, A., Steber, M., Mayer, G., Meitert, J., Klotzsche, M., Blind, M., Hillen, W., Berens, C., and Suess, B. (2009) An RNA Aptamer that Induces Transcription. *Chem. Biol. 16*, 173–180.

(137) Saenger, W., Hinrichs, W., Orth, P., Schnappinger, D., and Hillen, W. (2000) Structural basis of gene regulation by the tetracycline inducible Tet repressor-operator system. *Nat. Struct. Biol. 7*, 215–219.

(138) Ramos, J. L., Martı, M., Molina-henares, A. J., Tera, W., Brennan, R., and Tobes, R. (2005) The TetR family of transcriptional. *Microbiol. Mol. Biol. Rev. 69*, 1–31.

(139) Orth, P., Saenger, W., and Hinrichs, W. (1999) Tetracycline-Chelated Mg 2+ Ion Initiates Helix Unwinding in Tet Repressor Induction. *Biochemistry 38*, 191–198.

(140) Berens, C., and Hillen, W. (2003) Gene regulation by tetracyclines: Constraints of resistance regulation in bacteria shape TetR for application in eukaryotes. *Eur. J. Biochem. 270*, 3109–3121.

(141) Gossen, M., and Bujard, H. (1992) Tight control of gene expression in mammalian cells by tetracycline-responsive promoters. *Proc. Natl. Acad. Sci. USA 89*, 5547–5551.

(142) Gossen, M., Freundlieb, S., Bender, G., Müller, G., Hillen, W., and Bujard, H. (1995) Transcriptional Activation By Tetracyclines in Mammalian-Cells. *Science. 268*, 1766–1769.

(143) Urlinger, S., Helbl, V., Guthmann, J., Pook, E., Grimm, S., and Hillen, W. (2000) The p65 domain from NF-κB is an efficient human activator in the tetracycline-regulatable gene expression system. *Gene 247*, 103–110.

(144) Gatz, C., and Quail, P. H. (1988) Tn10-encoded tet repressor can regulate an operator-containing plant promoter. *Proc. Natl. Acad. Sci. U. S. A. 85*, 1394–7.

(145) Urlinger, S., Baron, U., Thellmann, M., Hasan, M. T., Bujard, H., and Hillen, W. (2000) Exploring the sequence space for tetracycline-dependent transcriptional activators: novel mutations yield expanded range and sensitivity. *Proc. Natl. Acad. Sci. U. S. A. 97*, 7963–8.

(146) Resch, M., Striegl, H., Henssler, E. M., Sevvana, M., Egerer-sieber, C., Schiltz, E., Hillen, W., and Muller, Y. A. (2008) A protein functional leap: How a single mutation reverses the function of the transcription regulator TetR. *Nucleic Acids Res. 36*, 4390–4401.

(147) Steber, M., Arora, A., Hofmann, J., Brutschy, B., and Suess, B. (2011) Mechanistic basis for

RNA aptamer-based induction of TetR. *ChemBioChem 12*, 2608–2614.

(148) Goldfless, S. J., Belmont, B. J., De Paz, A. M., Liu, J. F., and Niles, J. C. (2012) Direct and specific chemical control of eukaryotic translation with a synthetic RNA-protein interaction. *Nucleic Acids Res. 40*, 1–12.

(149) Goldfless, S. J., Wagner, J. C., and Niles, J. C. (2014) Versatile control of Plasmodium falciparum gene expression with an inducible protein-RNA interaction. *Nat. Commun. 5*, 5329.

(150) Wieland, M., Ausländer, S., Tigges, M., and Fussenegger, M. (2011) Rational design of a small molecule-responsive intramer controlling transgene expression in mammalian cells. *Nucleic Acids Res. 39*, e155.

(151) Esteller, M. (2011) Non-coding RNAs in human disease. *Nat. Rev. Genet. 12*, 861–74.

(152) Sayed, D., and Abdellatif, M. (2011) MicroRNAs in Development and Disease. *Physiol. Rev. 91*, 827–887.

(153) Saito, H., Fujita, Y., Kashida, S., Hayashi, K., and Inoue, T. (2011) Synthetic human cell fate regulation by protein-driven RNA switches. *Nat. Commun. 2*, 160–168.

(154) Feng, Y., Zhang, X., Graves, P., and Zeng, Y. A. N. (2012) A comprehensive analysis of precursor microRNA cleavage by human Dicer. *RNA 18 (11)*, 2083–2092.

(155) Choudhury, N. R., and Michlewski, G. (2012) Terminal loop-mediated control of microRNA biogenesis: selectivity and mechanism. *Biochem Soc Trans. 41*, 789–793.

(156) Michlewski, G., Guil, S., Semple, C. A., and Cáceres, J. F. (2008) Posttranscriptional Regulation of miRNAs Harboring Conserved Terminal Loops. *Mol. Cell 32*, 383–393.

(157) Gu, S., Jin, L., Zhang, Y., Huang, Y., Zhang, F., Valdmanis, P. N., and Kay, M. A. (2012) The loop position of shRNAs and pre-miRNAs is critical for the accuracy of dicer processing in vivo. *Cell 151*, 900–911.

(158) Taylor, D. W., Shigematsu, H., Cianfrocco, M. A., Noland, C. L., Nagayama, K., Nogales, E., Jennifer, A., Wang, H., Biology, C., Division, S., Berkeley, L., Division, B., and Berkeley, L. (2013) Substrate-specific structural rearrangements of human Dicer. *Nat. Struct. Mol. Biol. 20*, 662–670.

(159) Mayr, and Bartel. (2010) Widespread shortening of 3′UTRs by alternative cleavage and polyadenylation activates oncogenes in cancer cells. *Cell 138*, 673.

(160) Ziebarth, J. D., Bhattacharya, A., and Cui, Y. (2012) Integrative Analysis of Somatic Mutations Altering MicroRNA Targeting in Cancer Genomes. *PLoS One 7*, 1–10.

(161) Jin, H. Y., Gonzalez-Martin, A., Miletic, A. V., Lai, M., Knight, S., Sabouri-Ghomi, M., Head, S. R., Macauley, M. S., Rickert, R. C., and Xiao, C. (2015) Transfection of microRNA mimics should be used with caution. *Front. Genet. 6*, 1–23.

(162) Cloonan, N. (2015) Re-thinking miRNA-mRNA interactions: Intertwining issues confound target discovery. *BioEssays 37*, 379–388.

(163) Kulkarni, V., Naqvi, A. R., Uttamani, J. R., and Nares, S. (2016) MiRNA-Target interaction reveals cell-specific post-transcriptional regulation in mammalian cell lines. *Int. J. Mol. Sci. 17*.

(164) Chou, C.-H., Chang, N.-W., Shrestha, S., Hsu, S.-D., Lin, Y.-L., Lee, W.-H., Yang, C.-D., Hong,

H.-C., Wei, T.-Y., Tu, S.-J., Tsai, T.-R., Ho, S.-Y., Jian, T.-Y., Wu, H.-Y., Chen, P.-R., Lin, N.-C., Huang, H.-T., Yang, T.-L., Pai, C.-Y., Tai, C.-S., Chen, W.-L., Huang, C.-Y., Liu, C.-C., Weng, S.-L., Liao, K.-W., Hsu, W.-L., and Huang, H.-D. (2016) miRTarBase 2016: updates to the experimentally validated miRNA-target interactions database. *Nucleic Acids Res. 44*, D239–D247.

(165) Aranda, J. F., Canfran-Duque, a., Goedeke, L., Suarez, Y., and Fernandez-Hernando, C. (2015) The miR-199-dynamin regulatory axis controls receptor-mediated endocytosis. *J. Cell Sci. 128*, 3197–3209.

(166) Lino Cardenas, C. L., Henaoui, I. S., Courcot, E., Roderburg, C., Cauffiez, C., Aubert, S., Copin, M. C., Wallaert, B., Glowacki, F., Dewaeles, E., Milosevic, J., Maurizio, J., Tedrow, J., Marcet, B., Lo-Guidice, J. M., Kaminski, N., Barbry, P., Luedde, T., Perrais, M., Mari, B., and Pottier, N. (2013) miR-199a-5p Is Upregulated during Fibrogenic Response to Tissue Injury and Mediates TGFbeta-Induced Lung Fibroblast Activation by Targeting Caveolin-1. *PLoS Genet. 9*.

(167) Mukherji, S., Ebert, M. S., Zheng, G. X. Y., Tsang, J. S., Sharp, P. A., and van Oudenaarden, A. (2011) MicroRNAs can generate thresholds in target gene expression. *Nat. Genet. 43*, 854–859.

(168) Hydbring, P., and Badalian-Very, G. (2013) Clinical applications of microRNAs. *F1000Research 2*, 136.

(169) Choudhuri, S. (2010) Small noncoding RNAs: Biogenesis, function, and emerging significance in toxicology. *J. Biochem. Mol. Toxicol. 24*, 195–216.

(170) Tuleuova, N., An, C. Il, Ramanculov, E., Revzin, A., and Yokobayashi, Y. (2008) Modulating endogenous gene expression of mammalian cells via RNA-small molecule interaction. *Biochem. Biophys. Res. Commun. 376*, 169–173.

(171) Beisel, C. L., Bayer, T. S., Hoff, K. G., and Smolke, C. D. (2008) Model-guided design of ligand-regulated RNAi for programmable control of gene expression. *Mol. Syst. Biol. 4*, 224.

(172) Berens, C., Lochner, S., Löber, S., Usai, I., Schmidt, A., Drueppel, L., Hillen, W., and Gmeiner, P. (2006) Subtype Selective Tetracycline Agonists and their Application for a Two-Stage Regulatory System. *ChemBioChem 7*, 1320–1324.

(173) Beilstein, K., Wittmann, A., Grez, M., and Suess, B. (2014) Conditional control of mammalian gene expression by tetracycline- dependent hammerhead ribozymes. *ACS Synth. Biol. 4*, 526–534.

(174) Livak, K. J., and Schmittgen, T. D. (2001) Analysis of relative gene expression data using real-time quantitative PCR and. *Methods 25*, 402–408.

(175) Chen, C., Ridzon, D. A., Broomer, A. J., Zhou, Z., Lee, D. H., Nguyen, J. T., Barbisin, M., Xu, N. L., Mahuvakar, V. R., Andersen, M. R., Lao, K. Q., Livak, K. J., and Guegler, K. J. (2005) Real-time quantification of microRNAs by stem-loop RT-PCR. *Nucleic Acids Res. 33*, 1–9.

8 Talks and Poster Presentations

2014

Summer School, Pottenstein, Germany

Talk: Kontrolle der miRNA Funktion durch Liganden-gesteuerte RNA-basierte Regulatorsysteme

2015

Winter School SFB902, Obergurgl, Austria

Talk: Control of miRNA function by ligand dependent RNA-based regulators

International Synthetic and Systems Biology Summer School SFB902, Taormina, Sicily

Poster: Control of miRNA function by ligand-dependent RNA-based regulators

9 Publications

Klauser B, Atanasov J, Siewert LK, Hartig JS: **Ribozyme-based aminoglycoside switches of gene expression engineered by genetic selection in S. cerevisiae.** (2015) *ACS Synth Biol*. 4(5): 516-25

Atanasov J, Weigand JE and Suess B: **Design and implementation of a synthetic pre-miR switch for controlling miRNA biogenesis in mammals.** (2017), manuscript submitted

10 Curriculum Vitae

Name	Janina Atanasov
Date of birth	29.09.1987 in Nuremberg
Address	Darmstädter Straße 35a
	64807 Dieburg
	Germany

Professional experience

01/2014 - present **Institute for Biology | Synthetic genetic circuits |**

Technische Universität Darmstadt, Germany

Graduate student in the Lab of Prof. Dr. Beatrix Suess
Doctoral thesis: Design and implementation of a synthetic pre-miR switch for controlling miRNA biogenesis in mammals

Degree: Dr. rer. nat.

Education

10/2011-12/2013 **Master of Science in Life Science**
Universität Konstanz
Master thesis: Design of Aptazymes with Novel Ligand Selectivity

Degree: M. Sc.

04/2008 - 03/2011 **Bachelor of Science in Pharmaceutical Sciences**
Ludwig-Maximilians-Universität München
Bachelor thesis: Detection of HCN3 surface expression

Degree: B. Sc.

09/1998 - 06/2007 **Wolfram-von-Eschenbach-Germany, Schwabach, Germany**

University-entrance diploma

11 Ehrenwörtliche Erklärung

Ich erkläre hiermit ehrenwörtlich, dass ich die vorliegende Arbeit entsprechend den Regeln guter wissenschaftlicher Praxis selbstständig und ohne unzulässige Hilfe Dritter angefertigt habe.

Sämtliche aus fremden Quellen direkt oder indirekt übernommenen Gedanken sowie sämtliche von Anderen direkt oder indirekt übernommenen Daten, Techniken und Materialien sind als solche kenntlich gemacht. Die Arbeit wurde bisher bei keiner anderen Hochschule zu Prüfungszwecken eingereicht.

Darmstadt, den 06.03.2017

.....

(Janina Atanasov)